One half will never be believed,
the other never read.

Alexander Pope (Epigrams)

FORMATIVE TIME LAG STUDIES IN NEON

being a thesis on the secondary ionization mechanisms leading to the Townsend breakdown in low pressure neon

by

M. J. FULKER, B.A., M.Sc., Grad.Inst.P.

and

submitted to the University of Keele
in candidature for the degree of Ph.D.

January 1967

ABSTRACT

Formative time lags have been measured in neon using variable gap nickel electrodes for a reduced pressure range from 18 to 59 torr. The results cover an E_s/p_o range from 15 to 32 volt cm^{-1} $torr^{-1}$ (that is an E_s/N range from 4.3 to 9.0 x 10^{-16} volt cm^2.) Theoretical formative time lags have been calculated using Davidson's current growth theory for various assumed values of the secondary ionization coefficients. Comparison between theoretical and experimental formative time lags showed that the predominant secondary ionization processes leading to electrical breakdown were the emission of electrons from the cathode induced by positive ions (coefficient γ) and by radiation from the destruction of atomic neon metastable states at two body collisions with gas atoms (coefficient δ_1/α). The coefficient γ included ionization from undelayed photons reaching the cathode (coefficient δ/α). Diatomic metastable molecules were not thought to contribute significantly to secondary ionization for the range covered by this work. Approximate values of the coefficients γ and δ_1/α were calculated as functions of E_s/p_o and p_o. For low E_s/p_o and high p_o the δ_1/α process provides most of the secondary ionization, the γ process becoming more important at high E_s/p_o and low p_o.

ACKNOWLEDGMENTS

My thanks are due to Professor D. J. E. Ingram for the use of laboratory facilities, A.E.R.E., Culham for a research grant, Professor D. E. Davies and Dr. N. A. Surplice for supervision of this work and Mrs. J. Grange and Mrs. E. Fenn of Edwards High Vacuum International Ltd. for typing the thesis.

CONTENTS

CHAPTER I

BASIC PROCESSES IN A LOW PRESSURE TOWNSEND GAS DISCHARGE

CHAPTER II

A REVIEW OF PREVIOUS WORK

CHAPTER III

DAVIDSON'S THEORY FOR THE TEMPORAL GROWTH OF CURRENT

CHAPTER IV

EXPERIMENTAL APPARATUS

CHAPTER V

EXPERIMENTAL RESULTS

CHAPTER VI

DETERMINATION OF SECONDARY IONIZATION COEFFICIENTS USING DAVIDSON'S THEORY

LIST OF FIGURES

CHAPTER I

BASIC PROCESSES IN A LOW PRESSURE TOWNSEND DISCHARGE

1.1. INTRODUCTION

The application of a D.C. voltage to parallel plate electrodes in a gas at low pressure may result in the passage of a current through the gas. Such a current may be initiated by the emission of electrons from the electrode at the negative potential or by externally induced ionization of gas molecules. The emission of electrons from the cathode is commonly induced by raising the cathode temperature or illuminating the cathode surface with ultra-violet radiation. This externally induced current is denoted by I_o. If the electric field applied between the two electrodes is sufficiently low the total current I flowing in gap (or the current of electrons arriving at the anode) is related to the current I_o by the equation:

$$\frac{I}{I_o} = \frac{e^{\alpha d}}{1-\omega/\alpha(e^{\alpha d}-1)} \qquad (1)$$

where d is the separation of the electrodes in centimetres. α is the average number of ionizing collisions made by an electron travelling 1 cm in the direction of the field, and is called the primary ionization coefficient. Thus, if only this primary process operates, one electron leaving the cathode results in

$e^{\alpha d}$ electrons arriving at the anode. However, secondary ionization processes are normally present in the discharge. These processes which involve ions, photons, and excited molecules formed in the discharge, are all included in the generalized secondary ionization coefficient ω/α which is the average number of electrons contributed to the discharge by secondary processes per primary ionizing collision in the gas. As the field is increased these secondary processes increase and contribute significantly to the discharge current, which remains, however, proportional to the externally induced electron current I_o. For a particular value of the electric field the generalized secondary coefficient ω/α reaches such a value that the denominator of equation (1) falls to zero and the total current I therefore becomes independent of I_o and is only limited by the external circuit. This was first used as the criterion for electrical breakdown of the gap by Townsend (Townsend 1910). The criterion only applies where the breakdown involves many electron avalanches crossing the gap. i.e. at low gas pressures where the space charge of the charge carriers in the gas is not sufficient to distort the field. In a few simple cases the secondary ionization processes, which lead to breakdown of the gap, can be evaluated from study of the growth of current with time. The Townsend breakdown of a uniform field gap in low pressure hydrogen is known to be the result of secondary electron emission from the cathode by positive ions and photons formed in the gas. The Townsend breakdown of the rare gases has been studied for a number of years but the mechanisms are still not completely clear. The current growth as a function of time is

much slower than for hydrogen. This has been attributed to the presence of low energy metastable states in the rare gas.

There are two main approaches to this problem. One is to observe the current resulting from a short pulse of electrons leaving the cathode under a steady electric field. The secondary electrons which result from the arrival of ions and undelayed photons at the cathode can be separated temporally from those caused by the arrival of diffused metastable atoms and photons which have been delayed. The second approach, which is used in the present work, is to apply to the gap a step voltage, slightly greater than the breakdown voltage, with constant ultra-violet illumination of the cathode, and observe the resulting growth of current with time. In cases where metastable atoms or molecules are involved this approach requires a knowledge of the lifetime and diffusion rates of these particles. This information is provided by measurements of the density of metastable particles, by an optical absorption method, as a function of time following the passage of a short burst of electrons through the gap.

In this first chapter some of the basic concepts of the Townsend breakdown theory for low pressure gases under uniform electric field will be introduced. The theoretical and experimental work which directly concerns the problem of secondary ionization mechanisms in neon will be discussed in chapters II and III.

1.2. COLLISION PHENOMENA IN GASES

The build-up of a current in a gas is the result of a large number of interactions initiated by the electric field. The interactions, or collisions may involve electrons, ions, neutral and excited gas molecules, photons, the electrodes and the surrounding walls, and may be elastic, involving no change in the internal energy of the particles involved, or inelastic, involving excitation or ionization. Diffraction effects may occur if the kinetic energy of the incident particle is such that the wavelength is of the same order of magnitude as the diameter of the impacting particle. For example, diffraction effects occur for low energy electrons (below 1 electron volt) in the heavier noble gases, Ar, Kr, Xe. In helium and neon however electron diffraction is not significant.

1.3. EXCITATION BY ELECTRON IMPACT

Electron impact with a neutral gas molecule can cause excitation of the gas molecule, called a collision of the first kind. For this to occur two conditions must be satisfied.

(1) The kinetic energy of the electron must exceed the critical excitation energy of the gas molecule.

(2) The linear and angular momentum must be conserved. It follows that the probability for excitation is negligible at the threshold.

The gas molecule may be excited to a normal excited state with a typical lifetime of 10^{-8} seconds, or to a metastable

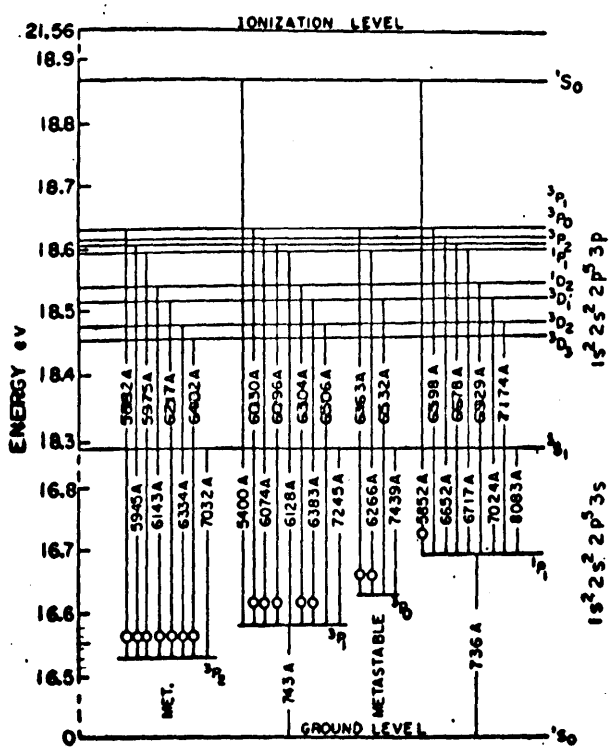

FIG. 1. Energy level diagram, first two excited configurations of neon.

state where the lifetime may be 10^{-3} seconds or greater. Fig. 1 shows the energy level diagram of the first two excited configurations of the neon atom. The ground state of neon is denoted by $1s^2 2s^2 2p^6$, where 1,2 denote the principal quantum number of each electron orbit, s,p correspond to the electron angular momentum values of $\ell = 0$ and $\ell = 1$. The superscript denotes the number of electrons in each orbit. The ground state may be more conveniently expressed as $^1S_0$ where S denotes a value of 0 for L, the orbital angular momentum quantum number of the atom. The subscript gives the value of the total angular momentum quantum number J obtained by coupling the orbital angular momentum quantum number L and the spin angular momentum quantum number S. The superscript denotes the multiplicity or the number of possible levels with the same L value.

The first excited configuration of neon consists of those energy levels where one electron is raised from the 2p to the 3s orbit, i.e. the configuration is $1s^2 2s^2 2p^5 3s$. This configuration consists of the triplet levels, $^3P_2$, $^3P_1$ and $^3P_0$, and the singlet level $^1P_1$. Transitions between the $^1S_0$ state and the $^3P_2$ and $^3P_0$ states are prohibited by the selection rule that $\Delta J = \pm 1$ or 0 with the transition $0 \rightarrow 0$ forbidden. The $^3P_2$ and $^3P_0$ states are therefore metastable and play an important part in the secondary ionization mechanisms which lead to the Townsend breakdown. Transitions between the $^3S_1$ state and higher energy D states and between the $^3S_1$ state, the D states and the $^1S_0$ ground level, are prohibited by a second selection rule that $\Delta L = \pm 1$.

FIG. 2 THE PROBABILITY OF IONIZATION AT A COLLISION AS A FUNCTION OF ELECTRON ENERGY.

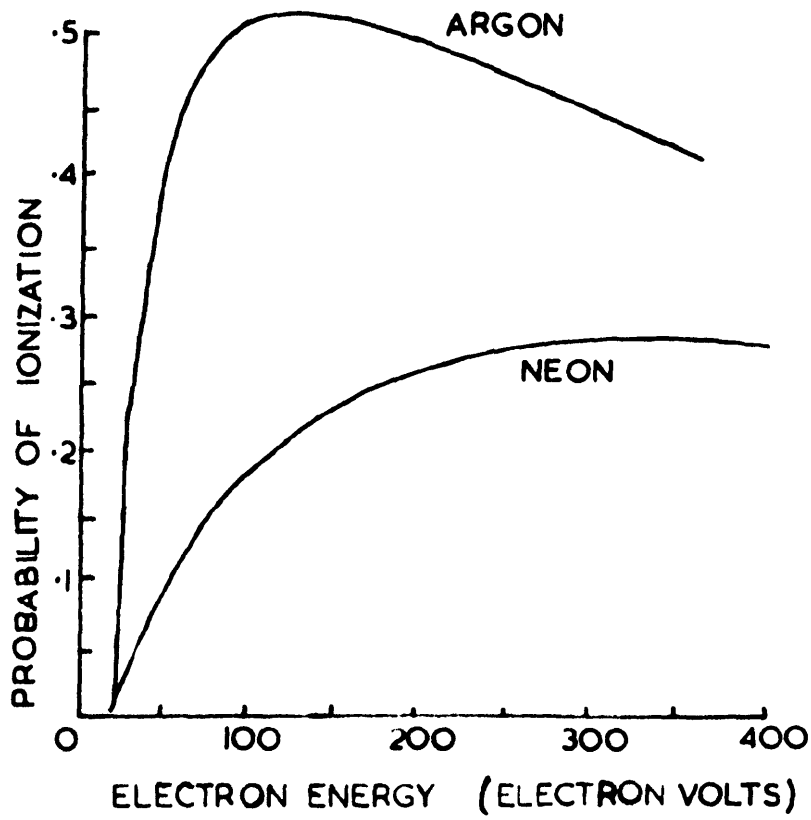

1.4. IONIZATION BY ELECTRON IMPACT

Ionization of gas atoms or molecules by electron impact can occur if the electron kinetic energy exceeds the ionization of the atom or molecule. The probability of ionization for neon as a function of electron energy is shown in Fig. 2. (Compton and VanVoorhis 1926). The probability is negligible at the threshold but increases approximately linearly with electron energy above that, reaching a maximum at about 350 eV. Above this energy the probability slowly decreases. For a given electron energy the number of ions produced per second is proportional to the primary electron current.

The probability of ionization for electrons of a given energy cannot be directly related to gas discharge conditions unless the electron energy distribution is known. Under Townsend discharge conditions, the primary ionization coefficient is the average number of ion pairs produced in the gas by one electron moving 1 cm. in the direction of the field. This coefficient is denoted by α.

For sufficiently low value of uniform electric field ionization of gas molecules by electron impact is the only significant ionization process and results in multiplication of any initial electron current emitted from the cathode. In this case the total electron current I at the anode distance d cm. from the cathode is given by $I = I_o e^{\alpha(d-d_o)}$ (Llewelyn Jones 1957, p. 3). I_o is the initial electron current at the cathode. d_o is the average distance an electron must travel from the cathode in order to acquire sufficient energy from the field to be capable of ionizing a gas molecule. In practice d_o is usually small compared with d.

The measured current for a given uniform electric field between two electrodes (i.e. voltage per unit gap distance) should increase exponentially with gap distance. In practice, for sufficiently large gap distances, the current increases with d at a faster rate than this due to the operation of other, secondary, ionization processes. Some of these processes will now be considered.

1.5. IONIZATION OF GAS MOLECULES BY POSITIVE ION IMPACT

The secondary ionization in the Townsend discharge, which can lead to breakdown of the gap, was originally thought to be the result of ionization of gas molecules when in collision with positive ions formed in the primary ionization process. Later work has shown this process to be of little importance.

According to the classical treatment for ion-atom or atom-atom collisions, only about half the energy of the incident particle can be transferred. Thus an ion or neutral atom must have at least twice the ionization energy to be capable of ionizing an atom. Experimental work by Utterback and Miller (Utterback 1961) has shown that the threshold of ionization for neutral nitrogen molecules occurs at about this value. Calculations by Little (Little 1956, p. 625) have shown that the probability of ionization for neon atoms by neutral neon atoms or neon ions is negligible in the Townsend discharge region, so that this process need not be considered in the present work.

1.6. COLLISIONS BETWEEN ELECTRONS AND EXCITED ATOMS OR MOLECULES

Electrons with energy less than the ionization energy

can ionize an already excited atom or molecule. This two-stage ionization process depends on the square of the electron current and on the lifetime of the excited states. Although metastable excited states are present in the neon Townsend discharge, the electron current is not sufficient to make this ionization process appreciable.

1.7. DESTRUCTION OF METASTABLE STATES

The neon atom can be easily excited to low energy metastable states. The dissipation of the metastable excitation energy on destruction of a metastable level can affect the excitation and ionization of the gas discharge in several ways.

The metastable atom may be destroyed at a collision with a neutral gas atom or molecule, causing ionization, excitation or dissociation of that atom or molecule. For example, if the metastable excitation energy E_{met} exceeds the ionization energy E_i of an atom of a different species, the metastable state can be destroyed at a collision causing ionization of the second atom. The Penning effect (Penning 1929 (1,2); Pike 1936) was first observed in neon-argon mixtures where argon atoms were ionized (E_i = 15.7 electron volts) by collision with metastable neon atoms (E_{met} = 16.53 electron volts). Quantum mechanical considerations show that the cross section for this process is large because of the particular energy difference between the two states. Slight contamination of neon with argon can therefore seriously affect

the ionization processes operating in a discharge. For example, Penning showed that argon impurity of 10 parts per million of neon could reduce the sparking potential of the gap by 50% and increase $\frac{\alpha}{p}$ (the primary ionization coefficient per unit pressure) by as much as several orders of magnitude. Therefore the purity of neon used for experimental measurements is very important.

A metastable particle may revert to the ground state on collision with one of the electrodes or the wall of the chamber to liberate an electron. The electron emission is by an Auger potential energy process discussed in a later section. If the probability of metastable atoms reaching the cathode is large this process may contribute appreciably to secondary ionization.

An atom in a metastable state may be excited to a higher energy non-metastable state on collision with a neutral gas atom. The higher state can then revert to the ground level with emission of a photon. This process can occur for neon, since the energy gaps between the excitation states are comparable with the thermal energy of a neutral gas atom. For helium the energy gaps are larger and metastable states are unlikely to be destroyed by this process.

Metastable states may be destroyed at two or three body collisions involving one or two neutral gas atoms producing a collision induced photon. This photon may result in electron emission from the cathode. (Such photons are sometimes referred to as 'non-resonance photons' to distinguish them from 'resonance photons'. Resonance photons travel through the gas by exciting gas atoms to non-metastable

resonance levels which quickly decay, re-emitting photons of the same energy. As a result the photons travel through the gas by a process similar in some respects to diffusion. After each absorption the photon is emitted in a random direction.) The production of collision induced photons by metastable atoms is proportional to the pressure in the two body case, and the square of the pressure in the three body case.

From these considerations it is apparent that the lifetime of a metastable state is dependent on gas purity, geometrical factors, temperature and pressure. Experimental measurements of the lifetime can provide information about the relative importance of the different destruction processes. These measurements will be considered in chapter III.

1.8. EXCITATION OF GAS MOLECULES BY PHOTONS

An atom or molecule of a gas can be excited by a photon which has energy $h\nu$ exactly equal to the excitation energy. In this respect photo-excitation differs from excitation by electron impact where the probability of excitation is zero at the threshold. However if the photon energy is not exactly equal to the excitation energy, the probability is small (the excess energy being radiated at longer wavelength).

One consequence of the high probability of excitation when the photon energy is exactly equal to the excitation energy E_{ex} is that a photon which has been emitted by the decay of an excited state (after about 10^{-8} seconds) has a high probability of being absorbed by an adjacent molecule. Such a photon is said to be

'trapped' and moves through the gas being repeatedly absorbed and re-emitted. The photon is emitted in a random direction after each absorption so that scattering results. The delayed passage of the photon through the gas is by a diffusion type process and results in long transit times. This trapped or resonance radiation might explain the relatively slow (millisecond) build-up of secondary ionization which is sometimes observed in a gas if the photon can cause electron emission when it finally reaches the cathode. The resonance process is most important for excitation levels near the ground state. It can work for higher excitation levels, but there is then a considerable volume destruction of photons. (Holstein 1947, Biberman 1947).

1.9. IONIZATION OF GAS MOLECULES BY PHOTONS

Ionization of gas molecules in the ground state by a photon of energy h can occur if hν is greater than or equal to the ionization energy E_i. The cross section for photo-ionization in many cases reaches a maximum close to the threshold in contrast to ionization by electron bombardment where the cross section is zero at the threshold. Photo-ionization cross sections are generally about 1000 times smaller than cross sections for ionization by electron impact. Therefore the contribution to ionization by this process is usually insignificant.

1.10. SURFACE PHENOMENA CONTRIBUTING TO IONIZATION IN A GAS

The interaction of photons, electrons, ions, and excited atoms or molecules with the solid or liquid surfaces in contact with a gas can cause electrons to be released into the gas. Electrons can also be released by field emission where high electric fields are applied or where the field is enhanced by surface irregularities.

An electron in a metal must be supplied with at least a well defined minimum energy, (known as the work function and denoted by ϕ,) in order to escape. An electron which lies below the Fermi level of the metal will require greater energy than this.

1.11. PHOTO-ELECTRIC EMISSION FROM METALS

Emission of an electron from the metal by an incident photon is possible if the photon energy $h\nu$ is equal to or greater than the work function ϕ of the metal. The ejected electron will have energy $h\nu - \phi$ if it comes from the Fermi level of the metal. For example, to release an electron from a gold surface with a work function of 4.7 electron volts the photon must have a wavelength less than 2630Å which means that it must be in the ultra-violet region. The electrons will have various energies even if all the photons have the same wavelength because the electrons are ejected from different depths in the conduction band. For photons of a given energy the electron emission current is proportional to the intensity of the radiation.

The photo-electric yield (electrons emitted per incident photon) depends on the nature and state of the surface as measured by the work function. The work function can be affected by absorbed gas layers on the surface and by insulating surface layers, such as an oxide. The photo-electric yield also depends on the angle of incidence and polarization of the incident radiation.

For all metals except the alkali metals and those with surface layers, the wavelength required to produce electron emission is in the ultra-violet region. Irradiation of a cathode with ultra-violet radiation is a common method of producing an initial current of electrons in a gas.

1.12. SECONDARY EMISSION OF ELECTRONS BY ELECTRON IMPACT

An electron striking a solid surface may be reflected or it may cause secondary electrons to be emitted from the solid. These secondary electrons are often accompanied by the emission of soft X-rays. The primary electron energy must exceed the work function (in electron volts) of the solid. No completely satisfactory theory exists for secondary emission by electrons. Under Townsend discharge conditions, electrons arriving at the anode of a uniform field gap may cause secondary electrons to be emitted. However, these will have a negligible contribution to the ionization of the gap because they are prevented by the field from travelling far from the anode and they are mostly of low energy (a few electron volts only).

FIG 3. POTENTIAL ENERGY DIAGRAM AND ELECTRON TRANSITIONS FOR NEON IONS ON A NICKEL SURFACE

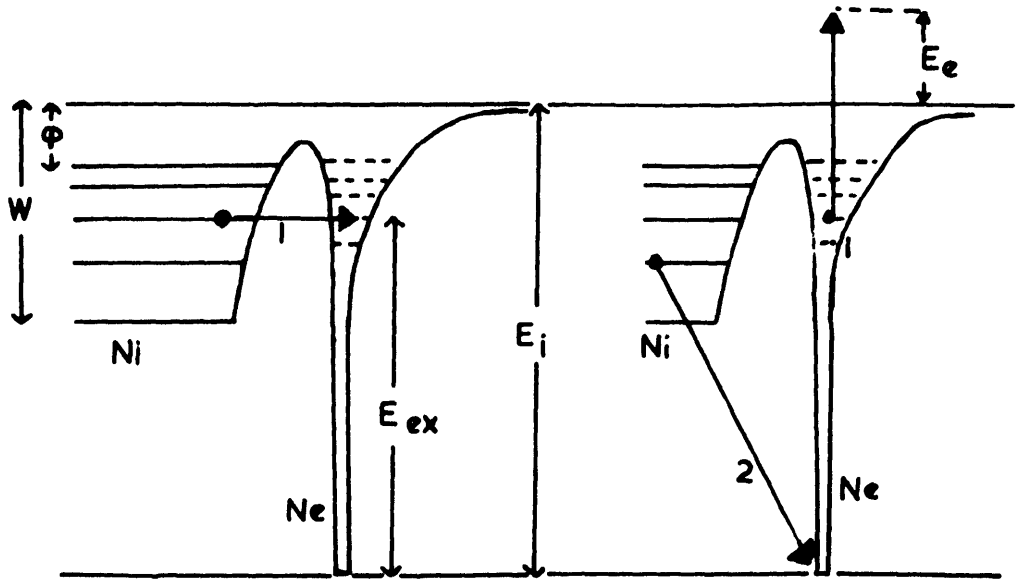

(a) RESONANCE NEUTRALIZATION (b) AUGER DE-EXCITATION

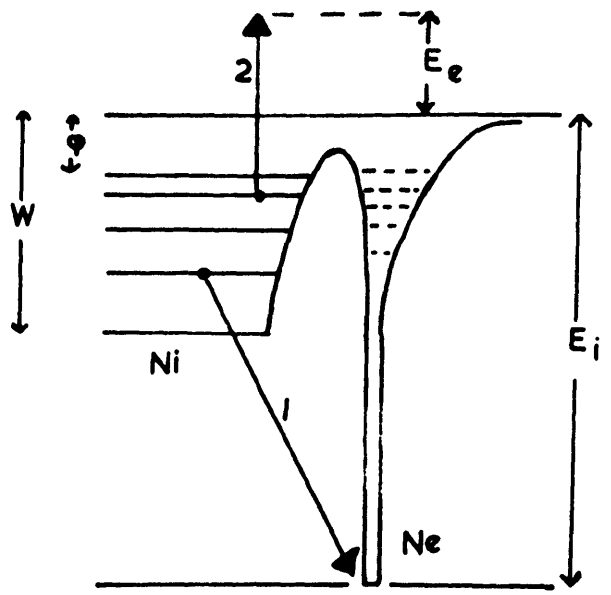

(c) DIRECT AUGER NEUTRALIZATION

1.13. EMISSION OF ELECTRONS FROM METALS BY POSITIVE IONS

The secondary emission coefficient γ_i for ions incident on a surface is defined as the number of secondary electrons emitted from the surface per incident ion of a specified energy. For positive ions of low energy it is found that γ_i is almost independent of ion kinetic energy and depends only on the potential energy. Little (1956, p. 651) describes two alternative Auger processes in which two electrons are involved at the same time. The two stage process is illustrated in Fig. 3 (a and b) for the case of emission of an electron from nickel by a neon ion. The first stage is the resonance capture of an electron from the Fermi level of the metal by the ion, the electron going to an excited level which may be metastable (Fig. 3a). This is possible if $W > (E_i - E_{ex}) > \phi$ where

W is the maximum depth of the Fermi level in electron volts.

ϕ is the minimum depth or work function of the nickel.

E_i is the ionization energy of the neon in electron volts.

E_{ex} is the excitation energy of the neon in electron volts.

The second stage shown in Fig (3b) involves the ejection of this electron by the neon and at the same time the transfer of another electron from the Fermi level of the metal to the ground state of the neon. This is called Auger de-excitation. (For some excitation states the excited electron may decay to the ground state at the same time as an electron is emitted directly from the metal.) The energy of the electron released, E_e, lies in the range

$$E_{ex} - \phi \geq E_e \geq E_{ex} - W$$

The alternative single stage process described by Little

(illustrated in Fig. 3c) involves the simultaneous emission of two electrons from the metal, one being released and the other going to the ground state of the gas ion. In this case the energy of the released electron lies in the range

$$E_i - 2\phi > E_e \geq E_i - 2W.$$

In either case, the process is dependent on the work function and the maximum depth of the Fermi level of the metal, and also on the ionization energy of the ion. The two stage process also requires the existence of a suitable excitation level in the gas. Neither process depends on the kinetic energy of the ion. Recent experimental measurements of the electron emission from metals by rare gas ions of low kinetic energy have confirmed the operation of a potential emission process. (Hagstrum, 1954, Rakimov and Dzhurakulov 1964, Magnuson and Carlston 1963).

Under gas discharge conditions the situation may be complicated by the existence of several different species of ions. Single and double charged atomic and molecular ions will have different potential energies of ionization and therefore they will have different secondary emission coefficients. The proportion of each ion species will depend on the voltage and pressure conditions in the gap.

1.14. SECONDARY ELECTRON EMISSION BY EXCITED AND METASTABLE ATOMS AND MOLECULES

As previously mentioned, a metastable particle may liberate an electron at a collision with a solid boundary. If the excitation energy of the metastable particle is M electron volts, and the solid surface has a work function of ϕ electron volts, the ejected electron

energy E_e will be given by

$$E_e \leq M - \phi.$$

For the low energy metastable atomic states of helium and neon M has values of about 19.8 and 16.5 electron volts respectively. These metastable atoms would clearly be capable of releasing electrons from a nickel surface with work function between 3.96 and 5.24 electron volts (Weissler 1956, p. 347). The electrons are emitted from the metal by the secondary stage of the two stage Auger process described in the previous section (MacLennon 1966). In the present work a metastable neon atom arriving at the nickel cathode could cause the release of a secondary electron.

Since metastable atoms are uncharged, only about 20% of those formed in the gas will diffuse to the cathode and be capable of returning electrons into the discharge. However the yield or average number of electrons produced per incident metastable atom can be quite high,

e.g. 10^{-2} for Hg metastable atoms on Hg

0.24 for 2^3S He metastables on Pt

0.5 for 2^1S He metastables on Pt

0.4 for A metastables on Cs
(Weissler 1956, p. 84).

1.15. SUMMARY OF SECONDARY IONIZATION PROCESSES

The processes mentioned in this chapter which contribute to secondary ionization in a gas discharge can each be represented by an ionization coefficient which is the number of electrons contributed by that process per primary ionizing collision in the gas.

If several secondary processes are operating at the same time it can be shown that, to a good approximation, the secondary coefficients are additive and the total secondary ionization can be expressed by a generalized secondary ionization coefficient ω/α which is the sum of the individual coefficients. (Llewellyn Jones, 1957, p. 54). The spatial growth of current in the steady state can then be expressed by the equation

$$\frac{I}{I_o} = \frac{e^{\alpha d}}{1-\omega/\alpha(e^{\alpha d}-1)} \qquad (1)$$

where I is the current measured at the anode, I_o is the initial externally induced electron current at the cathode, d is the gap distance and α is the primary ionization coefficient. All the ionization coefficients, both primary and secondary, are functions of the electric field per unit pressure, E/p. Some of the secondary ionization coefficients may also be functions of pressure and gap distance.

1.16. THE SPARKING CRITERION AND THE PHYSICAL SIGNIFICANCE OF BREAKDOWN

If there is some secondary ionization in a gas discharge a graph plotted of $\log.(I/I_o)$ against the gap distance d for a given value of E/p will show some upcurving for large d values. If d is made sufficiently large the slope of this graph becomes infinite and the current I flowing through the gap is limited only by the external circuit. The physical significance of this phenomenon is that the current I in the gap is no longer a function of I_o the externally induced photocurrent at the cathode. In other words the current has

become self-maintained and will continue to flow even if the current I_o is reduced to zero. From equation (1) it will be seen that when this state is reached

$$1 - \omega/\alpha(e^{\alpha d}-1) = 0 \qquad (2)$$

This expression is known as Townsend's criterion for breakdown, and can be used to determine the generalized secondary coefficient ω/α where α is known.

1.17. DISTINGUISHING THE SECONDARY IONIZATION PROCESSES IN A GAS DISCHARGE

Consideration of the spatial growth of current for a gap which has reached equilibrium without breaking down does not provide a means of distinguishing which of the several possible secondary ionization processes are operating in the discharge. Measurement of the breakdown potential (V_s) and the generalized secondary ionization coefficient, ω/α, may provide some indirect information. For example the existence of a sharp peak in the curve of ω/α against E/p at low E/p values (less than 10 volts cm^{-1} $torr^{-1}$) can sometimes be attributed to photo-emission from the cathode. In some simple cases it is possible to relate the temporal growth of current as the discharge reaches the breakdown condition, to the life-times and transit times across the gap of the active particles. In this way it may be possible to estimate the importance of some of the secondary ionization processes. This approach has however three serious weaknesses. The theory required is complicated and necessarily involves a number of simplifying assumptions, all of which may not

be justified. The current growth is not always a sensitive function of the secondary ionization coefficients. If this is the case the information obtained about the secondary coefficients will be correspondingly inaccurate. The theory requires values of diffusion coefficients, drift velocities of ions and electrons, metastable lifetimes and primary ionization coefficient under the conditions of the experiment. The data may not always be available under conditions which are strictly comparable. The calculated current growth is a particularly sensitive function of the primary ionization coefficient α.

The various theories for the temporal growth of current at the beginning of a gas discharge will be considered in detail in Chapter II and III. One of the simplest methods of observing the temporal growth is to measure the 'time lag'. This time lag is the total time required for the formation of a self maintained discharge measured from the application of the voltage to the gap. The first part of the time lag is the time which elapses before primary current of electrons begins to flow from the cathode. This is called the 'statistical time lag' since it involves statistical events. The second part of the time lag is the time required for the primary current to lead to a self maintained discharge. This is called the 'formative time lag'. In practice the statistical time lag can be made very short by ensuring that the appearance of electrons in the gap is highly probable. This can be done, for example by irradiating the cathode with ultra-violet light. The measured total time lag is then equal to the formative time lag. The formative time lag can be predicted theoretically in certain simple cases by assuming values

for the secondary ionization coefficients which are thought to be operative. Comparison of these calculated time lags with the experimentally measured values for a number of values of the applied field can provide approximate values for the secondary coefficients provided agreement between theory and experiment can be found. This procedure, considered in detail in chapter 3, has been used in the present study of the secondary ionization processes involved in the onset of breakdown in low pressure neon under uniform field conditions.

CHAPTER II

A REVIEW OF PREVIOUS WORK

2.1. INTRODUCTION

This chapter contains a review of experimental and theoretical work relevant to the problem of evaluating the secondary mechanisms of the Townsend breakdown of neon. The neon atom has two low energy metastable levels, excitation to either of which requires less energy than ionization. Atoms in a metastable state will be present in a gas discharge initiated by emission of electrons from the cathode and have an important effect on the secondary ionization processes which lead to breakdown. The secondary electron current which results from processes involving metastable atoms can be observed by initiating a short burst of primary photoelectrons from the cathode. The metastable processes are much slower than the positive ion and undelayed photon processes, and can therefore be separated temporally.

The temporal growth of current resulting from the application of a step voltage to a gap constantly illuminated with ultra-violet light involves a more complicated theory but can still be related to the secondary ionization processes. In addition, optical absorption methods applied to recently excited gaps can be used to provide information about the lifetimes and decay processes of metastable atoms. The work will be described in order of historical development, the formative time lag theory of Davidson and its application to the rare gases helium and neon being considered separately in Chapter III.

The energy levels of the first two excited configurations of neon are shown in Fig. 1 in Chapter I (Dixon and Grant 1957). The first configuration consists of the $^1P_1$ singlet level of energy 16.7 electron volts, and the triplet levels $^3P_0$, $^3P_1$, and $^3P_2$ on the energies 16.62, 16.58 and 16.53 eV. The $^3P_0$ and $^3P_2$ levels are metastable because selection rules prohibit transition to the ground state.

2.2. THE LIFETIME OF NEON METASTABLE STATES

F.A. Grant used absorption of mohochromatic light of a suitable wavelength by excited neon gas to measure the lifetimes of the neon excited levels. (Grant 1950) He used neon purified by a potassium pool discharge to remove mercury vapour, the electrodes of the system were rigorously outgassed and the system used for the purified gas contained no stopcocks. Despite these precautions, a trace of argon remained in the gas. Grant found that the lifetime of the $^3P_2$ metastable state depended on the size of the absorption tube. The $^3P_2$ lifetime τ was related to the neon pressure P by the equation:

$$\frac{1}{\tau} = \frac{B}{P} + CP \qquad (3)$$

where B and C are constants for a given tube. Earlier theoretical treatment by Meissner and Graffunder (1927), Anderson (1930) and Zemansky (1929) gave the constant B as

$$\frac{23.2}{D^2} + \frac{\pi^2}{L}$$

where D and L are the diameter and length of the discharge tube.

Grant's results however showed widespread disagreement with this expression for B. The term CP had a predominant effect on the lifetime at high pressures, although it was thought that argon impurity could have been partly responsible for this term. The lines used for absorption were 6402, 5945, 6143, 6334 and 5882 Å. All these wavelengths excite atoms in the $^3P_2$ state to higher levels in the second configuration which may decay to the ground state via the $^3P_1$ or $^1P_1$ non-metastable levels. The density and lifetime of the $^3P_2$ metastable atoms can thus be calculated from the absorption of radiation of these wavelengths. Grant also observed long lifetimes for the $^1P_1$ and $^3P_1$ radiating levels. This was thought to be due to a resonance radiation process where photons from the decay of these states are quickly re-absorbed by ground state atoms.

An important contribution to the study of rare gases has been made by Phelps and Molnar using pulsed light beam techniques. In a theoretical paper published in 1951, Molnar calculated the form of the slow current build up for a Townsend discharge in a rare gas stimulated by a pulsed light beam. The form of the calculation is based on a previous paper by Engstrom & Huxford (1940). The metastable components of this current can be separated from the much faster effects resulting from the action of photons and ions. He considered two mechanisms: (1) emission of electrons from the cathode by metastable atoms, and (2) conversion of metastable atoms into radiating atoms with the consequent emission of a photon and photoelectric ejection of electrons at the cathode. Two further processes:
(3) collision of two metastable atoms to produce one atom in the ground state and one ion, and (4) collision of a metastable atom

with an electron to produce an ion and two electrons, were not included in the analysis because they are only of importance at high metastable density or high electron current density. The analysis based on (1) and (2) enabled the fundamental time constant τ_1 of the metastable decay to be calculated. It is this decay of metastable particles which gives rise to the slow component of the current following a pulse of light. This slow component could be described by a single exponential plus a second term of higher time constant but much smaller amplitude. Experimentally, values for the time constant τ_1 could be obtained from the form of the current growth. Comparison with the calculated values over a range of gap distance and pressure made it possible to calculate the diffusion constant and the volume destruction probability of the metastable atoms.

In a paper published concurrently (Nolnar 1951 (2)) Nolnar applied this method to experimental results for argon and neon. The experimental method was similar to that used in earlier work by Engstrom and Huxford (1940). The results for argon cover an E/p range from 50 to 200 volts cm^{-1} $torr^{-1}$. The gas was purified by Batalum getters and liquid nitrogen traps. The operation of a cataphoresis discharge had little beneficial effect. The fundamental time constant τ_1, was calculated from the current growth of the slow component. A graph of $\frac{1}{\tau_1}$ against π^2/x^2, where x was the anode-cathode gap, enabled the metastable diffusion coefficient D_m and G, the probability of volume destruction of the metastable states per second, to be obtained from the equation

$$\frac{1}{\tau_1} = \left(\frac{\pi^2 D_m}{x^2}\right) + G$$

FIG. 4 GRAPH OF $\frac{1}{\tau_1}$ AS A FUNCTION OF $\frac{\pi^2}{X^2}$ FOR ARGON METASTABLE ATOMS IN ARGON.

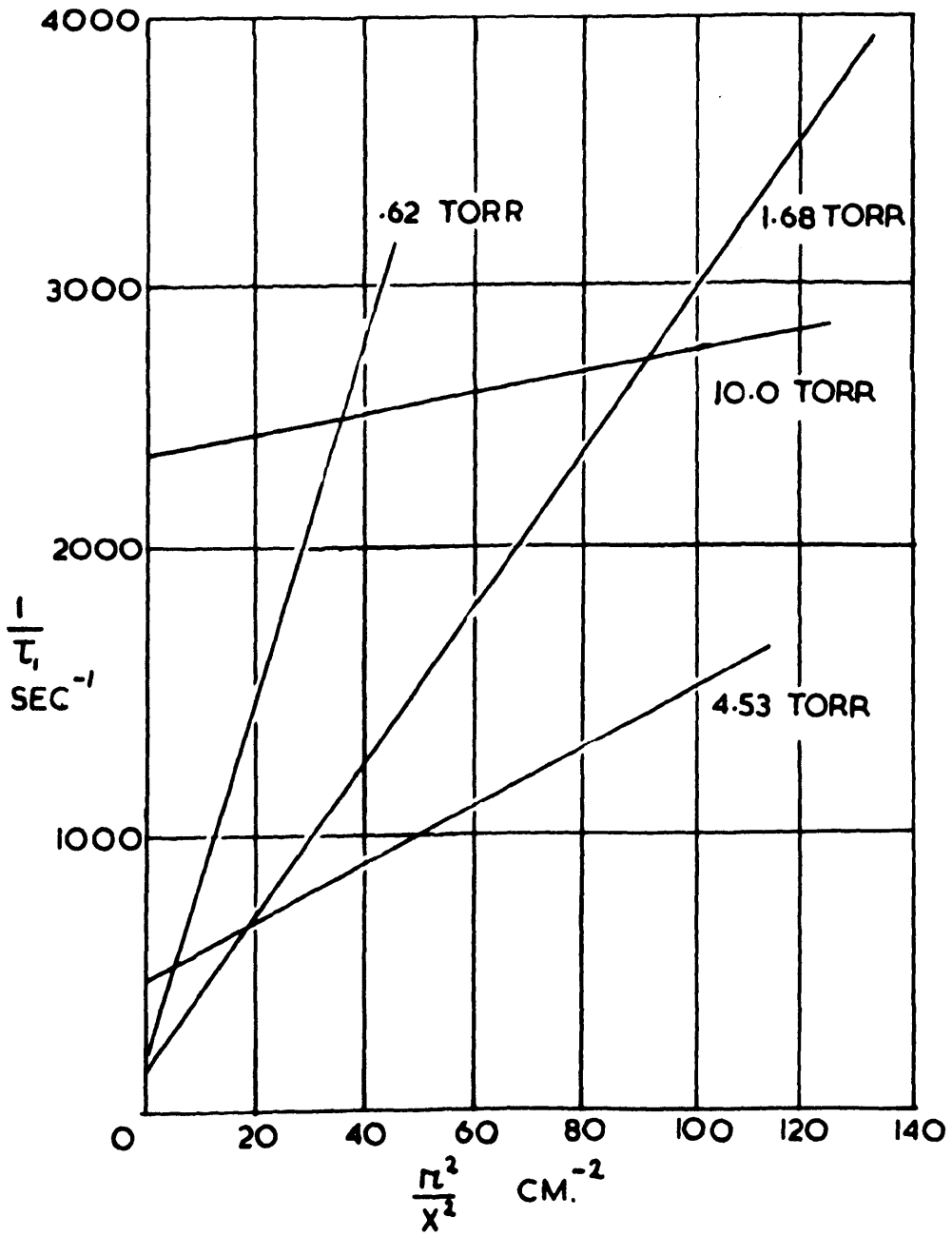

The argon results showed that D_m varied inversely with pressure as expected. For a given pressure, results obtained using different electrodes fell on the same straight line giving values for D_m and G which were independent of electrode material. Fig. (4) shows some of these results for argon. The diffusion coefficient for argon metastable atoms was found to be 45 ± 4 cm^2 sec^{-1} for a pressure of 1 torr at 25°C. The diffusion coefficient for the neon metastable states was 120 ± 10 cm^2 sec^{-1} at the same pressure and temperature. The probability of volume destruction, G, was found to be 80 sec^{-1} at 1 torr for argon metastable atoms corresponding to an argon metastable lifetime of 2×10^5 impacts with normal atoms. The probability of volume destruction for neon metastable atoms at 20 torr and a gap of .5 cm was 870 sec^{-1}.

By introducing suitable radiation, the metastable atoms can be excited into higher radiating levels which may decay (1) back to metastable levels, or (2) to other lower radiating states. If (1) occurs there is no net change in the metastable density. If (2) occurs it results in radiation of a photon whose energy is very nearly the same as that of the metastable level because of the closeness of the $3p^5 4s$ levels in argon. Molnar used this method to compare the efficiencies of metastable atoms and photons of about the same energy for emission of electrons from the cathode. He found that the metastable atoms were considerably more efficient.

This approach used by Molnar has the advantage of physical, if not mathematical simplicity. It does however ignore many possible mechanisms for loss and decay of metastable states. For example, measurements and calculations by Biondi (1952) in the afterglow of

helium and neon mixtures following a pulsed discharge suggested that the Schade and Büttner reaction (Schade 1937, 1938; Büttner 1939) produced significant ionization. In this reaction two metastable atoms interact to form one ion and one ground state atom,

e.g. $Ne^* + Ne^* \longrightarrow Ne + Ne^+ + e^-$

This is possible because $2E_{met} > E_i$, where E_i is the ionization energy and E_{met} the excitation energy of the metastable atom. However, this process was not observed by later workers (e.g. Phelps and Molnar 1953, Dixon and Grant 1957, Phelps 1959). Molnar's theory is extended in a later paper (Phelps and Molnar 1953). The processes considered in this paper by which metastable gas atoms can be lost are as follows:

(1) Diffusion to the walls and de-excitation.

(2) Two body collisions with neutral atoms resulting in (a) excitation to a nearby higher radiating state, (b) de-excitation to a lower state (this of course only applies to the higher metastable states which have greater energy than a radiating state), (c) formation of unstable diatomic molecules which may radiate before dissociation occurs (collision induced radiation).

(3) Three body collisions with two neutral atoms resulting in the formation of a stable excited molecule.

(4) Collisions between pairs of metastable atoms resulting in the ionization of one of them and de-excitation of the other. Process 2(a) is possible for neon and argon because the energy gap between the lowest metastable state $^3P_2$ and the higher $^3P_1$ radiating state is less than $\frac{1}{10}$eV and this is comparable with the thermal energy

FIG 5. $\frac{1}{\tau}$ AS A FUNCTION OF PRESSURE FOR THE NEON $^3P_2$ METASTABLE STATE AT 77°K AND 300°K.

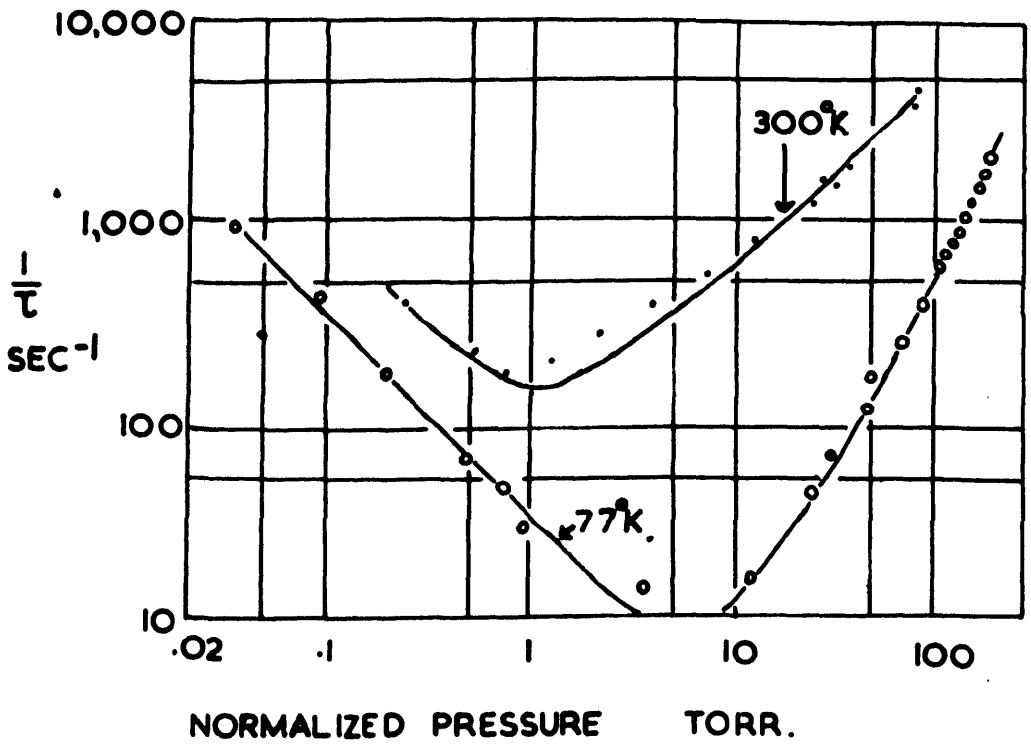

of the neutral atom. The process is not possible in helium because the energy gap is too large.

Using a similar approach to the simpler theory, an expression is derived for the fundamental time constant of the exponential decay of the metastable density resulting from a pulse of ultra-violet radiation directed on to the cathode. (The decay is exponential if the metastable density is not too large). This expression is:

$$\frac{1}{\tau} = \frac{D_o}{p\Omega^2} + Ap + Bp^2 \qquad (4)$$

where Ω is the diffusion length given by

$$\Omega = \left[\left(\frac{\pi}{L}\right)^2 + (2.4/R)^2\right]^{-\frac{1}{2}}$$

for a cylindrical vessel of length L and radius R. D_o is the metastable diffusion coefficient at 1 torr pressure. A is the frequency of destruction by two body collisions (process 2); B is the frequency of destruction by three-body collisions (process 3). p is the pressure in torr. A process of curve fitting for an experimental graph of $\frac{1}{\tau}$ against p enabled D_o, A and B to be evaluated.

The results obtained from the absorption of the 6143Å line by the lower neon metastable level ($^3P_2$) are shown in Fig. 5. The $^3P_2$ neon metastable atoms, for a temperature of 300°K were lost mainly by diffusion at the lower pressures and by destruction at two body collisions at the higher pressures used. De-excitation of the metastable atoms to a lower radiating state (process 2b) is not possible for the $^3P_2$ metastable level. At a temperature of 77°K it was found that the $^3P_2$ metastable loss processes were diffusion at

FIG.6 VARIATION OF THE MEAN LIFETIME OF THE $^3P_2$ NEON LEVEL WITH PRESSURE.

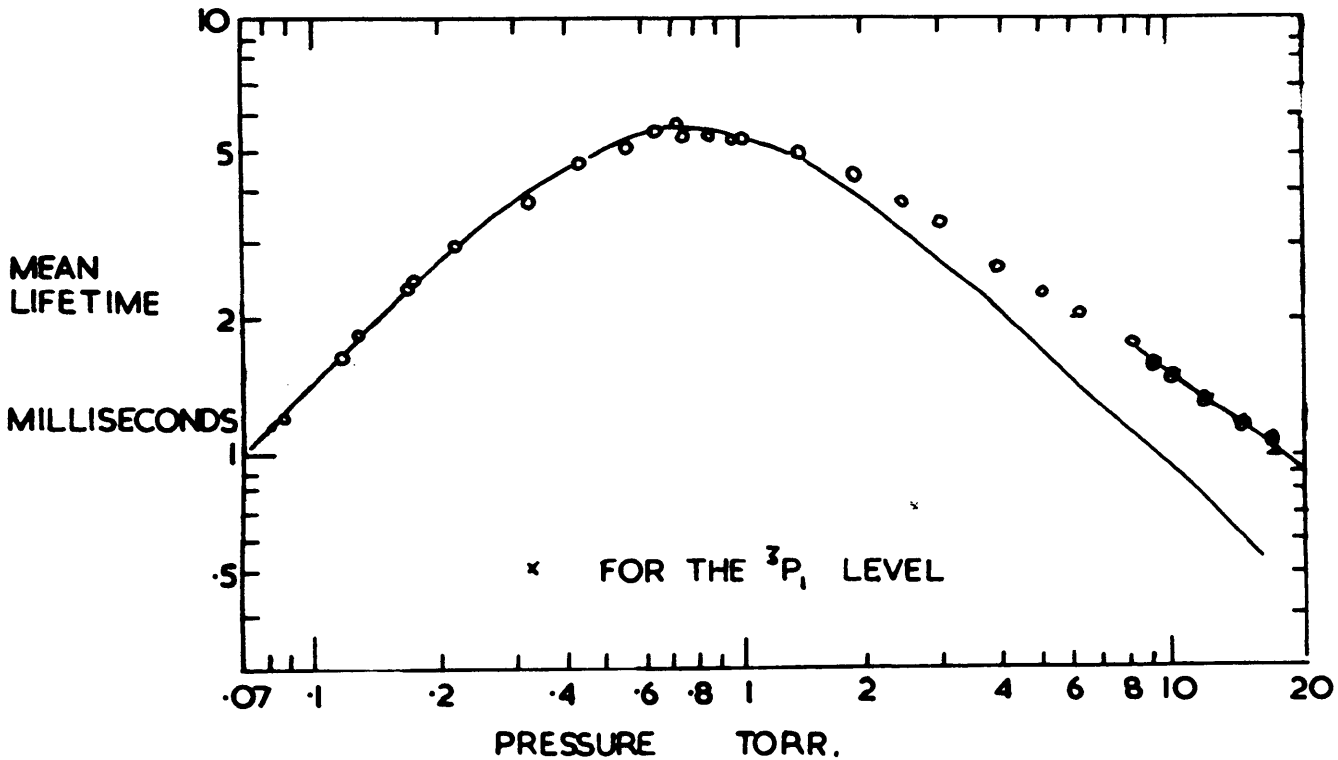

lower pressures and destruction at three-body collisions at the higher pressures. The average diffusion coefficients found from these results were 150 cm^2 sec^{-1} at 300°K and 60 cm^2 sec^{-1} at 77°K. There is, however, some departure between the experimental and theoretical $\frac{1}{\tau}$ values at intermediate pressure, as can be seen from Fig. 5.

In a paper published in 1957 Dixon and Grant used the optical absorption method for investigation of the decay in the afterglow of neon metastable atoms.

The neon metastable loss processes considered were:

(1) Diffusion and de-excitation at the walls.

(2) Emission of forbidden radiation.

(3) Radiation resulting from two-body collisions.

(4) Transition to radiating levels by two-body collisions.

(5) Ionization of impurities with ionization energy lower than the neon metastable excitation energy. (The Penning effect).

(6) Formation of metastable molecules by three-body collisions.

(7) Metastable collisions with ions.

(8) Metastable-metastable collisions producing an ion.

In this work processes (2), (5), (6) and (8) were not observed. There was no evidence to show that the three-body collison process occurred at 300°K. This agrees with results of Phelps and Molnar (1953) where the three-body process was only apparent at low temperature.

FIG.7 VARIATION OF THE MEAN LIFETIME OF THE $^3P_0$ NEON LEVEL WITH PRESSURE

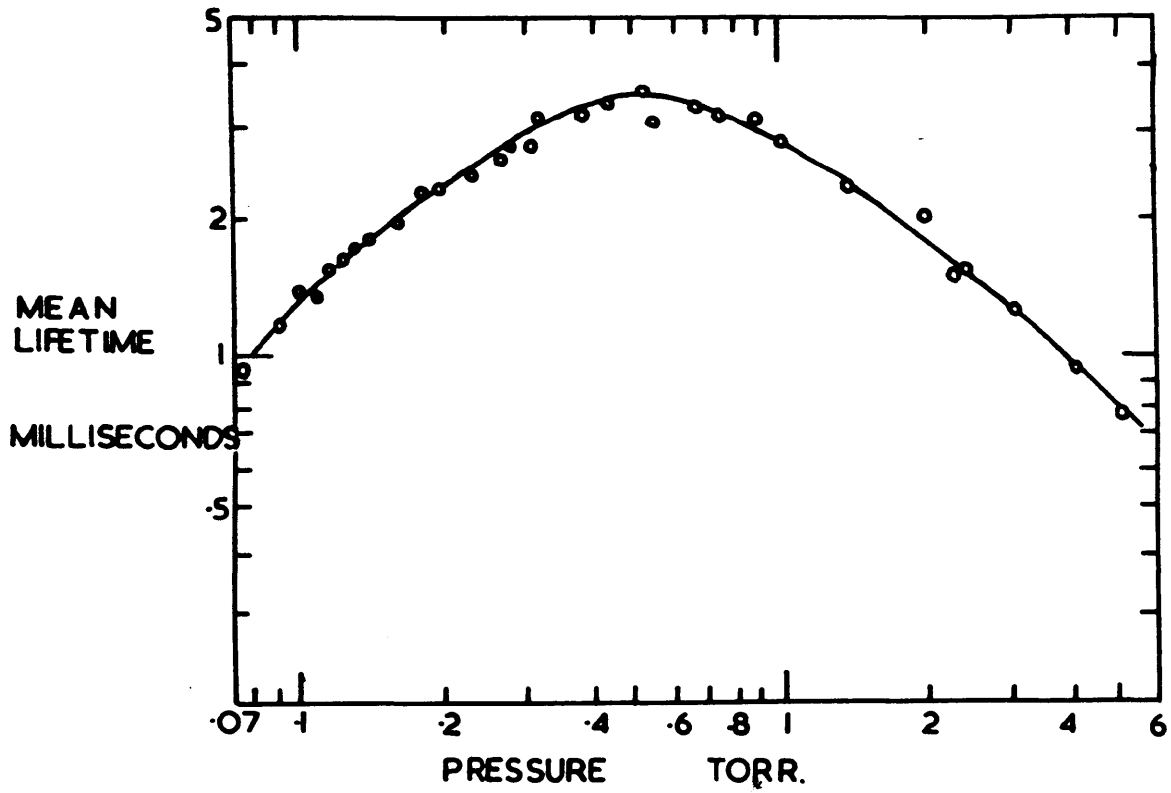

The mean lifetime measurements for the $^3P_1$ and $^3P_2$ neon levels as a function of pressure are shown in Fig. (6). The $^3P_1$ and the $^3P_2$ values fall on the same curve, and over a pressure range from 9 to 17 torr the lifetimes were the same within the limits of experimental error. This implies that the $^3P_1$ radiating level is filled from the $^3P_2$ metastable level, and therefore governed by the lifetime of the $^3P_2$ level. The solid curve was obtained by using the formula

$$\frac{1}{\tau} = \frac{D_1}{\Omega^2 p} + Ap \qquad (6)$$

where D_1 is the diffusion coefficient of the $^3P_2$ level, Ω the diffusion length given by equation (5). A is the frequency of two-body quenching collisions per unit pressure. Equation (6) is identical with the equation (4) used by Phelps and Molnar (1953), if B, the three-body process destruction frequency, is put equal to zero.

The value of D_1 used to give this curve was 170 cm^2 torr sec^{-1}. It can be seen that this equation describes the experimental results reasonably well, except at the higher pressures. Dixon and Grant state that the short straight line on the right of the graph was obtained by allowing for resonance radiation using an approach due to Phelps (1955). It is not explained in either paper how this curve is arrived at.

Fig. (7) shows the lifetime of the $^3P_0$ metastable neon states obtained by Dixon and Grant using absorption of the 6266Å line. At the lower pressures, where diffusion is the predominant loss mechanism, the lifetimes for the $^3P_0$ and $^3P_2$ states fall approximately

FIG 8. DIFFUSION COEFFICIENT AT UNIT GAS DENSITY OF $^3P_2$ NEON ATOMS AS A FUNCTION OF TEMPERATURE.

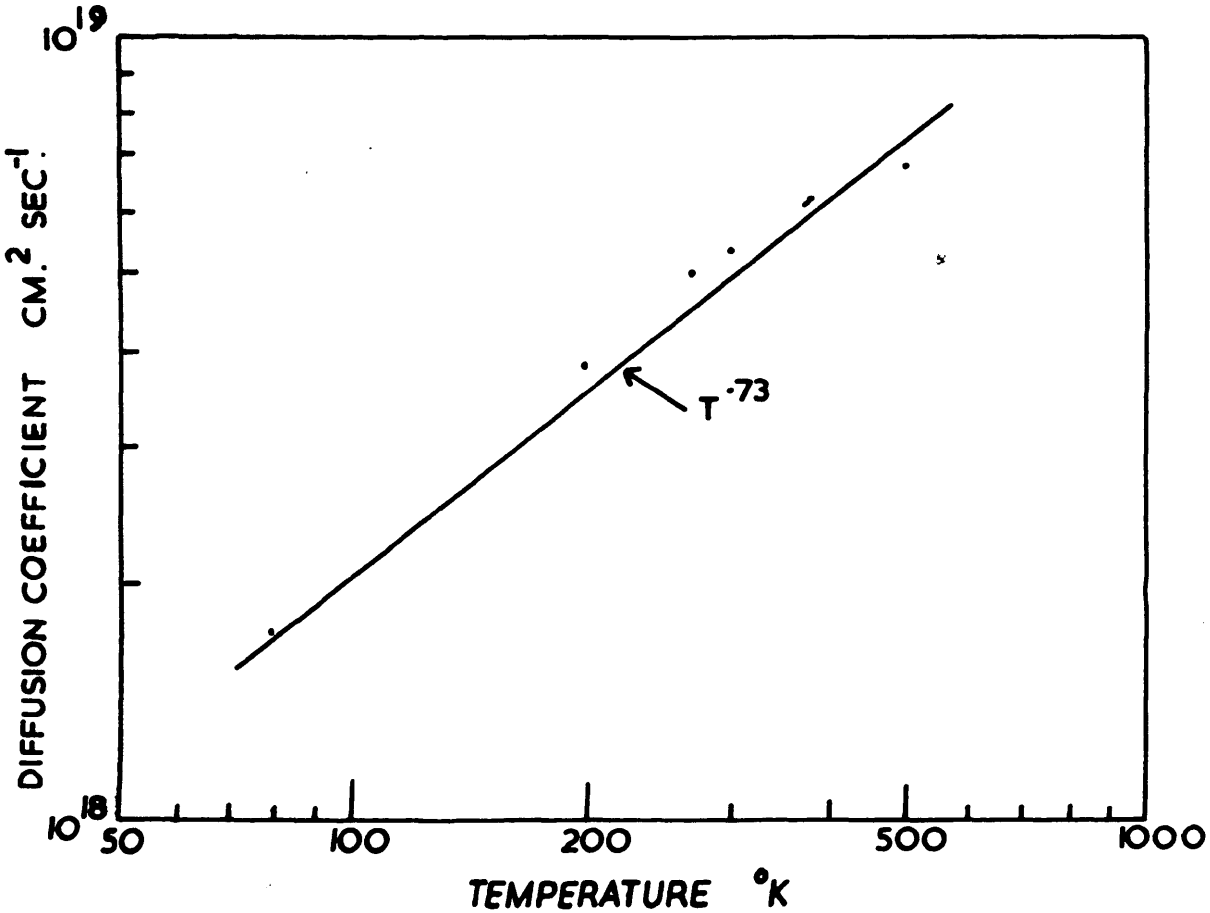

on the same curve. This implies that the two types of atom have the same diffusion coefficient (equation 6). The ^3P_o lifetimes are however shorter at the higher pressures. The theoretical curve shown on Fig. 7 was obtained by using equation 6 with the same value for D_1 as used for the $^3P_2$ case, but with a larger value for the destruction frequency.

The optical absorption method has been used by Phelps (1959) to measure the lifetimes of neon excitation states in the afterglow, the theory being extended to include the imprisonment of resonance radiation. The results show that the $^3P_2$ metastable atomic state is destroyed by:

(1) Diffusion to the walls.

(2) Two-body collisions involving a ground state neon atom which causes the $^3P_2$ state to be excited to the $^3P_1$ radiating state.

(3) Three-body collisions involving two ground state atoms.

The $^3P_1$ states are destroyed by:

(1) Two-body collisional de-excitation to the $^3P_2$ metastable state.

(2) Escape of the imprisoned resonance radiation.

The ^3P_o metastable states are destroyed by:

(1) Diffusion to the walls.

(2) Two-body collisional de-excitation to the $^3P_1$ or $^3P_2$ states.

The ^3P_o states may also be produced by collisional excitation of the $^3P_2$ and $^3P_1$ states. It was found that the $^1P_1$ state played no significant part in the decay of the $^3P_2$, $^3P_1$ or ^3P_o states. (This agrees with the findings of Dixon and Grant in 1957). The diffusion coefficients of the two metastable states were found to be

FIG. 9 PREDICTED GROWTH CONSTANTS AS FUNCTIONS OF APPLIED VOLTAGE FOR HELIUM.

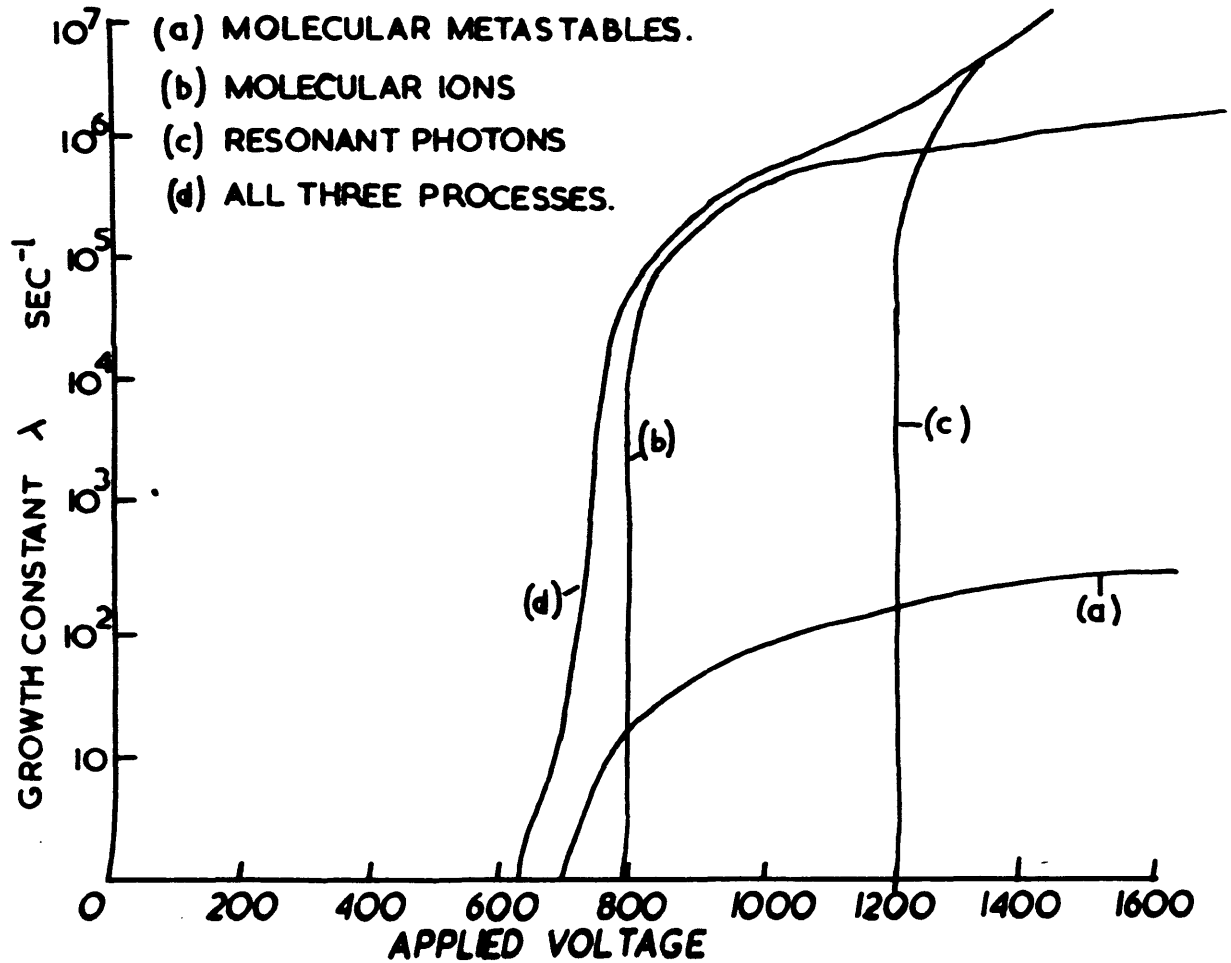

equal, and in agreement with those of Dixon and Grant. Fig. 8 shows Phelps' results for the metastable diffusion coefficient as a function of temperature.

2.3. PHELPS' THEORY OF CURRENT BUILD-UP

Phelps has further extended his theory to include the effects of molecular ions, molecular metastable particles and non-resonance radiation and used it to calculate the build-up of current preceeding the Townsend breakdown of a rare gas. (Phelps 1960). A parallel plane electrode system is considered and the rates of arrival at the cathode calculated for atomic and molecular ions, atomic and molecular metastable particles and resonance and non-resonance photons. For this theory it was assumed that the electron current increased exponentially with time, although Phelps pointed out that this is not strictly true in the initial stages of the current build-up because of the discrete nature of the electron. The Holstein-Biberman theory for the imprisonment of resonance radiation was used to find the spatial distribution and the rate of arrival at the cathode of the resonance radiation. (Holstein 1947, Biberman 1947, Biberman and Gurevich 1950). This avoids the inaccuracies which are introduced if the passage of resonance radiation through the gap is treated as a diffusion process. The molecular ions are considered to be formed by two or three-body interactions between excited and ground state atoms. Phelps applied this theory to the case of current growth in helium for which the required data is available. The growth constant λ of the exponential pre-breakdown current was calculated from the theory as a function of the amplitude of the applied voltage pulse. Fig. (9) shows the predicted growth constant as a function

FIG. 10. THE FRACTION OF THE CATHODE CURRENT CONTRIBUTED BY THE VARIOUS SECONDARY PROCESSES AS A FUNCTION OF THE GROWTH CONSTANT.

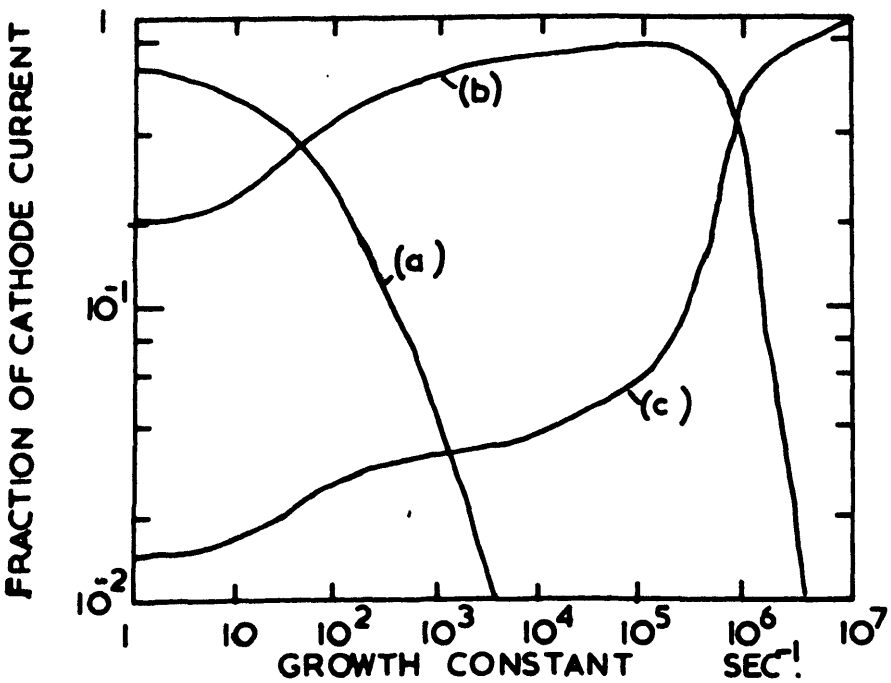

(a) MOLECULAR METASTABLES

(b) MOLECULAR IONS

(c) RESONANT PHOTONS

of applied voltage for helium at 300°K and 100 torr for a number of possible secondary ionization processes. The secondary electron current at the cathode is assumed to be due to the arrival of (a) diatomic metastable helium molecules, (b) diatomic helium ions, (c) resonance photons, and (d) all three processes together. Fig. (10) shows the calculated fractions of the cathode current resulting from each process as a function of the growth constant. These results show that for low time constants (slow current growth) the diatomic metastable molecules provide the main contribution to the slow components of the current. At intermediate λ the molecular ions dominate and at large λ the resonance radiation process is most important. The threshold voltages for the appearance of each process is shown in Fig. (9).

This approach to the problem of pre-breakdown currents is at present limited to the case of helium because of the availability of the data required. Phelps considers that the existence of four closely spaced metastable and resonance levels in neon and argon would lead to a more complicated situation than for helium. This theory does not take into account faster ionization processes such as electron emission from the cathode by atomic positive ions and undelayed photons. These processes can never-the-less have an important effect on the Townsend breakdown even though slower metastable effects are present.

2.4. MOLECULAR IONS

Mass spectrometer measurements by Arnot and M'Ewan (1938, 1939)

suggested that the ion He_2^+ could be produced by a collision between a low energy excited helium atom (e.g. the metastable state at 19.8 eV) and a neutral atom. However, more recent measurements by Hornbeck and Molnar (1951) have shown that the appearance potential is too high for this. It is thought that the molecular ions are produced by excitation of a helium atom to a high energy non-metastable state by electron impact. The molecular ion is produced by impact between this excited atom and a ground state atom, i.e.

$$He + e + K.E. \longrightarrow He^* + e$$

$$He^* + He \longrightarrow He_2^+ + e.$$

Similar processes led to the formation of Kr_2^+, Xe_2^+, Ne_2^+ and A_2^+. The appearance potentials measured were $23.18 \begin{smallmatrix} +.2 \\ -.7 \end{smallmatrix}$ volts for He_2^+ and $20.86 \begin{smallmatrix} +.3 \\ -.7 \end{smallmatrix}$ for Ne_2^+. Thus the $^3P_0$ and $^3P_2$ metastable states of neon would not have sufficient energy for the formation of molecular ions, although they could be produced by a high energy non-metastable excitation state.

2.5. METASTABLE MOLECULES

Colli (1954) observed ultra-violet radiation from avalanches in a couter tube containing argon at pressures from 70 to 650 torr. This radiation was thought to result from the destruction of metastable atomic states. The lifetime of these states, determined

from the temporal variation of the radiation, was found to be inversely proportional to the square of the argon pressure implying a three body destruction process for the pressure range used. The hypothesis suggested by Colli was that the $^3P_2$ argon metastable atom was destroyed in a three body collision involving two ground state atoms to give a diatomic metastable molecule, one ground state atom and a photon in the ultra-violet region

$$A^* + A + A \rightarrow A_2^* + A.$$

This process would however be much less important at lower pressures. A similar process could occur for neon at high pressures.

2.6. McCLURE'S THEORY FOR THE TOWNSEND BREAKDOWN OF NEON

The temporal growth of current for the Townsend breakdown of neon has been measured by McClure (1962). A step voltage was applied to a plane parallel electrode system with variable gap distance where the cathode was continuously illuminated with ultra-violet radiation. The voltages used were slightly greater than the voltage required for breakdown (i.e. overvoltages up to about 1%). All results were for a neon pressure of 40 torr. An electrical circuit was used directly to measure the time constant θ of the growth of current in the gap at breakdown. McClure attempted to explain the variation of θ with gap voltage by a theory where it was assumed that only two secondary ionization processes were concerned in the breakdown. These were the emission of secondary electrons

from the cathode resulting from the arrival of positive ions and metastable atoms. An explicit expression for the time constant θ was obtained by using a return function $L(V,t)$. An electron leaving the cathode at time $t = 0$, with a gap voltage of V volts, causes an average $L(V,t)dt$ secondary electrons to leave the cathode during the interval $(t, t + dt)$. However it was found that the experimental values of θ exceeded the calculated ones by about 15%. Thus it was concluded that the breakdown could not be explained by the action of positive ions and metastable atoms at the cathode and that some other process was required. The Townsend breakdown of helium has been examined by D.K. Davies (1963) using Davidson's formative time lag theory. This will be discussed in chapter III, but it is of interest to note here that a conclusion similar to McClure's was reached.

2.7. CONCLUSION

In recent years the mechanisms by which metastable atoms of rare gases are destroyed have been extensively studied and the processes are now reasonably well understood. The work of Phelps and Molnar has been particularly valuable. At pressures of a few torr the predominant loss of neon metastable atoms is by diffusion. At higher pressures (20 to 50 torr) destruction of metastable atoms at two body collisions involving gas atoms becomes important. This

experimental work has provided values of the meanlife time of metastable atoms as a function of pressure and geometry, and also values of the diffusion coefficient of the metastable atoms as a function of pressure. This data is required for formative time lag calculations.

The extensive analysis by Phelps of the slow component of current resulting from a pulse of electrons is at present limited to helium. A study of the Townsend breakdown by McClure has shown that breakdown cannot be explained by the action of positive ions and metastable atoms at the cathode. Davidson's formative time lag theory provides an analysis of the Townsend breakdown which is more complete and more rigorous than McClure's simple approach. This theory, and its application to the rare gases helium and neon, will be considered in the next chapter.

CHAPTER III

DAVIDSON'S THEORY FOR THE TEMPORAL GROWTH OF CURRENT

3.1. INTRODUCTION

Formative time lags in the Townsend breakdown of low pressure gases under uniform electric field have been studied at the University College of Swansea for a number of years. A temporal growth theory developed by Davidson enables the experimentally measured formative time lags to be related to the secondary ionization processes which lead to the electrical breakdown of the gap. The theory enables the formative time lag to be calculated if the secondary ionization coefficients are known. The usual procedure therefore is to assume values for the coefficients, calculate the theoretical formative time lag, and compare it with the experimental value. The coefficients are adjusted until agreement is found between the theoretical and experimental formative time lags. In this way the importance of various secondary ionization processes can be estimated. A particularly simple case is the Townsend breakdown of low pressure hydrogen where only two secondary ionization processes are of importance. These processes are emission of electrons from the cathode resulting from the impact of photons and positive ions. The theory developed by Davidson (Dutton et al. 1953) will be outlined here since it forms the basis for the more complex theory used for the breakdown of the rare gases.

3.2. DAVIDSON'S THEORY FOR HYDROGEN

In a uniform field gap between two electrodes the steady state pre-breakdown current I is given by Townsend's formula

$$I = \frac{I_o \exp(\alpha d)}{1 - {}^{\omega}/_{\alpha}(\exp(\alpha d) - 1)}$$

where I_o is the current of electrons generated at the cathode by external means, and d is the gap distance; α is the primary ionization coefficient for electrons, and ${}^{\omega}/_{\alpha}$ is the generalized secondary ionization coefficient which includes contributions from the two operative processes. If ${}^{\delta}/_{\alpha}$ is the coefficient for the emission of electrons from the cathode by photons generated in the discharge, and γ the coefficient for emission of electrons from the cathode by positive ions formed in the discharge, then, for hydrogen ${}^{\omega}/_{\alpha} = {}^{\delta}/_{\alpha} + \gamma$.

In the non steady state, when the applied voltage V exceeds the sparking voltage V_s, the rate of increase of current in the gap with time will depend on which of the two processes is the dominant one. Thus the measured formative time lag, which is the time required for the gap current to grow to a given value, will depend on the relative importance of the ion and photon processes.

The continuity equations for ions and electrons are:

$$\frac{\partial\left(\frac{I_-}{v_-}\right)}{\partial t} = -\frac{\partial I_-}{\partial x} + \alpha I_- \quad \text{for electrons} \qquad (7)$$

and

$$\frac{\partial\left(\frac{I_+}{v_+}\right)}{\partial t} = \frac{\partial I_+}{\partial x} + \alpha I_- \quad \text{for ions} \qquad (8)$$

where I_- is the electron current

I_+ the ion current

v_- the electron drift velocity

and v_+ is the ion drift velocity.

The distance from the cathode is x cm, and the time measured from the application of the voltage V is t secs. Bartholomeyczyck (1940) produced an approximate solution for these equations, but Von Gugelberg (1947) pointed out that Batholomeyczyck's solution ignored the current of electrons from the cathode induced by ultra-violet illumination. This omission has been allowed for in a modified solution by Davidson (Dutton et al. 1953). An exact form of this solution allows for the presence of an initial distribution of change particles in the gap at the time of application of the breakdown voltage (Davidson 1955). This is important in cases where continuous backing voltage is applied to the gap and a pre-breakdown current is already flowing when the voltage pulse, which leads to breakdown, is applied. However, this form is difficult to apply in practice because of the lengthy calculations involved. The approximate form of Davidson's solution outlined below can be applied where there are no charged particles present in the gap at t = 0, or if particles are present it can be

applied with a small error.

The electron current I_- flowing at time t at the cathode ($x = 0$) is given by the equation:

$$I_-(0,t) = \frac{I_o(1 - \exp\lambda t)}{1 - (\gamma + \delta/\alpha)(\exp\alpha d - 1)} \qquad (9)$$

where I_o is the externally induced current at the cathode. The value of λ is calculated by solving the equation:

$$F(\lambda) = 1 - \frac{(\gamma\alpha)}{\phi}(e^{\phi x} - 1) - \frac{\delta}{\psi}(e^{\psi x} - 1) \qquad (10)$$

for $F(d) = 0$

where $$\phi = \alpha - \frac{\lambda}{v} \qquad (11)$$

$$\psi = \alpha - \mu - \frac{\lambda}{v_-} \qquad (12)$$

$$\frac{1}{v} = \frac{1}{v_-} + \frac{1}{v_+} \qquad (13)$$

v_- is the electron drift velocity in cm. sec^{-1}.

v_+ is the positive ion drift velocity.

μ is the coefficient of photo-absorption in the gas.

γ is the secondary ionization coefficient for the release of electrons from the cathode by positive ions (expressed as the number of electrons released per primary ionizing collision in the gas).

δ/α is the secondary ionization coefficient for the release of electrons from the cathode by photons formed in the discharge (defined as the number of electrons emitted per primary ionizing collision in the gas).

The calculation of formative time lags is carried out as follows:

(1) The value of ω/α is calculated from the value of the sparking potential using the value of the primary ionization coefficient α for the value of the electric field per unit pressure E/p_o existing in the gap. (p_o is the pressure reduced to 0^oC).

(2) Values of γ and δ/α are chosen to satisfy

$$\gamma + \delta/\alpha = \omega/\alpha. \qquad (14)$$

(3) Equation (10) is now solved for λ; this is done in practice by calculating $F(d)$ for various values of λ until a value is found which satisfied $F(d) = 0$.

(4) Using this value of λ equation (9) is solved for t assuming suitable values for I_o and I_-. In the solution for λ and t, the relevant value of α is the value for the E/p_o which obtains as the chosen value of the overvoltage $\Delta V = V - V_s$. It is assumed that ω/α is the same at the sparking voltage as it is at the given overvoltage. This is approximately true for small values of overvoltage.

Repeating the above procedure for a number of low values of overvoltage, a curve showing the variation of formative time lag with overvoltage can be obtained for a given ratio of $\frac{\gamma'}{\delta/\alpha}$. A series of curves for various values of $\frac{\gamma'}{\delta/\alpha}$ can be obtained, and a process of curve fitting with the experimental results can give an estimate of the value of $\frac{\gamma'}{\delta/\alpha}$ under experimental conditions.

This solution has been successfully used by a number of workers for the use of hydrogen (Dutton et al. 1953, Gozna 1960, Betts 1963, Fulker 1963).

3.3. EXTENSION OF THE THEORY FOR RARE GASES (I)

Phelps' theory for the growth of the slow component of current in the Townsend breakdown of rare gases has been described in 2.3. This theory enabled the time constant of the current growth to be calculated. Measurements of the growth constant are required for interpretation of the theory. However, Phelps has pointed out (1960) that the current build-up will not be exactly exponential for very short times after the initiation of the discharge owing to the discrete nature of electron avalanches. The theory does not take into account the faster ionization processes which may also be present. The solution developed by Davidson for rare gas breakdown enables the current flowing in the gap to be calculated as a function of time for cases where the growth is not exponential.

This solution also includes the effects of faster processes involving positive ions and undelayed photons. The theory which will now be described includes the emission of electrons from the cathode by impact of metastable atoms produced in the gas discharge (Davidson 1958). It was suggested that this same theory could also be applied to the resonance radiation process (which does not involve a metastable state) since the photons move through the case by a process analagous to diffusion. However, it was pointed out by Phelps (1960) that the resonance radiation should obey the Holstein-Biberman theory and not diffusion laws. The parameter of the solution for resonance radiation derived from the Holstein-Biberman theory is independent of the gas density and varies only as the square root of the electrode separation. On the other hand the parameter of the diffusion theory is proportional to the density and to the square of the electrode separation.

The complete solution for the Holstein-Biberman resonance radiation theory is given in a later paper (Davidson 1962).

For the case of electron-emission from the cathode by metastable atoms formed in the gas discharge, the basic diffusion equation for a region of gas x cm. from the cathode is

$$\frac{\partial n(x,t)}{\partial t} = - \frac{\partial j(x,t)}{\partial x} + \alpha_1 e^{\alpha x} i_-\left(t - \frac{x}{w_-}\right) - \frac{n(x,t)}{\tau_1} \qquad (15)$$

(Davidson 1958)

$n(x,t)$ is the spatial density of active particles at a distance x from the cathode, at time t.

$j(x,t)$ is the current density in the x direction of active particles.

i_- is the electron current at the cathode.

w_- is the electron drift velocity.

α is the average number of electrons generated by an electron per centimetre path length in the direction of the field, (the primary ionization coefficient).

α_1 is the average number of active particles generated by an electron per centimetre path length in the direction of the field.

$\frac{1}{\tau_1}$ is the fraction of the active particles destroyed per unit time by collisions with unexcited atoms. It is assumed that destruction of metastable atoms by electrons can be ignored. For this reason the theory is not applicable for high current densities where the field would in any case be distorted by space change.

In the steady state the diffusion coefficient D for the metastable atoms or active particles will be given by

$$j = -D\frac{\partial n}{\partial x} \qquad (16)$$

Assuming that this also applies to the non-steady state we can write

$$-\frac{\partial j(x,t)}{\partial x} \text{ as } D\frac{\partial^2 n(x,t)}{\partial x^2} \qquad (17)$$

the diffusion equation then becomes:

$$\frac{\partial n(x,t)}{\partial t} = D \frac{\partial^2 n(x,t)}{\partial x^2} + \alpha_1 e^{\alpha x} i_-(t - \frac{x}{w_-}) - \frac{n(x,t)}{\tau_1} \qquad (18)$$

For metastable atoms the diffusion coefficient D can be written approximately at $\frac{1}{3} \ell.\bar{v}$ where ℓ is the mean free path and $\bar{v}$ the mean kinetic velocity.

Davidson gives the solution for current growth in two forms, one valid at all times and one valid for time t where $\frac{t}{T}$ is a small fraction, e.g. $\frac{1}{4}$, T being the active particle transit time. The transit time for a diffusion process is $\frac{x^2}{D} = \frac{3x^2}{\ell \bar{v}}$.
For example with a gap distance of .5 cm. and diffusion coefficient of 4 $cm.^2 sec^{-1}$ the transit time is about 10^{-1} sec.

The solution is written as a Laplace contour integral.
The boundary conditions are:

(i) at $t < 0$, $n(x,t) = i_-(t) = 0$;

(ii) at $t > 0$, $i_-(t) = I_o + g_1 D \frac{\partial n(x,t)}{\partial x}$ at $x = 0$.

[This follows from Fick's first law of diffusion which states that J, the current density of metastable atoms is given by $J = -D$ grad. n. g_1 is the secondary emission coefficient at the cathode for the metastable atoms.]

(iii) at $t > 0$ $n(0,t) = n(d,t) = 0$

[d being the electrode separation]

(iv) at $t > 0$ the differential equation (18) holds throughout the gas.

The solution of (i) - (iv) given by Davidson is as follows:

$$\frac{n(x,t)}{I_o} = \frac{i\alpha_1}{\pi D} \cdot \int_c \frac{Ze^{D(Z^2-\mu^2)t}}{(Z^2-\mu^2)\Theta} \left[(1 - e^{-2Zd})e^{\psi x} + (e^{(\psi-Z)d} - 1)e^{-Zx} + (e^{-2Zd} - e^{(\psi-Z)d})e^{xZ} \right] dZ \tag{19}$$

$$\frac{i_-(t)}{I_o} = \frac{i}{\pi} \int_c \frac{Ze^{D(Z^2-\mu^2)t}(Z^2-\psi^2)(1-e^{-2Zd})dZ}{(Z^2-\mu^2)\Theta} \tag{20}$$

where $\psi = \alpha - \frac{D(Z^2-\mu^2)}{w_-}$ (21)

$$\Theta = \xi + 2\delta_1 Ze^{(\psi-Z)d} - (2\delta_1 Z + \xi)e^{-2Zd} \tag{22}$$

$$\xi = \{Z+\psi\}\{(Z-\psi)F - \delta_1\} \tag{23}$$

$F = 1$

$\delta_1 = g_1\alpha_1$ (Thus $\frac{\delta_1}{\alpha}$ is the secondary ionization coefficient for the metastable process more usually denoted by ϵ/α).

$\mu = \frac{1}{\sqrt{D\tau_1}}$ For the metastable process, where the active particles are assumed to be destroyed only at the cathode, μ becomes infinitesimal because $\frac{1}{\tau_1} \to 0$.

However, experimental measurements discussed in the previous chapter have shown that this assumption is only valid for low pressures. The function F, given equal to 1 here, provides for later generalization to allow for the contribution to ionization by positive ions and undelayed.photons. The contour c is a quarter of an infinite circle with its centre at the origin traversed clockwise, the centre of the arc being the positive real axis. Calculation of the current ratio $\frac{i_-}{I_o}$ requires solution of equation (22) for Z. In general there are an infinite number of complex solutions. The contour c may be deformed and the integral can be expressed as a series. For the case where the time t is small compared with the metastable transit time T, (e.g. for $t \ll 10^{-1}$ sec.) the expression $i_-(t - \frac{x}{w_-})$ may be replaced by $i_-(t)$ and Ψ may be replaced by α. The contour c of equation (20) can be deformed to form a semi-circle to the right of the imaginary axis. This integral can be expressed as $\frac{1}{2}$ the integral round an infinite circle since the integrand of (20) is an odd function of Z. By considering residues at the poles Davidson showed that

$$\frac{i_-}{I_o} = R\left[A + \sum \frac{2f\gamma(\lambda^2-\psi^2)(1-e^{-2\lambda d})e^{D(\lambda^2-\mu^2)t}}{(\lambda^2-\mu^2)\left(\frac{\partial\theta}{\partial Z}\right)_\lambda}\right] \quad (24)$$

f is a factor which is unity for the poles on the axes and 2 for poles elsewhere. The summation extends over all values λ of Z other than 0 and ψ which satisfy $\Theta(Z) = 0$. The expression for $\frac{i_-}{I_o}$ can in practice be evaluated since it is possible to show that only one real λ value need be considered for a good approximation.

The effect of positive ions and unscattered photons causing emission of electrons from the cathode can be included by replacing F by the expression:

$$1 - (\delta/\psi)(e^{\psi d} - 1) - (\alpha\gamma/\phi)(e^{\phi d} - 1) \qquad (25)$$

where $\phi = \alpha - \frac{D(Z^2 - \mu^2)}{w}$ and $\frac{1}{w} = \frac{1}{w_-} + \frac{1}{w_+}$.

The term A in equation (24) has the value $\frac{1}{1 - \omega/\alpha(e^{\alpha d} - 1)}$

The above temporal growth theory, has been applied to the case of helium by D.K. Davies et al. (1963) with little success as will be described in section 3.4. The theory was also used by the author in an attempt to describe experimental current growth in neon, but again the theory met with no success. The application of the theory to a practical case will now be described.

The expression 22) for Θ has one real solution for λ and an infinite number of imaginary ones. None of the λ's are complex since F is real, so that f is 1. In practice the

imaginary solutions can be neglected in comparison with the real solution. (D.K. Davies, 1961). Thus the complete solution is as follows:

$$\frac{i\_(0,t)}{I_o} = \frac{1}{1-\omega/\alpha(e^{\alpha d}-1)} + \frac{2(\lambda^2-\alpha^2)(1-e^{-2\lambda d})e^{D\lambda^2 t}}{\lambda\left(\frac{\partial\theta}{\partial Z}\right)_\lambda} \qquad (26)$$

(Putting $f = 1$, $\mu = 0$)

By differentiating equation (22):

$$\left(\frac{\partial\theta}{\partial Z}\right)_\lambda = 2\lambda F - \Gamma - 2\Gamma(\lambda d - 1)e^{(\alpha-\lambda)d} \qquad (27)$$

$$-e^{-2\lambda d}\left\{2Fd(\alpha^2 - \lambda^2) + 2d\Gamma(\alpha - \lambda) + 2\lambda F + \Gamma\right\}$$

$$F = 1 - (\gamma + \delta/\alpha)(e^{\alpha d} - 1) \qquad (28)$$

where λ is the real value satisfying $\theta(Z) = 0$

$$\text{where } \theta(Z) = (\alpha - Z)\left\{(\alpha + Z)F + \Gamma\right\}e^{-2Zd} + 2\Gamma Z e^{(\alpha-Z)d} \qquad (29)$$

$$-(\alpha + Z)\left\{(\alpha - Z)F + \Gamma\right\} = 0$$

$$\text{and } \Gamma = \frac{\mathcal{E}/\alpha(\alpha^2 d)(e^{\alpha d}-1)}{(e^{\alpha d} - \alpha d - 1)} \qquad (30)$$

The main assumptions applicable to this modified solution are given below.

(i) There is negligible destruction of diffusing metastable atoms in the gas.

(ii) The electron and ion transit times $\frac{d}{w_-}$ and $\frac{d}{w_+}$ may be regarded as infinitely small compared with t, the time at which it is required to calculate the ratio $\frac{i_-(0,t)}{I_o}$.

(iii) All the contributions to the current arising from the imaginary roots may be neglected.

The procedure for calculating the formative time lag t, or the time required for the current to rise to a given value, is as follows.

(1) The externally maintained electron current I_o is determined.

(2) The value of ω/α is determined from the Townsend breakdown criterion, by measuring the field at which the current is just self-maintained. The value of α at that field is used to calculate ω/α. It is necessary to assume that ω/α does not vary appreciably with the overvoltage ΔV. In other words ω/α, determined at the sparking potential where $\Delta V = 0$, is assumed to remain the same for the higher overvoltages used in formative time lag measurements.

(3) The values of the secondary ionization coefficients γ, δ/α, ε/α are chosen such that

$$\gamma + \delta/\alpha + \varepsilon/\alpha = \omega/\alpha.$$

In practice the γ and δ/α components are so much faster than the ε/α component that they cannot be distinguished from each other, they are therefore taken together.

(4) The value of α is selected for the field unit pressure existing at the overvoltage ΔV to be considered.

(5) Γ and F are then determined from equations (30) and (28).

(6) The real solution λ is then determined from equation (29). This represents the main difficulty in the calculation since numerical methods are required.

(7) The value of λ obtained is inserted in equation (27) and $(\frac{\partial\theta}{\partial Z})_{\lambda}$ is determined.

(8) From equation (26) Dt can then be calculated. t is the time required for the current to reach the value $i_{-}(0,t)$, and D is the diffusion coefficient. If D is known, t is then determined.

In this way the formative time lag can be calculated for several small values of overvoltage for a given choice of secondary ionization coefficients. The choice of these coefficients is adjusted in an attempt to get agreement with experimentally measured curves of formative time lag as a function of overvoltage.

It is of interest to observe that if the ε/α value is chosen as zero, $\Gamma = 0$ and the expression for $\theta(Z)$ becomes

$$\theta(Z) = (\alpha + Z)(\alpha - Z)F\left[e^{-2Zd} - 1\right] \qquad (31)$$

In general F is not zero.

The solutions for $\Theta(Z) = 0$ are then

$$Z = -\alpha$$

$$Z = +\alpha$$

and $$Z = 0$$

These are the trivial solutions referred to on page 48 which are not included in the summation. Thus in this case ($\eta/\alpha = 0$) there is no solution for λ. This is not surprising since the assumption that w_- and w_+ are zero is clearly no longer valid if the δ/α and γ processes are the only two secondary ionization processes operating.

3.4. EXPERIMENTAL MEASUREMENTS IN HELIUM AND APPLICATION OF THEORY (I)

Formative time lags have been measured in low pressure helium by D.K. Davies et al. (1963) using parallel plate silver electrodes. The field per unit pressure, E/p_o was varied from 8.61 to 38.08 volts cm^{-1} $torr^{-1}$ for a constant electrode separation. The helium used was initially spectrally pure, active charcoal being used in an attempt to maintain this purity in the system. In this experiment the α values used in the calculations were actually measured in the same gas sample and were therefore directly applicable. This is an important advantage since current growth measurements are particularly sensitive to small changes in α which may result from slight variation for the gas purity. The measurement of the longer

formative time lags at low overvoltages, which are most sensitive to changes in secondary ionization, were found to be consistent, with a coefficient of variation of less than 1%. The voltage was applied to the electrodes in two parts. A steady D.C. 'backing voltage' was applied continuously, and a square wave voltage pulse used to raise the total voltage above the sparking voltage for the gap. This arrangement simplifies pulse generator requirements, but the continuous presence of the backing voltage may affect conditions in the gap. If the electrodes have slightly insulating layers it is possible for the continuous flow of small pre-breakdown currents in the gap to cause the build up of a charge layer on the cathode and thus alter the work function, and the sparking potential of the gap. This effect has been shown in previous work by the author using an oxide coated cathode (Fulker 1963). The flow of current at time t = 0 also gave a charge distribution in the gap at t = 0 and thus violates one of Davidson's boundary conditions. However, D.K. Davies found that the measured formative time lags were substantially independent of the magnitude of the backing voltage and of the initial current in the gap, so that the effect of departure from the boundary condition was small.

Instead of the more direct measurement of current to determine formative time lag, D.K. Davies used the collapse of

FIG. 11 EXPERIMENTAL AND THEORETICAL FORMATIVE TIME LAGS FOR D.K. DAVIES' HELIUM RESULTS

$$E_{s/p} = 8.61$$

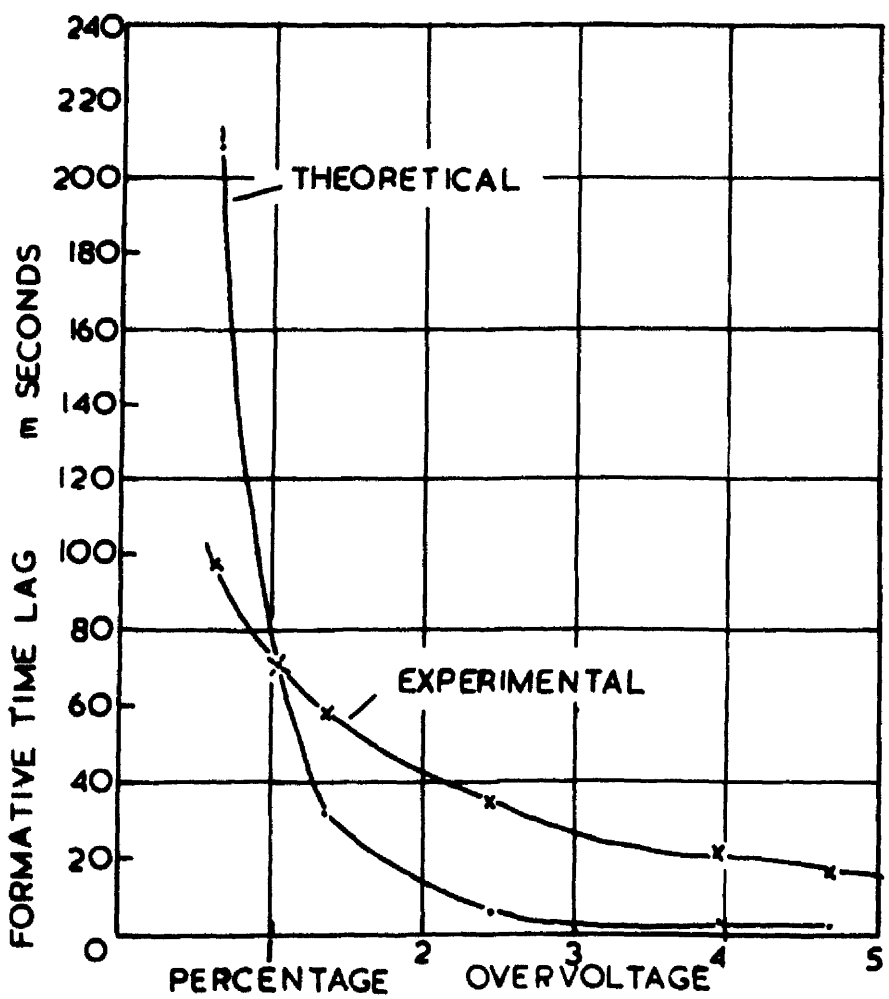

FIG. 12 EXPERIMENTAL AND THEORETICAL FORMATIVE TIME LAGS FOR D.K. DAVIES' HELIUM RESULTS

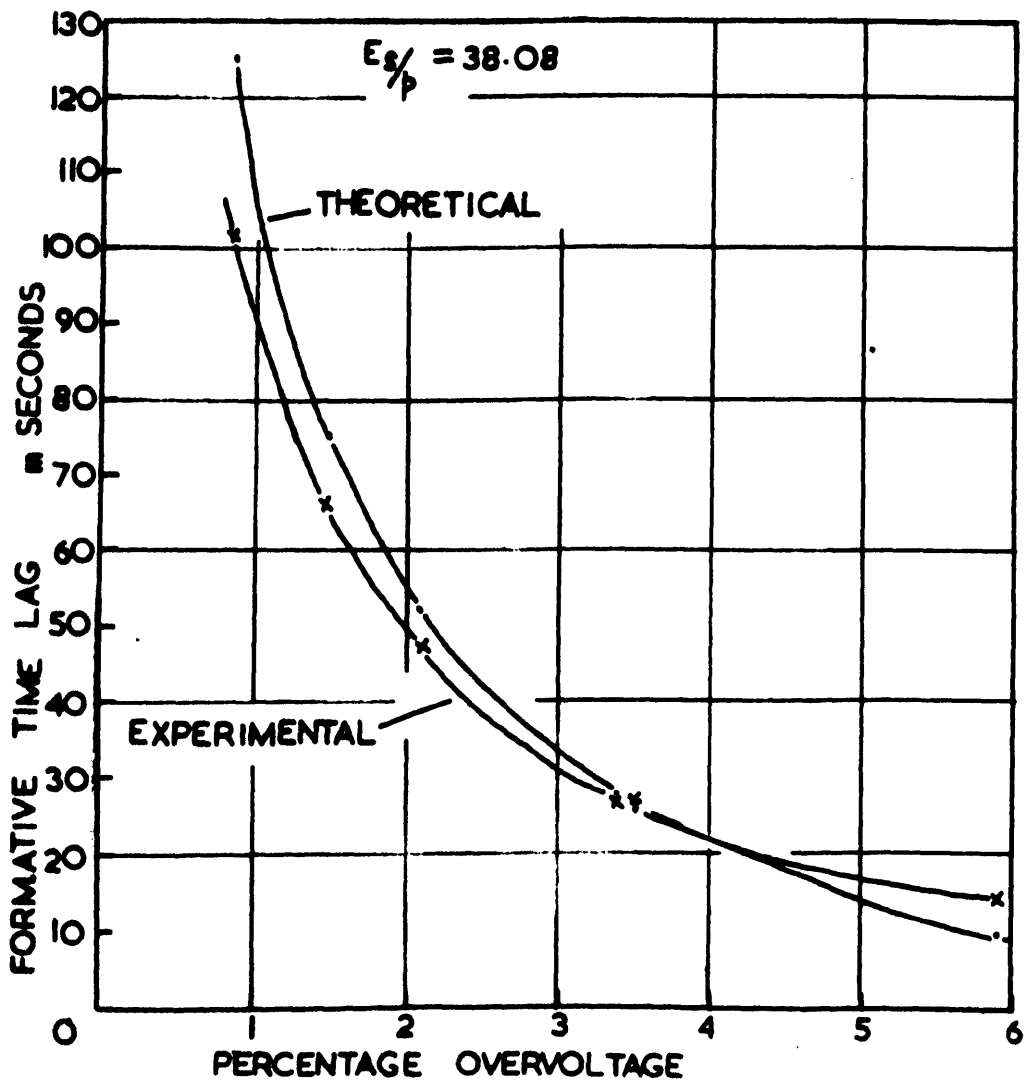

the applied voltage as the criterion. This, of course, is dependent on the electrical circuit. The breakdown current can be calculated from the voltage collapse.

The experimental results of formative time lag as a function of overvoltage were analysed using theory I, on the assumption that any or all of the γ, δ/α, ε/α processes were active. It was found that a process slower than the γ process was necessary to explain the results. Combinations of the fast processes (γ and δ/α taken together) and the slower ε/α process would not give sufficient agreement between experimental and theoretical results for a range of overvoltage from 0 to 5%. Figures (11) and (12) show the calculated formative time lags which give closest agreement at two different values of E_s/p_o. For Fig.(11) $E_s/p_o = 8.61$, $p_o = 38.51$, $\alpha = 8.17$ cm., $\omega/\alpha = .53$, ε/α is 4.2% of ω/α, and γ is 95.8% of ω/α. The agreement here is very poor.

For Fig. (12) $E_s/p_o = 38.08$, $p_o = 5.07$, $\alpha = 8.17$, $\omega/\alpha = .25$, ε/α is 19.5% of ω/α, and γ is 80.5% of ω/α. Here the agreement is much better, but the theory fails to explain the experimental results over a range of E_s/p_o.

An attempt was also made to explain the results by the theory which treats resonance radiation as a diffusion process (although, as has already been pointed out, this is not valid) (D. K. Davies, 1961). This also failed to explain the results.

3.5. MODIFICATION OF THE THEORY TO ALLOW FOR DESTRUCTION OF METASTABLE STATES IN THE GAS (II)

In a paper published in 1962 Davidson extended his temporal growth theory so that it could include other secondary ionization processes, in particular the destruction of metastable atoms at collisions with gas molecules and the transmission of the resulting radiation to the cathode, without appreciable scattering, to cause electron emission.

Davison derived two types of solution. One of these is a simple exponential solution where the current of each type of active particles is of the form $i_K(x,t) = i_K(x,0)e^{\lambda t}$ (32) This assumes that the time constant λ is the same for all types of active particles and that λ is real and non zero. The spatial densities of active particles contain the same time factor λ. This can be applied to the complicated cases such as that suggested by Phelps (1960) where molecular ions and molecular metastables are included. Formulae can be set up for each ratio

$$\frac{i_K(0,t)}{i_-(0,t)} = f_K(\lambda) \qquad (33)$$

where i_K is the active particle current and i_- the electron current, using the differential equation and boundary conditions for the active particles. Each function $f_K(\lambda)$ is a function of the time constant λ, but does not involve time.

The $f_K(\lambda)$ functions can then be inserted into the electron boundary condition .

$$i_-(0,t) = I_o + g(t) \tag{34}$$

where $$g(t) = \sum_K \gamma_K i_K(0,t) \tag{35}$$

where $i_K(0,t)$ is the active particle current at the cathode and γ_K the secondary emission coefficient for that species of active particle. If $I_o(t)$ is zero this equation becomes

$$i_-(0,t) = \sum_K \gamma_K i_K(0,t) \tag{36}$$

or $$1 - \sum_K \gamma_K f_K(\lambda) = 0 \tag{37}$$

If $I_o(t)$ is not zero the equation (34) becomes

$$i_-(0,t) = I_o(t) + \sum_K \gamma_K i_K(0,t) \tag{38}$$

$$\therefore \quad 1 = \frac{I_o(t)}{i_-(0,t)} + \sum_K \gamma_K f_K(\lambda) \tag{39}$$

$$\therefore \quad \frac{I_o(t)}{i_-(0,t)} = 1 - \sum_K \gamma_K f_K(\lambda) \tag{40}$$

$$\therefore \quad i_-(0,t) = \frac{I_o(t)}{1 - \sum_K \gamma_K f_K(\lambda)} \tag{41}$$

and $i_-(0,t) \neq i_-(0,0)e^{\lambda t}$.

Thus if the externally maintained current I_o is present a simple exponential solution which does not involve t does not exist. If, however, I_o is zero a simple exponential solution exists if λ satisfies a relation

$$F(\lambda) = 0 \text{ where } F(\lambda) = 1 - \sum \gamma_K f_K(\lambda) \qquad (42)$$

In general there will be an infinite number of λ's satisfying $F(\lambda) = 0$. These λ's may be complex and change continuously with V. The simple exponential solution of $F(\lambda) = 0$ is the λ value which goes through zero as V goes through V_s. This follows from the equation

$$i(0,t) = i(0,0)e^{\lambda t}$$

or $$e^{\lambda t} = \frac{i(0,t)}{i(0,0)}$$

At the sparking voltage $V = V_s$ and the secondary current at the cathode $i(0,t)$ is just sufficient to maintain the discharge, i.e. $i(0,t) = i(0,0)$ so that $e^{\lambda t} = 1$ and $\lambda = 0$ [λ has units seconds^{-1}.]

For the case where there is a constantly maintained current I_o and no active particles present for times $t < 0$, Davidson writes the electron current $i_-(0,t)$ at the cathode in the form

$$\frac{i_-(0,t)}{I_o} = A - \sum B_\lambda e^{\lambda t} \qquad (43)$$

this is valid at all times $t > 0$. A and the B's have explicit expressions. The summation contains the simple exponential

solution λ and all the other λ's which satisfy $F(\lambda) = 0$. However, further approximations can be made. For sufficiently large times all the other λ's become negligible in comparison with the simple exponential λ, and the general solution reduces to the simple exponential solution:

$$\frac{i_-(0,t)}{I_o} = A - Be^{\lambda t} \qquad (44)$$

If $V > V_s$ λ is positive and the expression can be written as

$$\frac{i_-(0,t)}{I_o} = = - Be^{\lambda t} \qquad (45)$$

with only a small percentage error. The expression B here relates directly to the problem considered. The simple exponential solution considered by Phelps (1960) has a similar form

$$\frac{i_-}{I_o} = Ce^{\lambda t}$$

but in that case the function C was determined by an initial arbitary distribution of particles which is absent in the considered problem. Using Davidson's approach the functions A and B were calculated for the case where it was assumed that secondary electron emission from the cathode was caused by positive ions formed in the gas, or by delayed photons originating from destruction of metastable atoms in the gas.

The general form of the growth equation is

$$\frac{i_-(0,t)}{I_o} = \frac{1}{F(0)} + \sum_X \frac{e^{\lambda t}}{\lambda F'(\lambda)} \qquad (46)$$

i.e. $A = \frac{1}{F(0)}$ and $B = \frac{-1}{\lambda F'(\lambda)}$

As explained above, this can be approximated to

$$\frac{i_-(0,t)}{I_o} = -Be^{\lambda t} \qquad (47)$$

where $$B = \frac{-1}{\lambda F'(\lambda)} \qquad (48)$$

This expression is generally true even for the complicated case considered by Phelps (1960), if the appropriate expression for $F(\lambda)$ is used. For the positive ion and delayed radiation case

$$F(p) = 1 - \frac{\delta_1(e^{\psi d} - 1)}{(1 + p\tau_1)\psi} - \frac{\alpha\gamma(e^{\alpha\phi} - 1)}{\phi} \qquad (49)$$

δ_1/α is the delayed photon secondary ionization coefficient expressed as the number of secondary electrons released from the cathode by this process per primary ionizing collision in the gas.

α is the primary ionization coefficient.

γ is the secondary ionization coefficient for positive ions.

d is the gap distance.

τ_1 is the mean lifetime of the metastable states.

λ is the real value of p which satisfies the equation $F(p) = 0$

where

$$\psi = \lambda - \frac{p}{w_-} \tag{50}$$

$$\phi = \alpha - \frac{p}{w} \tag{51}$$

$$\frac{1}{w} = \frac{1}{w_-} + \frac{1}{w_+} \tag{52}$$

w_- is the electron drift velocity in cm sec^{-1}.

w_+ is the positive ion drift velocity.

The total secondary ionization coefficient ω/α is assumed to be given by $\omega/\alpha = \gamma + \delta_1/\alpha$ (53)

$B = \frac{-1}{\lambda F'(\lambda)}$ where

$$F'(\lambda) = \frac{\delta_1\left[w_-\psi\tau_1(e^{\psi d}-1)+(1+\lambda\tau_1)\left\{(\psi d-1)e^{\psi d}+1\right\}\right]}{w_-\psi^2(1+\lambda\tau_1)^2} + \frac{\alpha\gamma\left[(\phi d-1)e^{\phi d}-1\right]}{w\phi^2}$$

In the case where $\tau_1 = 0$, these equations reduce to those given earlier (Dutton et al. 1953) for the positive ion and undelayed radiation case.

3.6. APPLICATION OF THEORY II FOR HELIUM

This delayed radiation and positive ion theory has been applied to the helium results obtained by D.K. Davies et al. (1964). The same form of Davidson's solution can also be used for the resonance radiation process using a value for the average delay

given by

$$\tau_1 = \tau_0 \left(\frac{3\pi^2 d}{\lambda_0} \right)^{\frac{1}{2}} \frac{1}{1.15} \qquad (54)$$

τ_0 is the lifetime of the resonance state.

λ_0 is the wavelength of the centre of the broadened resonance spectral line.

There are no experimental values of τ_0 , but they can be calculated (Mitchell and Zemansky 1934). At first it was assumed that either the delayed radiation or the resonance radiation was entirely responsible for the breakdown. The equations of Davidson's theory (equations 47 - 53) were solved for the time constant λ by a process of trial and error and the formative time lag calculated. The delay time τ_1 was treated as a variable parameter and the τ_1 value found which gave the best fit with the formative time lag results for a particular value of E_s/p_o. Column (1) of table (1) shows the τ_1 values obtained for agreement to within 20% between the experimental and calculated results.

The τ_1 value calculated from the Holstein-Biberman theory for transport of resonance radiation, involving 2^1P excited state, is approximately 10^{-6} sec. It was therefore concluded that resonance radiation was not a significant process since the experimental delay times were considerably longer than this.

TABLE 1

Total radiation delay time τ_1

p_o	E_s/p_o	τ_1 calculated	τ_1 data from Phelps (1960)
38.51	8.61	1.2×10^{-4} sec	1.3×10^{-4} sec
29.43	10.04	2.4×10^{-4} sec	1.8×10^{-4} sec
23.01	11.43	2.1×10^{-4} sec	2.2×10^{-4} sec
19.17	12.93	2.3×10^{-4} sec	2.7×10^{-4} sec
14.54	15.74	1.5×10^{-4} sec	3.6×10^{-4} sec
10.10	20.82	1.7×10^{-4} sec	5.1×10^{-4} sec
5.07	38.08	1.5×10^{-4} sec	10.0×10^{-4} sec

If, however, the delay process is due to the volume destruction of 2^1S metastable helium atoms, then the values of the delay time τ_1 found from the experiment should agree with the value calculated from Phelps data using the formula $\tau_1 = \frac{1}{193 p_o}$ seconds, which are shown in column 2. This was found to be the case and comparison of columns 1 and 2 shows reasonable agreement from pressures greater than 19 torr. The discrepancy for lower pressures is an indication that some contribution to the ionization is made by a faster process which becomes more effective as the pressure is reduced. It can also be pointed out that if the three body destruction process for 2^3S metastable atoms was

an important process τ_1, would be inversely proportional to p_o^2, showing a greater variation than appears in column (1). This agrees with Phelps' (1960) view that the 2^3S metastable atoms form long lived metastable helium molecules at three body collisions.

The simultaneous action of the delayed radiation process and the positive ion process was then considered using τ_1 values given by $\tau_1 = \frac{1}{193 p_o}$. The results obtained are summarised in Table 2. The combination of delayed radiation and positive ion processes can explain the experimental results over the whole pressure range (though the closeness of the agreement is not given).

TABLE 2

p_o torr	E_s/p_o	$\lambda \times 10^{-2}$ sec^{-1}	δ_1%	γ%
38.51	8.61	9.9	100	0
29.43	10.04	7.8	100	0
23.01	11.43	7.1	88	12
19.17	12.93	7.9	76	24
14.54	15.74	9.4	43	57
10.10	20.82	8.9	37	63
5.07	38.08	12	24	76

The role of the positive ions becomes increasingly important as the pressure decreases and E/p_o increases, eventually becoming the dominant process for pressure below about 10 torr. At low E/p_o and high pressures the number of excitations to

FIG 13. VARIATION OF γ WITH E/p_0 AND p_0 FOR HELIUM IONS ON SILVER.

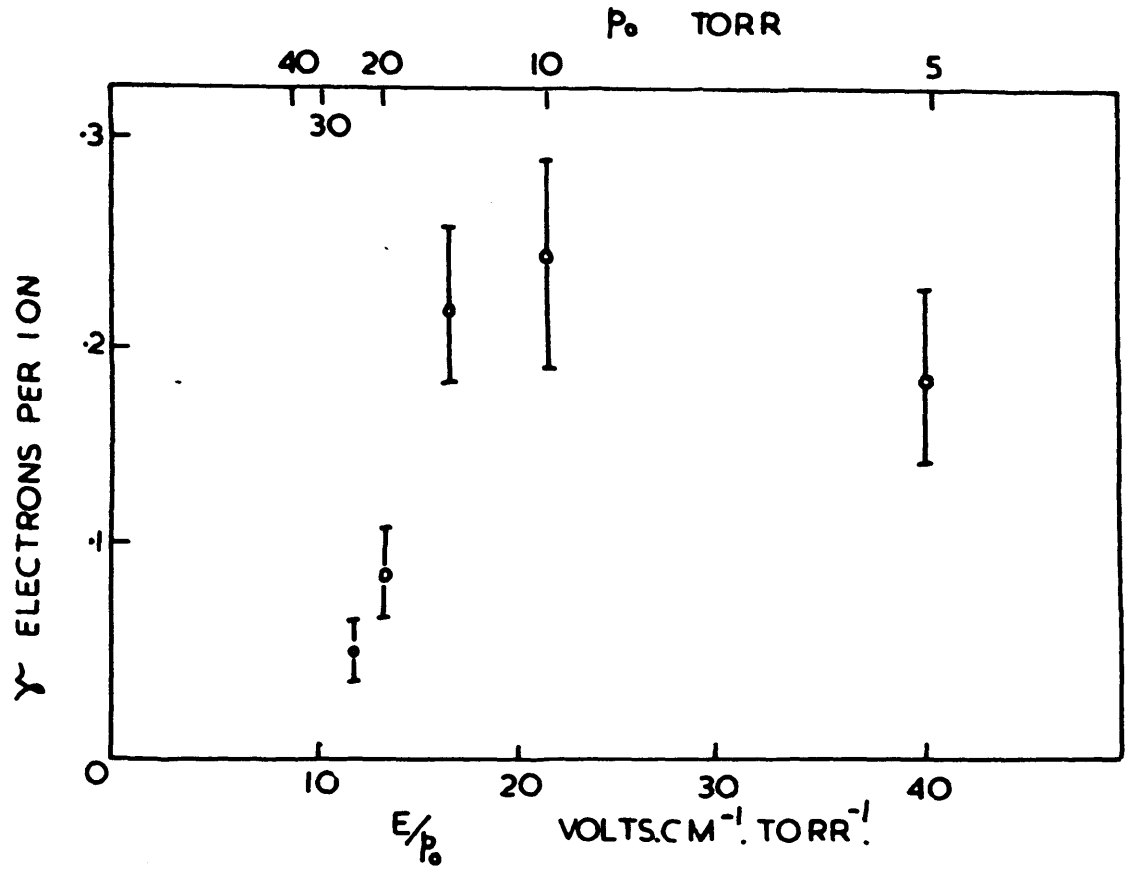

metastable states exceeds the number of ionizing collisions according to data of van Engel and Corrigan (1958). At lower pressures the ratio of metastables to ions is much reduced and the destruction of the metastables is reduced giving a qualitative explanation. It was not possible to distinguish between the atomic and molecular metastables. The values of γ (the number of secondary electrons emitted from the silver cathode per incident ion) in the helium measurements of D.K. Davies have been further analysed in a later paper. (C. G. Morgan et al. 1965). Fig. 13 shows the variation of γ with E/p_o and p_o obtained from the time lag analysis. It is assumed that back scattering of the secondary electrons can be neglected. For pressures less than about 18 torr γ is about .2 electrons per ion and roughly independent of E/p_o and kinetic energy of the ions considering the low accuracy of the γ values. For $p_o > 18$ torr γ decreases rapidly. The γ obtained for higher pressure was discarded as inaccurate because of the large change in $\delta 1/\alpha$ which occurred there. The variation of γ with E/p_o could be interpreted by supposing that two species of ions were present. One species was effective for $E/p_o > 14$ having a γ of about .2, and another ion with a lower γ becoming effective at lower E/p_o. The more effective ion was probably the He^+ ion formed by a two body electron atom collision in the gas. The lack of γ dependence on E/p_o and ion

FIG. 14. VARIATION OF δ_1/α WITH E/p_0 FOR SILVER ELECTRODES IN HELIUM.

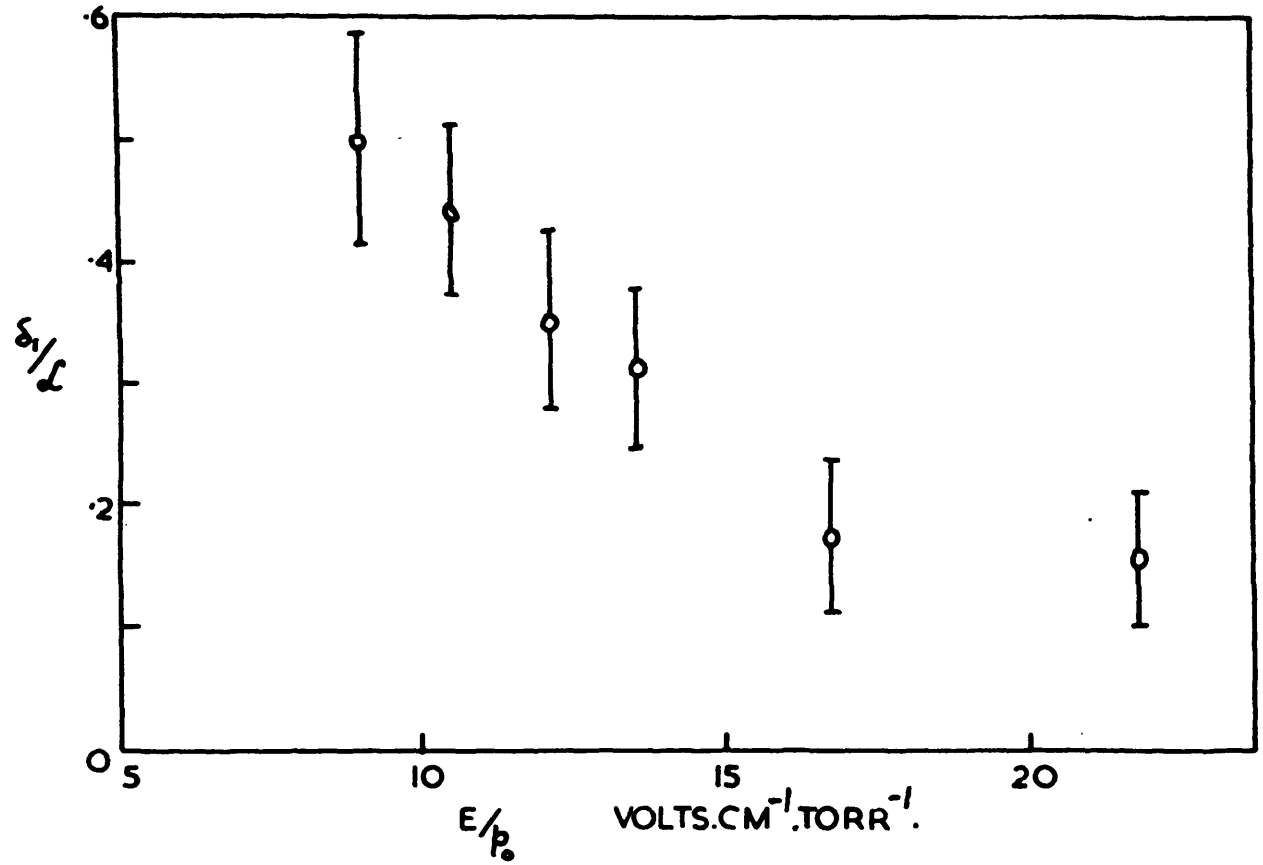

energy for higher E/p_o indicates that the secondary electrons are emitted from the silver cathode by a Auger potential energy process. Calculation by Hagstrum (1954) for this process with He^+ ions gave a γ value of .293 electrons per ion which agrees well with D.K. Davies values. Hagstrum's values were for tungsten which has a work function of about 4.5.eV which is not very different from the work function for silver. The lower γ values for $E/p < 14$ may be due to the presence of He_2^+ ions formed by three body collisions between a helium ion and two ground state helium atoms. Hagstrum's measurements for tungsten showed that He_2^+ was about half as effective as He^+ for causing emission of electrons (Hagstrum 1953). The molecular ions are more likely to be present at higher pressures because of the three body formation process. The variation of the delayed radiation ionization coefficient with E/p_o obtained from the D.K. Davies results are shown in Fig. 14. This radiation results from the destruction of the 2^1S helium metastable atom in two body collision with ground state atoms, and reaches the cathode without appreciable scattering to cause photo-emission of electrons.

More recent work on the Townsend breakdown in helium by Griffiths (1964), also using Davidson's theory, has shown that the action of three separate ionization processes can be distinguished.

(i) Emission of electrons from the cathode by positive ions. (Coefficient γ).

(ii) Destruction of the 2^1S metastable helium states at two body collisions with gas atoms, the resulting photons causing electron emission from the cathode. (Coefficient δ_1/α).

(iii) Dissociation of $2^3\Sigma$ molecular metastable states, the resulting radiation causing electron emission from the cathode. (Coefficient δ_2/α).

The $2^3\Sigma$ metastable molecule is considered to be produced by a three body collision involving a 2^3S metastable atom and two ground state atoms. Griffiths assumed that the 2^3S lifetime was long compared with the $2^3\Sigma$ lifetime and was thus the determining time factor for the process. The 2^3S lifetime τ_T was calculated from the equation

$$\tau_T = \frac{1}{0.26\ p^2} \text{ sec}$$

from data given by Phelps (1960) for the three body destruction process. Griffiths used a large range of over-voltage (5%) but calculated the value of the coefficients separately for each over-voltage to allow for the effect of the change in E/p_o. In agreement with the work of D. K. Davies he found that the collision induced radiation process (δ_1/α) and the positive ion process (γ) were able to account for the current growth at low

FIG 15. SECONDARY IONIZATION COEFFICIENTS δ_1/d, δ_2/d AND γ (EXPRESSED AS PERCENTAGES OF ω/d) AS FUNCTIONS OF E_s/p_0 FOR SILVER ELECTRODES IN HELIUM.

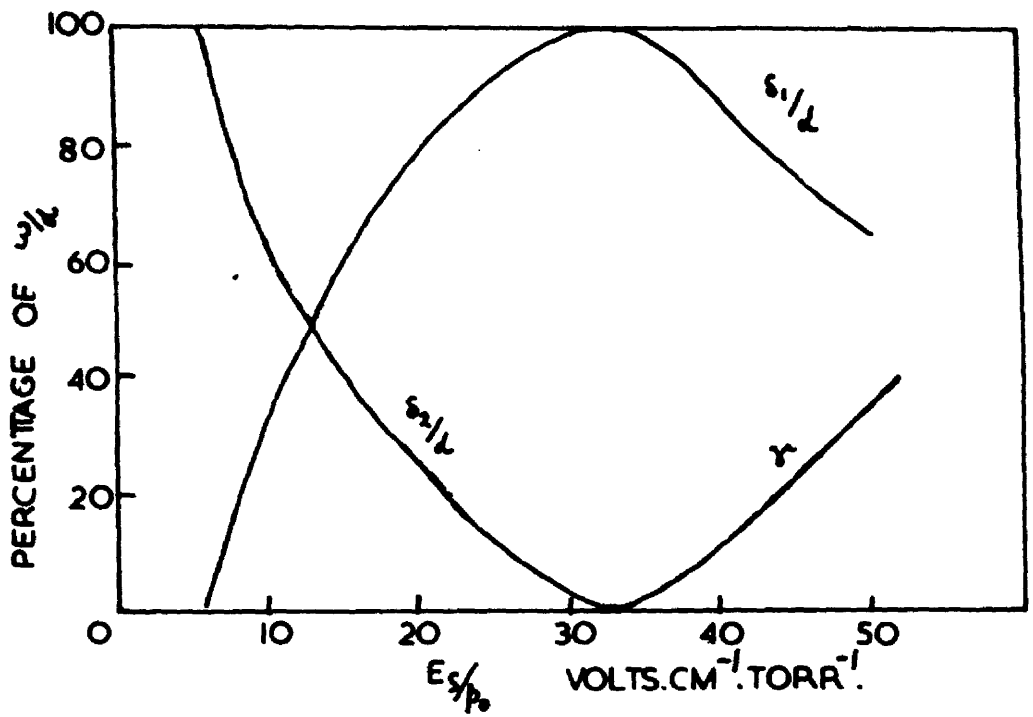

FIG. 16. IONIZATION COEFFICIENTS ω/d, δ_1/d, δ_2/d AND γ AS FUNCTIONS OF E_s/p_0 FOR SILVER ELECTRODES IN HELIUM.

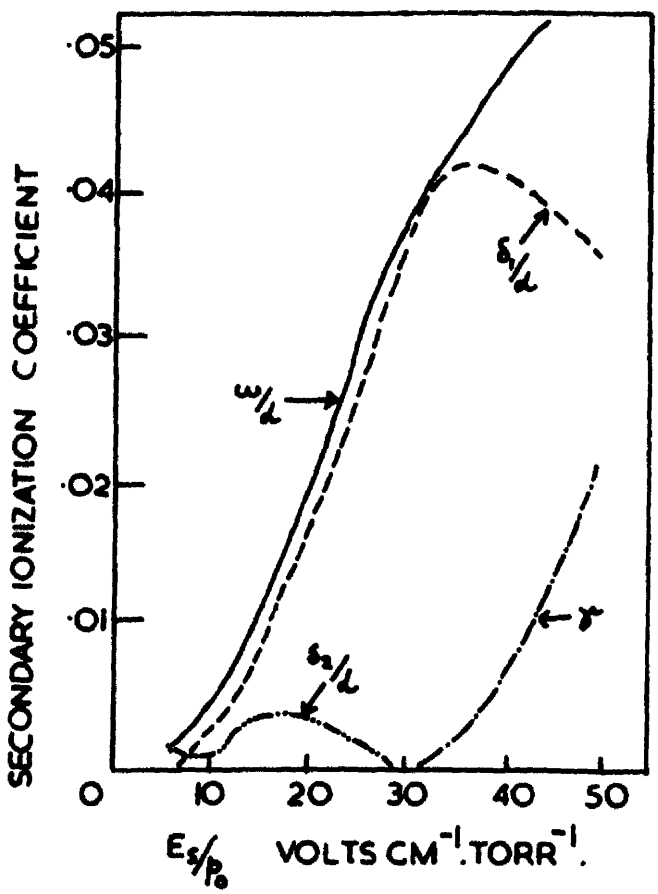

pressures (< 30 torr) and high E_s/p_o (> 10). For higher pressures and lower E_s/p_o the metastable molecule process (δ_2/α) replaced the faster positive ion process [Fig. 15, 16]. It was not possible to distinguish the possible effect of molecular helium ions since the drift velocities of the He^+ and He_2^+ ions are not sufficiently different. The values of the coefficients ω/α, γ and δ_1/α obtained by Griffiths (Fig. 16) are considerably lower than those obtained by D. K. Davies (Figs. 13, 14).

3.7. APPLICATION OF THEORY II FOR MEASUREMENTS IN NEON

A similar study of the temporal growth of current in a neon discharge using silver and gold electrodes has been made by R. D. Davies and F. Llewellyn Jones (1965). A gap distance of .4 cm was used, the pressure range extended up to 50 torr. Formative time lags of the order of 10^{-1} sec. at overvoltages below 1% were reported. These could be explained by a combination of positive ion action at the cathode and secondary emission resulting from delayed radiation from the destruction of neon metastable atoms at two body collisions. No evidence was found for a metastable molecular process.

3.8. CONCLUSIONS

The experimental and theoretical work described in this chapter indicates that Davidson's theories for current growth should be applicable to the analysis of formative time lag measurements in low pressure neon. It appears unlikely that the emission of electrons from the cathode by metastable neon atoms is an important secondary ionization process, because of the high cross sections that have been observed for destruction of metastable states in the gas. The radiation resulting from these destructions is more likely to provide significant electron emission from the cathode. The time constant of the current growth for slightly overvolted gap will then depend on the life time of the metastable states rather than on their diffusion coefficient.

The formative time lag measurements in low pressure neon by R.D.Davieshave only come to light since completion of the present work and in fact are not yet available in published form. However, they do enable a comparison to be made with the results which will be described in chapters V and VI.

CHAPTER IV

EXPERIMENTAL APPARATUS

4.1. INTRODUCTION

The determination of secondary ionization coefficients in the neon Townsend breakdown by the formative time lag method requires very high gas purity. If any impurity is present the Penning effect may operate, for example, if any argon impurity is present the cross section for ionization of an argon atom by a neon metastable atom is high. Penning showed that a few parts per million of argon could have a large effect on the ionization coefficients. Thus, if a neon gas pressure of 10 torr is to be used for formative time lag measurements, the partial pressure of impurities should be less than 10^{-5} torr. In the design of a system to meet these requirements it must be remembered that a vacuum system which is not continuously pumped will release gaseous impurities even though it has been carefully outgassed. For example, water vapour will be slowly released by glass walls. No leaks can be tolerated in a closed system since argon from the air will diffuse in through very small holes. Argon may even diffuse in through regions of very thin or badly annealed glass.

The molybdenum getters used for pumping are a potential source of hydrogen, methane and argon. Gases may also be released during the course of the experiment by ion or electron

FIG. 17 THE VACUUM SYSTEM.

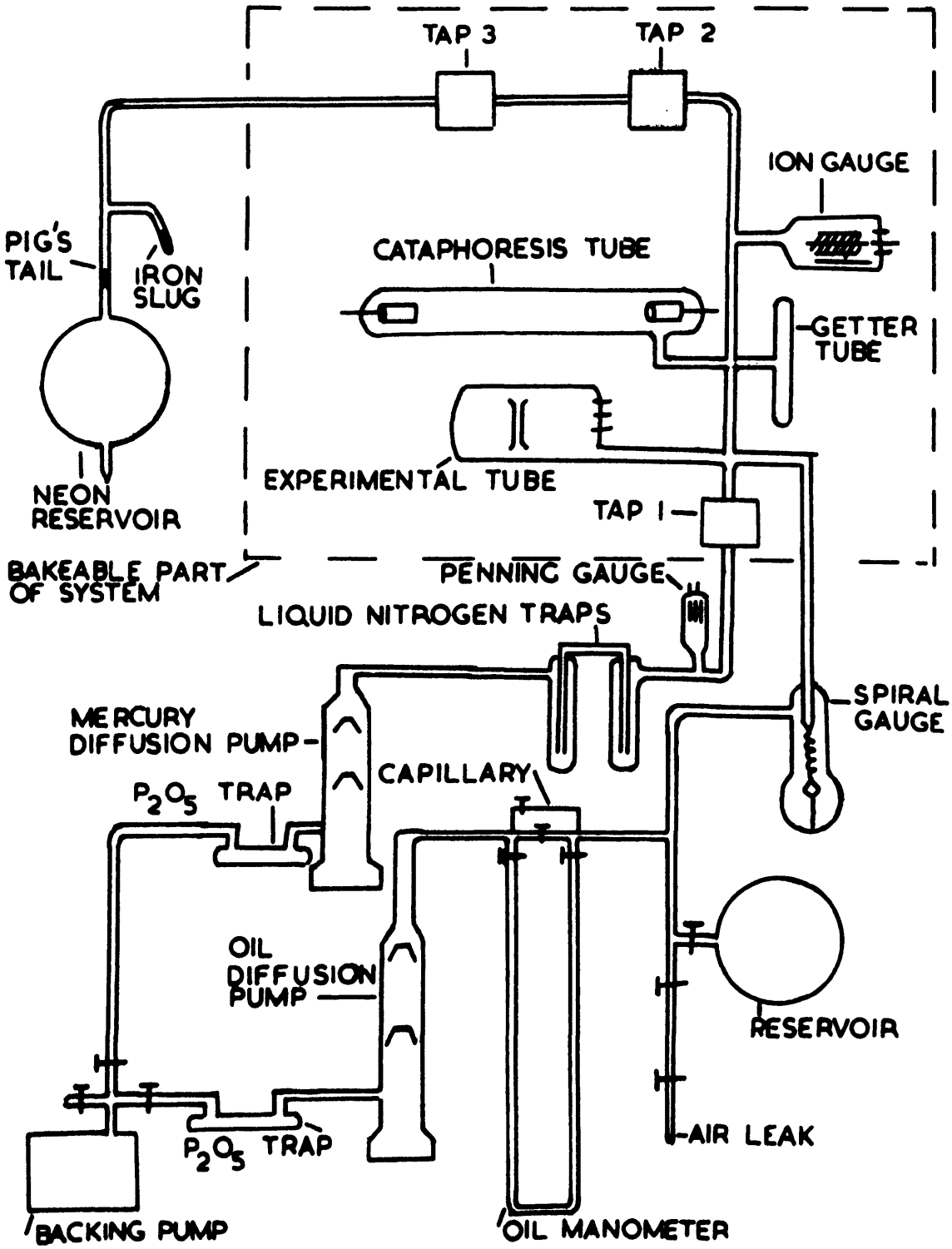

bombardment of electrodes or the containing walls.

Because of these considerations great care was taken to construct a leak tight system which could be thoroughly outgassed by baking and heating of internal parts. The only parts of the system which could not be baked were the glass spiral gauge used to measure the neon pressure and a short length of glass tubing leading to the gas reservoir. The system was equipped with a cataphoresis discharge tube to remove gaseous impurities from the area of the experiment.

4.2. THE VACUUM SYSTEM

The vacuum system, shown in Fig. 17, was mainly constructed of boro-silicate Pyrex glass. All metal bakeable valves were used in the high vacuum part of the system to avoid introducing grease or oil. Valve 1 was used to close off the system from the pumps. Valves 2 and 3 were used to control the introduction of the test gas into the system from the gas reservoir. These taps were a source of considerable trouble throughout the research programme. A leak developed in a welded joint, several glass-to-metal seals failed during baking because of faulty annealing, and the taps frequently failed to close completely. The use of three taps in a glass system made it necessary to use long lengths of $\frac{1}{2}$" diameter glass tubing between the taps to allow for differences in thermal expansion. This seriously limited the conductance of the system and the effective pumping speed of the system was therefore low.

The system was evacuated by a two-stage rotary backing pump connected through a P_2O_5 water vapour trap to a glass two-stage mercury diffusion pump. Two liquid nitrogen traps in series were used to prevent mercury from entering the system. It was found that one trap was not sufficient. No precautions were taken to prevent oil from the rotary pump from entering the system. Recent work by Baker (1966) has shown that oil diffuses back into the system especially when the pump is operating at it's ultimate pressure. This oil contamination can result in the formation of insulating polymer films on electrode surfaces. The oil is not effectively trapped by the tray type of P_2O_5 trap, nor is the liquid air trap effective because the mean free path of molecules is too small at backing pressure. Contamination can, however, be simply prevented by an "in-line" trap packed with activated alumina.

During evacuation pressures were measured by a Bayard-Alpert ionization gauge (Mullard IOG-12), the pressure during baking being measured by a Penning gauge mounted just below the oven.

Spectrally pure neon was used as the test gas in this investigation. This was contained in a glass bulb sealed to the vacuum system. When required the gas could be released from the bulb by breaking a thin glass "pig's tail" with a glass encased iron slug operated by an external magnet. Ultra-high vacuum

could be obtained by use of molybdenum getters and the Bayard-Alpert gauge used as a pump.

The pressure of neon in the closed off system during experimental measurements was determined by comparing it with the pressure in a separate system by observing the deflection of a beam of light reflected from a mirror on the spiral gauge. The pressure of the auxiliary system could be adjusted to equal the pressure of neon in the closed system, using the spiral gauge as a null indicator, and measured with a manometer containing silicone 704 diffusion pump oil.

The vacuum system was baked for 24 hours with all three bakeable taps open. Where possible, parts of the system outside the oven were outgassed by heating with a gas flame. The metal parts in the system were outgassed as soon as possible after removal of the oven. The grid of the ion gauge, the metal electrodes in the experimental tube and in the cataphoresis tubes, and the molybdenum getters, were outgassed by eddy-current heating. The gold evaporation source used in the first experimental tube was outgassed by passing a current through the tungsten core. The system was then baked for a further 24 hours, followed by outgassing of metal parts. After this treatment the system, if leak tight, would reach a pressure of 10^{-7} torr.

The firing of molybdenum getters inevitably causes the release of some gas. Consequently the getters were fired with

the system still open to the diffusion pump. Tap 1 was closed when the pressure fell back to the original level. In addition to the action of the getters, further pumping was obtained by pumping with the Bayard-Alpert gauge. The Mullard ICG-12 gauge used had a conducting tin oxide film on the inside of the glass envelope. This could be connected as an additional ion collecting surface. In practice it was found best to pump with a grid current of 1 mA. A higher current than this tended to cause the release of gas from the gauge. After ion pumping the ultimate pressure could in some cases be reduced to 5×10^{-9} torr. The pump down of experimental tube 2, from which most of the useful results were obtained, reached an ultimate pressure of 2×10^{-8} torr. The rate of pressure rise when ion pumping was discontinued was so small that it was realistic to expect a partial pressure of impurities of less than 10^{-6} torr from gas sources inside the vacuum system. The spectrally pure neon was a greater source of impurities than this. A typical chemical analysis of the neon supplied by the British Oxygen Company showed:-

Neon	99.9%
Helium	0.1%
Oxygen	approximately 2 parts per million.

The high percentage of helium made it necessary to use some additional means of purification.

4.3. CONSTRUCTION OF THE EXPERIMENTAL TUBES

The requirements of an experimental tube for the

FIG. 18 MOVABLE GOLD EVAPORATION SOURCE

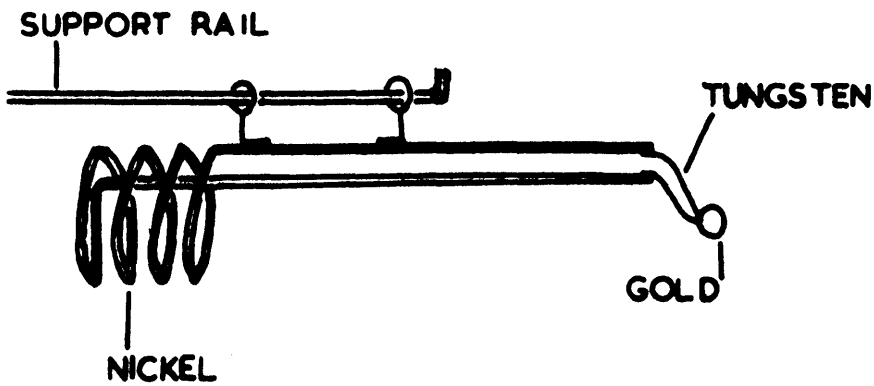

measurement of temporal growth of current are outlined below. The electrodes were required to produce a uniform electric field which would not be disturbed by the proximity of the containing vessel. It was also desirable that one electrode should be movable so that different gap distances could be used for a given pressure. Illumination of the cathode, the fixed electrode, was required to provide an initial photocurrent. It was necessary that both the electrodes should have known, uniform and stable work functions, and not to be sources of gaseous impurities.

Two experimental tubes were constructed, both from Pyrex glass and both having variable gas distances. Tube 1 had glass electrodes of 3 cms diameter. These were moulded, with a tungsten seal passing through the glass. The electrodes were ground flat on a grinding wheel, the edges rounded to avoid enhancing the field, and finally polished with jeweller's rouge. The anode was mounted so that it could be moved about 5 cms with respect to the cathode by means of an attached, glass encased, iron slug, operated by an external magnet.

A gold evaporation source, consisting of gold wire overwound on a tungsten filament, was mounted in a side tube. This source was purified, by pre-melting in a hydrogen atmosphere, before being mounted in the experimental tube. It is difficult to obtain a uniform gold coverage on the electrodes with a fixed gold source without the source being sufficiently close to the

FIG. 19 EXPERIMENTAL TUBE 1.

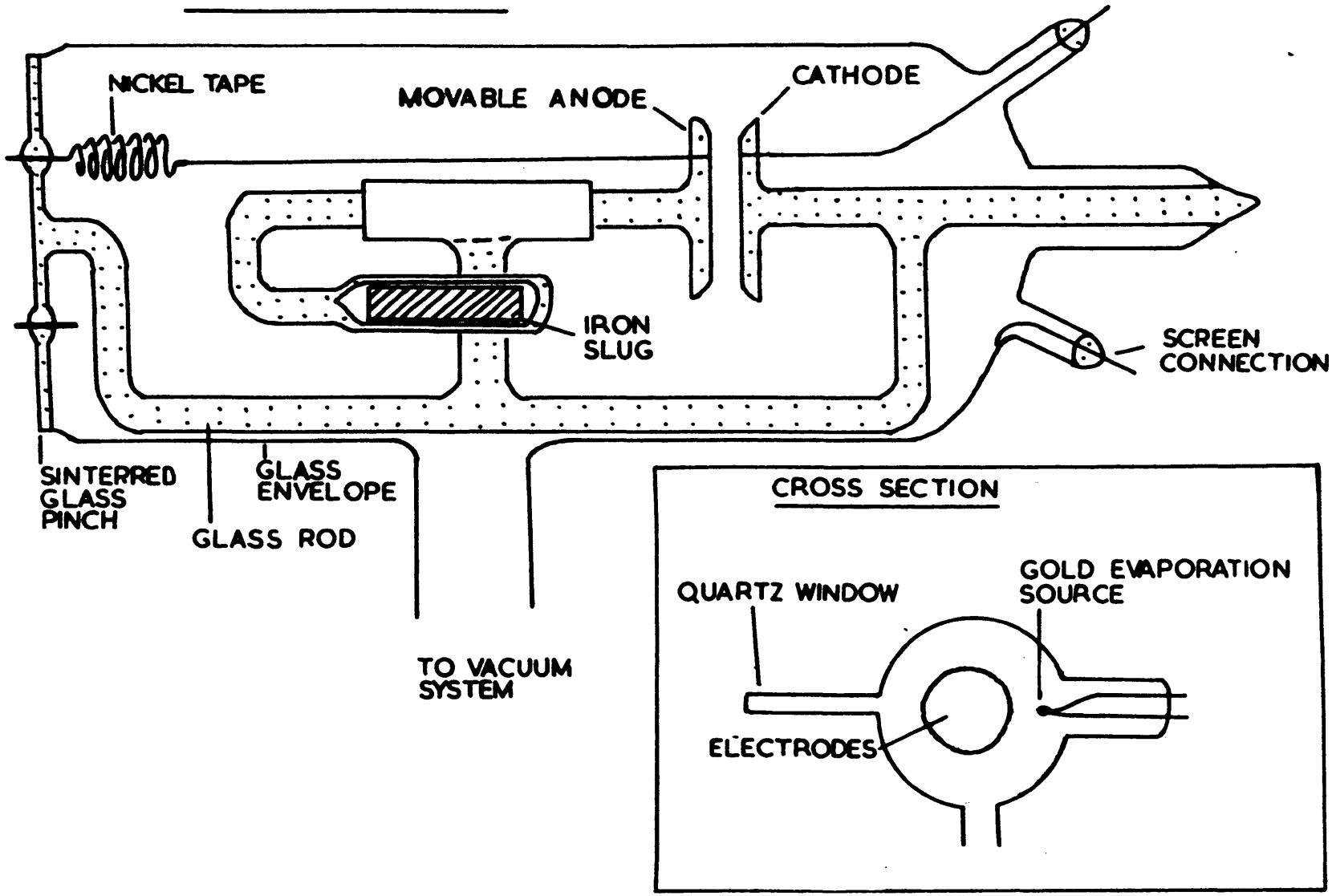

gap to disturb the field during the experimental measurements. It was hoped that this problem could be overcome using the movable gold source shown in Fig. 18. The filament was attached to a coil of 1.5 mm diameter nickel wire. This was mounted on a rail in a 4 cm diameter glass side-arm. The source could be moved along the wire with a magnet. The filament could be heated and gold evaporated by inducing eddy-currents in the nickel coil using an eddy-current heater coil. This system had the advantage that the gold source could be outgassed inside the side arm, well away from the electrode surfaces. The source could then be positioned between the electrodes to obtain a uniform gold evaporation on to the glass surfaces, and retracted for experimental measurements. Unfortunately the device was not successful because there was enough evaporation of nickel from the coil to form a conducting film on the glass. Currents were also induced in this film leading to failure of the glass. Time did not allow further attempts but the film could be prevented from forming a circuit by use of a glass rod to form a shadow across the film. The coil could be made of some other metal with a lower vapour pressure but this would require more complicated movement arrangements.

The construction of Tube 1 is shown in Fig. 19. The gold film evaporated on to the glass envelope provided a screen which could be earthed to prevent changes building up. A glass encased iron slug was magnetically held in position during the

evaporation of the gold in order to leave a window in the film for gap distance measurements.

Unfortunately no satisfactory time lag measurements could be made with this tube because the breakdown of the gap between the electrodes occurred in two stages. In the first stage the breakdown was limited to a filamentary discharge between the points on the electrodes where the tungsten pins contacted the gold film. This discharge was sometimes followed by complete breakdown, the discharge then filling the interelectrode space. This two stage breakdown was believed to be the result of poor electrical contact between the tungsten pins and the gold film, perhaps resulting from the formation of a high resistance tungsten oxide layer prior to evaporation. Bulk metal electrodes were used with Tube 2 to overcome this problem. These were made from die stamped 0.007" thick nickel sheet and could be outgassed by eddy-current heating to red heat. The electrodes were 4 cms diameter with rounded edges to prevent field enhancement. Tube 2 was otherwise similar to Tube 1, having a movable anode and a cathode illuminated by ultra-violet light.

The inside of the envelope was painted with colloidal graphite leaving a window for measurement of the gap distance. This screen could be earthed through a tungsten lead-through to prevent changes building up on the envelope. This use of colloidal graphite is not really desirable since the preparation contains organic binders. Some of these may remain even after baking and

act as a source of impurity gases, especially if bombarded by electrons or ions from the discharge. Other conducting paints such as liquid bright platinum would suffer from the same disadvantage.

Tube 2 was found to give consistent time lag results after an initial "conditioning" of the electrodes. This "conditioning" phenomena is possibly due to removal of slight oxide layers from the electrode surfaces and the consequent stabilization of the work function.

4.4. PURIFICATION OF NEON BY CATAPHORESIS

Cataphoresis, or the separation of different species of gas in a low pressure D.C. discharge, was observed by Baly in 1893 using hydrogen and carbon dioxide. The phenomenon was later observed with mixtures of rare gases and metal vapours such as magnesium. A theory to explain this separation was developed by Langmuir (1923) and Druyvesteyn (1935).

The concentration of the impurity is determined by the current of impurity positive ions towards the cathode and diffusion back of impurity atoms. Metal impurity atoms are more easily ionized than the rare gas atoms because of their lower ionization potential and this leads to a higher concentration of the metal impurity near the cathode of the discharge tube. Spectroscopic measurements by Penning (1934) for a mixture of 10% mercury in neon at a pressure of 12 torr and a discharge

current of 30 mA confirmed this theory.

Reize and Dieke (1954) used cataphoresis to separate rare gas mixtures using a discharge current of about 20 mA and total pressures from 5 to 55 torr. The minor constituent appeared to be concentrated at the cathode, whatever it's nature. For neon impurities in helium, this agrees with Druyvesteyn's theory because of the lower ionization potential of neon. For helium impurities in neon the mechanism appeared to be retrograde, that is, the constituent with the higher ionization potential concentrated at the cathode, in disagreement with the previously mentioned theory.

Retrograde cataphoresis was also observed by Kenty (1958) for mixtures of xenon and mercury, where the mercury was concentrated at the anode even though the ionization potential for mercury (10.43 eV) is less than that for xenon (12.12).

Loeb (1958) has suggested that the pumping action of electron impacts with mercury atoms may exceed the cataphoresis effect.

However, Schmeltekopf (1964) using helium and neon mixtures of about 1% impurity (about 10 times higher than used by Reize and Dieke) did not find retrograde cataphoresis with helium impurity in neon. Spectroscopic measurement for helium and neon lines indicated higher helium impurity concentration at the cathode, but observations with a mass spectrometer showed that

in fact the helium concentration was greatest at the anode. The anomalous spectroscopic observations were apparently due to the high degree of ionization in the cathode region. To remove the helium impurities from the neon used in the present work, it would therefore be advantageous for the anode of the cataphoresis tube to be furthest away from the experimental tube. To remove mercury which could be present as a result of backstreaming from the pumping system, the opposite would be the case. However, either helium or mercury would be concentrated in the cataphoresis tube and away from the experimental tube. In fact in the present work the cathode of the cataphoresis tube was furthest away from the experimental tube.

Schmeltekopf also showed that cataphoresis improved with increasing pressure up to about 40 torr, above which there was little improvement. The separation was improved by increasing the current from 20 to 100 mA, but eventually became independent of current. The effectiveness of cataphoresis was decreased by increasing temperature, increasing tube diameter and decreasing length. Thus a cataphoresis tube should be as long and narrow as practicable and should not be allowed to get hot.

4.5. CONSTRUCTION OF THE CATAPHORESIS TUBES

Two cataphoresis tubes were constructed and sealed to the manifold. Only one of these was in fact used because leakage of neon through control taps 2 and 3 did not allow sufficient time

FIG.20 CATAPHORESIS TUBE

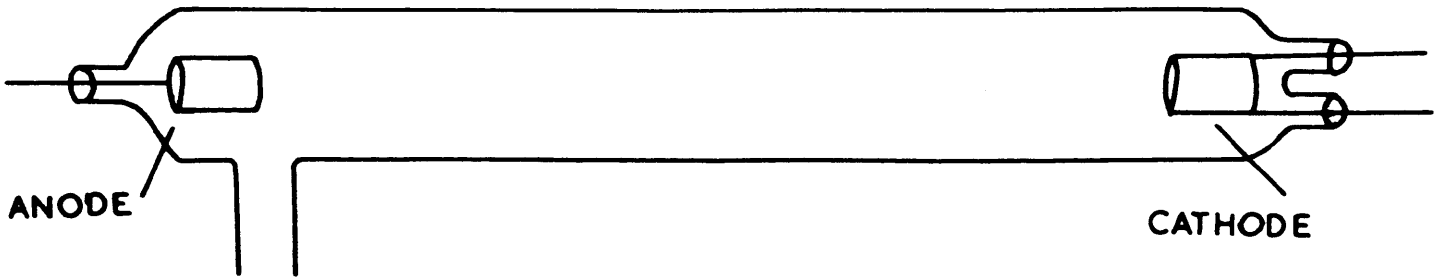

FIG. 21 WATER COOLED CATHODE

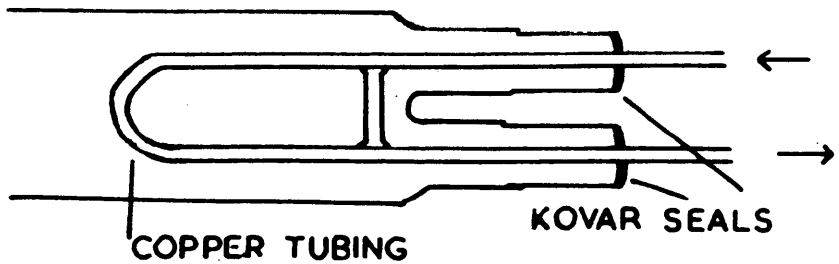

for the high current cataphoresis tube to be brought into operation.

The cataphoresis tube used in the experiments is shown in Fig. 20. Both electrodes were cylinders of 'O' nickel, 1 cm diameter and 2 cms long. This electrode shape could be easily outgassed by eddy-current heating. The enhanced field at the edge of the cylinder made the discharge easier to start. The cathode was supported by two 1 mm diameter tungsten rods passing through the glass. These rods were cooled externally by a heavy copper lead with one end in a water reservoir. The anode was supported by a single tungsten rod. The envelope was constructed of 4 cm diameter Pyrex glass. The distance between the electrodes was 25 cm. The cataphoresis tube was connected to the manifold by a $\frac{1}{2}$" diameter tube near the anode end.

The second cataphoresis tube, which was attached to the manifold but not used, was of basically similar construction except that the cathode consisted of a loop of 3/16" diameter copper tubing brazed to two 1/4" diameter Kovar seals, as shown in Fig. 21. A copper strip brazed across the tubes formed a loop for eddy-current heating. It was intended to cool this cathode by a flow of water through the copper tube so that a high cataphoresis current could be used without overheating the cathode.

The simple cataphoresis tube was kept running continuously throughout experimental measurements of formative

time lags. A discharge current of about 40 mA was obtained from a D.C. power supply supplemented with H.T. batteries. Starting of the discharge was assisted by the use of a high frequency leak detector.

4.6. THE ELECTRICAL CIRCUIT

At voltages near the sparking potential of the gap the temporal growth of current leading to Townsend breakdown becomes extremely sensitive to small voltage changes. For example, a change in the over-voltage from 0.05% to 0.5% might change the formative time lag from 50 msec to 16 msec. For a sparking potential of 300 volts this corresponds to a voltage change of less than 1.5 volts in 300. Considerably better voltage stability than this would be required to measure formative time lags at over-voltages of 0.5% or less. Formative time lags are measured by applying a step voltage to the gap. The rise time of the step must be short in comparison with the time lag to be measured. This requirement is less difficult to meet for neon than for some other gases, such as hydrogen, where the time lags are much shorter. The formative time lag for neon at 5% over-voltage is about 1 msec. A liquid mercury switch with a rise time of a few μsec can therefore be used to provide the step voltage. The voltage output is required to be continuously and finely variable up to about 500 volts. It was

FIG.22 ELECTRICAL CIRCUIT

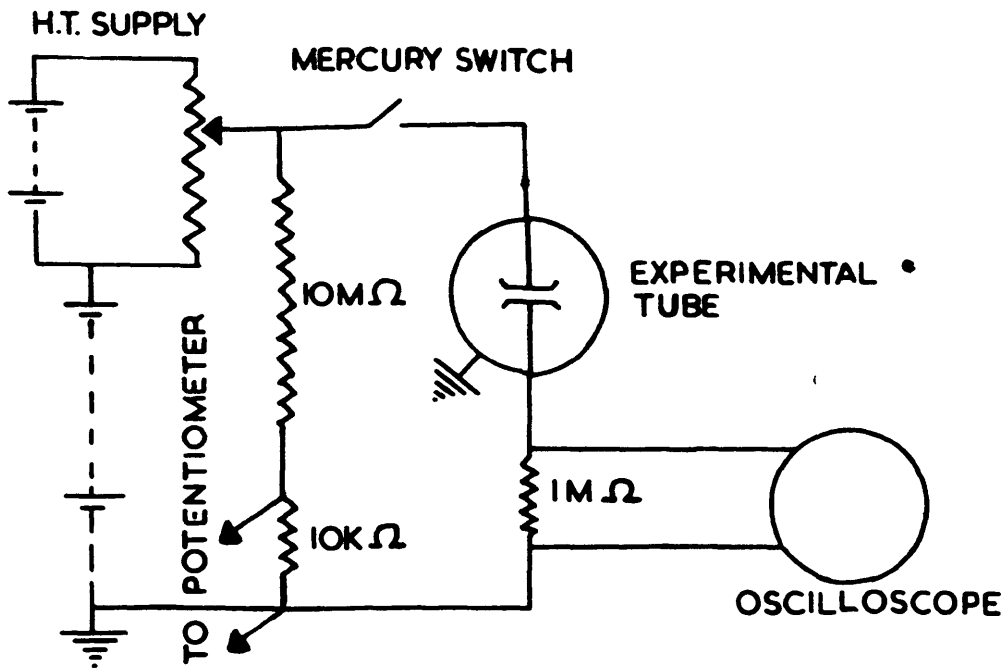

not thought desirable to use a continuously applied backing voltage (over-volting the gap with an additional voltage pulse) since this violates the initial boundary condition, used by Davidson, that the current in the gap be zero for $t < 0$. Previous experimental work by the author (1963) has shown that the use of a backing voltage can alter the temporal growth of current, particularly where an insulating layer is present on the cathode. The entire voltage step was therefore obtained by using a mercury switch and a bank of high tension batteries as shown in Fig. 22. The voltage was measured with a calibrated resistance divider and a potentiometer. The current flowing through the gap after breakdown was limited by a 1 MΩ resistor in series. The current rise in the gap at breakdown was observed by displaying the voltage drop across this resistor on a Textronic 545A oscilloscope. Quickly changing currents less than 1 μA could be easily observed by this method, the time constant of the circuit being of the order of 1 μsec. A current of 5×10^{-7} Amps was normally used as the criterion for breakdown. This value was not particularly critical because of the fast rise of the current above this value.

The measurements of formative time lag as a function of over-voltage obtained from the experimental tubes 1 and 2 will be described in the following chapter.

CHAPTER V.

EXPERIMENTAL RESULTS

5.1. INTRODUCTION

No reliable formative time lag results were obtained with Tube 1. Some of the preliminary results are included to show the effect of cataphoresis. The results used in the calculations described in Chapter VI were obtained with Tube 2. Some of the later results obtained were thought to be slightly unreliable as a result of the apparent release of some impurity gas, caused by the failure of a mercury switch.

5.2. EXPERIMENTAL PROCEDURE WITH TUBE 1.

After the system had been evacuated, baked and outgased, the bakable tap 1 was closed to seal the manifold from the pumping system. The gold film was then evaporated on to the glass electrodes. After final pumping with the Bayard Alpert gauge, the neon control taps 2 and 3 were closed and the neon reservoir opened by breaking the glass 'pig's tail'. The gas was then let into the system in small quantities by operating taps 2 and 3. For low neon pressure it was found that breakdown in the experimental tube gave a diffuse glow filling the whole tube. The sparking potential increased if the electrode gap was reduced so that breakdown was occurring to the left of the minimum of the Paschen curve (V_s as a function of $p_o d$ where V_s is the sparking potential, p_o the pressure reduced to 0^oC

FIG. 23 TYPICAL CURRENT GROWTH CHARACTERISTICS FOR TUBE I.

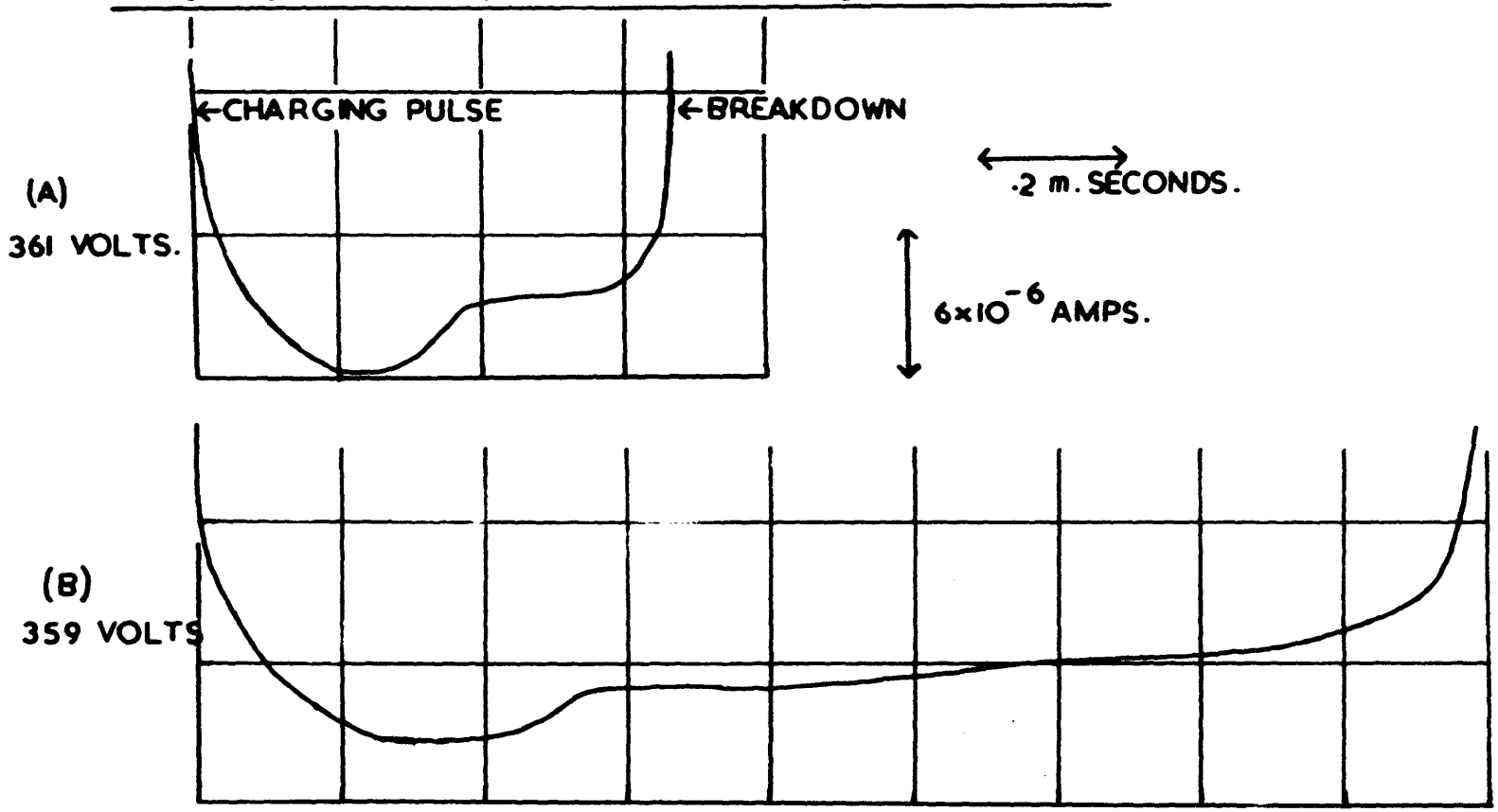

and d the gap distance). The pressure was increased until breakdown occurred to the right of the Paschen curve minimum.

The cathode was illuminated by a high pressure mercury lamp giving a high output in the ultra-violet region. This lamp was originally operated from a 2kV A.C. supply. However it was found that this caused 50 cycle modulation of the current flowing through the experimental tube because of modulation of the initial photo-current I_o. This problem was avoided by running the lamp from a 500 volt D.C. supply using a 60 watt light bulb in series as a ballast resistor.

With tube 1 it was found that the current growth occurred in two distinct stages. The current first rose to a limited value, the magnitude of which depended on the voltage. In the event of the voltage being sufficient this first stage was followed by complete breakdown, the current being unlimited by the gap. Two examples of the growth of current with time are shown in Fig. 23. During the first stage of breakdown a filamentary neon discharge was visible between the points on the electrodes where the tungsten rods contacted the gold films. The effect was probably due to a poor electrical connection between the tungsten and the gold film.

5.3. EXPERIMENTAL MEASUREMENTS WITH TUBE 1.

In formative time lag experiments it is necessary to compromise between making a large number of observations of the time

lag to improve accuracy, and completing all the measurements for several values of overvoltage before the pressure or temperature of the gas has had time to change. The interval between successive applications of the voltage can sometimes affect the breakdown. For example, if the interval is too short, some of the active particles from the previous breakdown may still be present. If charged particles from the discharge can reach an insulating surface near the discharge the surface may remain charged for some time after the discharge has ceased. This is not likely to be serious in the tubes used, since exposed glass surfaces have been kept well away from the discharge region. The absence of this effect was demonstrated by the fact that the formative time lag and sparking potential were not seriously affected by variation of the interval between successive breakdowns.

The procedure adopted was to measure 10 successive time lags for a given overvoltage with a standard interval of 10 seconds between each application of the voltage. The applied voltage was measured before and after each set of time lags. The sparking potential was measured by applying the voltage to the gap at 10 second intervals, reducing the voltage very slightly between each application. The lowest voltage for which the gap would just break down was then measured. The sparking potential was measured between each set of formative time lag measurements, since a small variation

FIG. 24
THE EFFECT OF CATAPHORESIS ON FORMATIVE LAG FOR TUBE I.

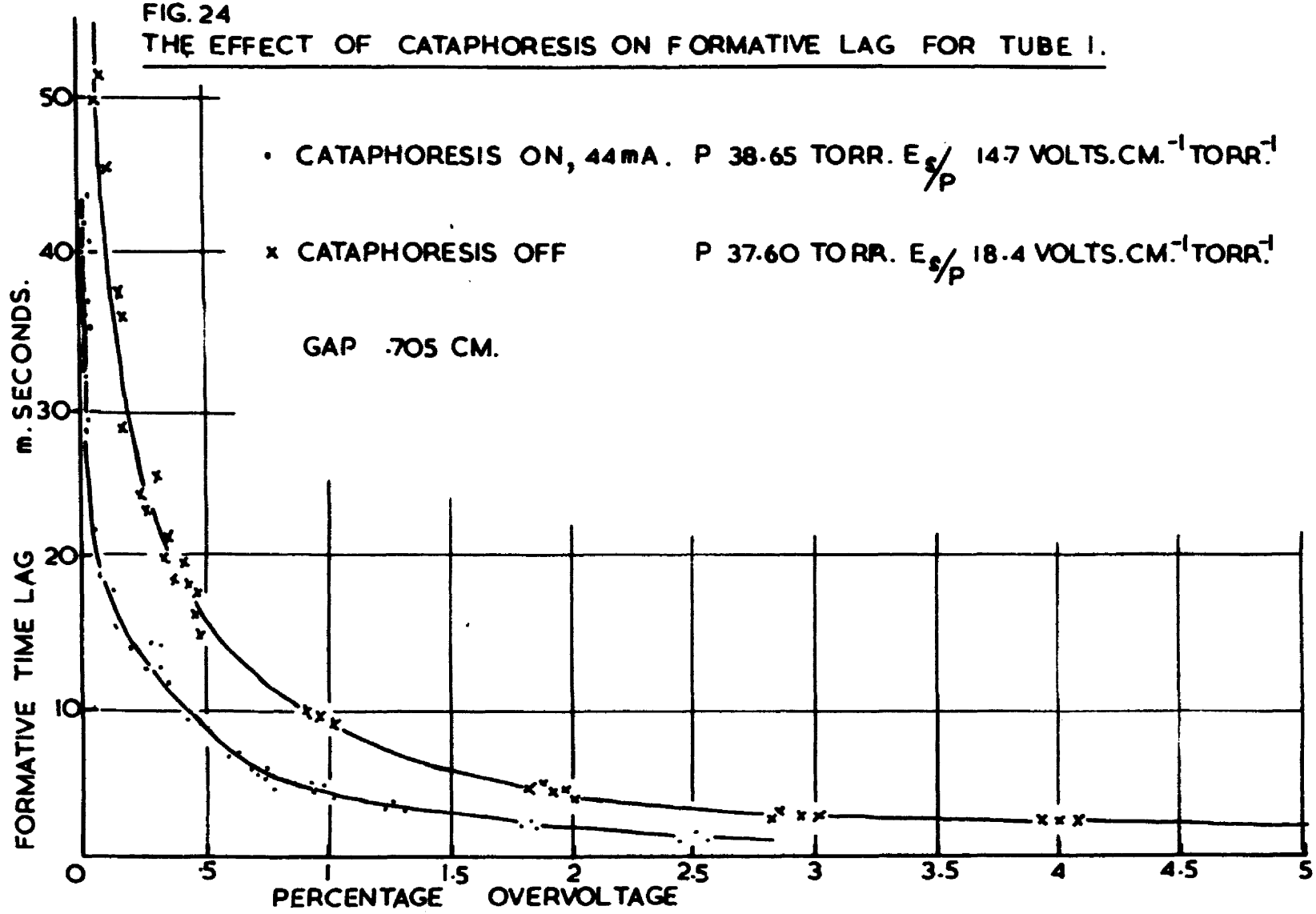

FIG.25 THE EFFECT OF CATAPHORESIS ON SPARKING POTENTIAL TUBE I.

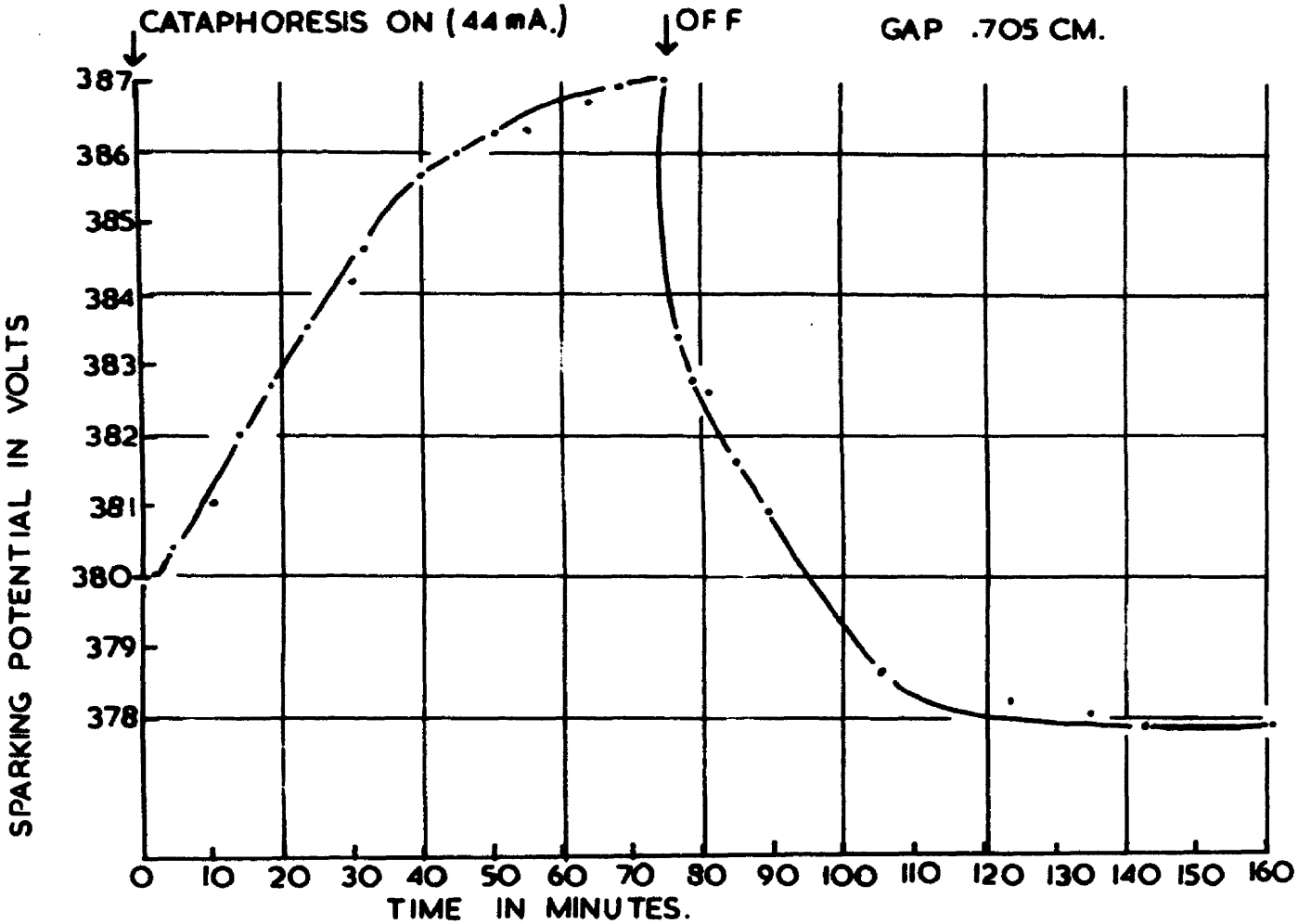

in the sparking potential could result in a large error in over-voltage. Formative time lags were measured for a number of over-voltages between 0 and 5%. The neon pressure was measured on the oil manometer of the auxiliary system using the spiral gauge to indicate equality of pressure between the two systems. This pressure was reduced to a temperature of $0^{\circ}C$.

A D.C. discharge of 44 mA in the cataphoresis tube caused a reduction in the formative time lag, as shown in Fig. 24. However, all or part of this effect could have been due to a rise of about 2% in the pressure when the cataphoresis discharge was running. The sparking potential increased slowly after starting the cataphoresis discharge, reaching a steady value after about 1 hour. This change was reversible and reproducible, falling back to the original value about 1 hour after the cataphoresis discharge had been switched off. This effect is shown in Fig. 25.

The reversible change in sparking potential appeared to be slower than the pressure change. However the pressure change was difficult to follow because of the lack of sensitivity of the spiral gauge system. In the later work with tube 2, with a more sensitive spiral gauge system, the pressure change could be followed more accurately and it was found that the change in sparking potential resulting from the operation of the cataphoresis discharge was accounted for by the corresponding change in pressure.

No attempt was made to apply Davidson's theory to the results from Tube 1 because of the complex form of the current growth observed at the breakdown of the gap.

5.4. EXPERIMENTAL PROCEDURE WITH TUBE 2.

The results finally used in calculations of secondary ionization coefficients using Davidson's theory were obtained with the second experimental tube with nickel electrodes. After the final pump down of the ultra-high vacuum system the 'pig's tail' of the neon reservoir was broken and neon let into the system, using the bakable taps 2 and 3. Unfortunately neither of these taps would close completely. This was the result of a series of vacuum system failures during the baking process caused by faulty metal-to-glass seals on these taps. The seating of the taps had been damaged by small glass fragments and by oxidation. The failure of these taps to close completely resulted in a continuous rise in the neon pressure. This rise was slow enough to enable formative time lag measurements to be made, but did not allow the consistency of results at a given pressure to be checked, nor did it allow time for the water cooled cathode cataphoresis tube to be brought into operation. For this reason the measurements of secondary ionization coefficients as functions of E/p_o, d, and p_o, which are given in Chapter VI, are somewhat limited.

FIG.26 THE EFFECT OF CATAPHORESIS ON SPARKING POTENTIAL FOR TUBE 2.

GAP .456 CMS. CATAPHORESIS CURRENT 50 mA.

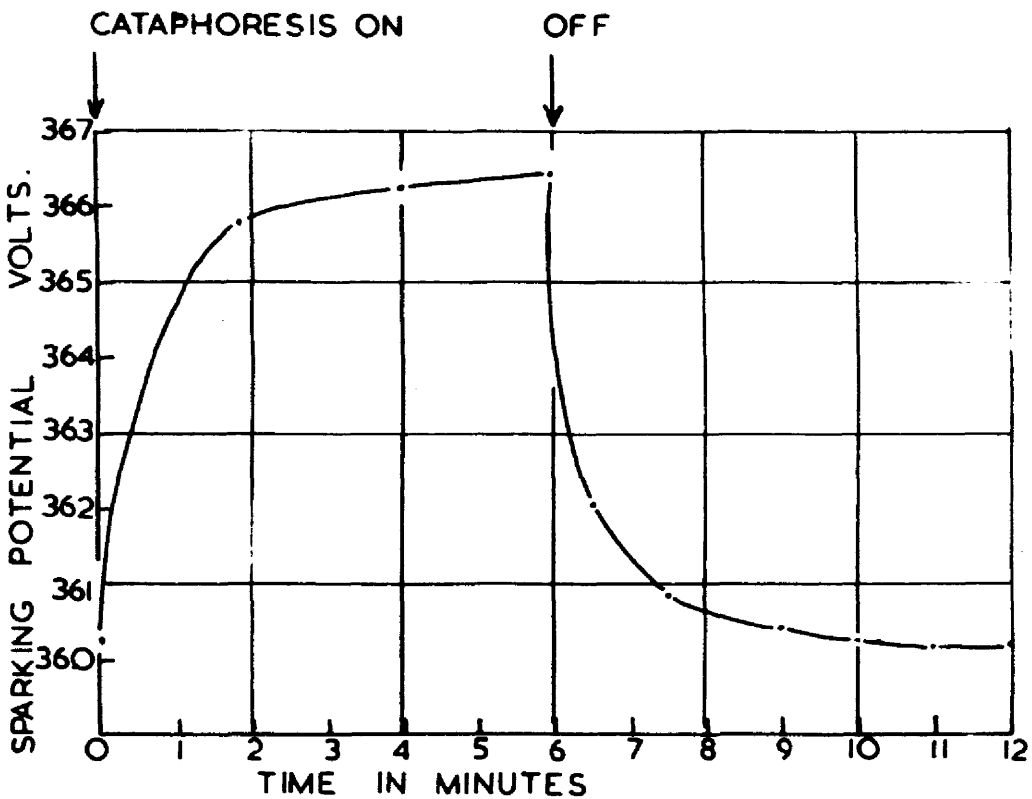

FIG 27 THE EFFECT OF CATAPHORESIS ON PRESSURE FOR TUBE 2 GAP ·456 CM.

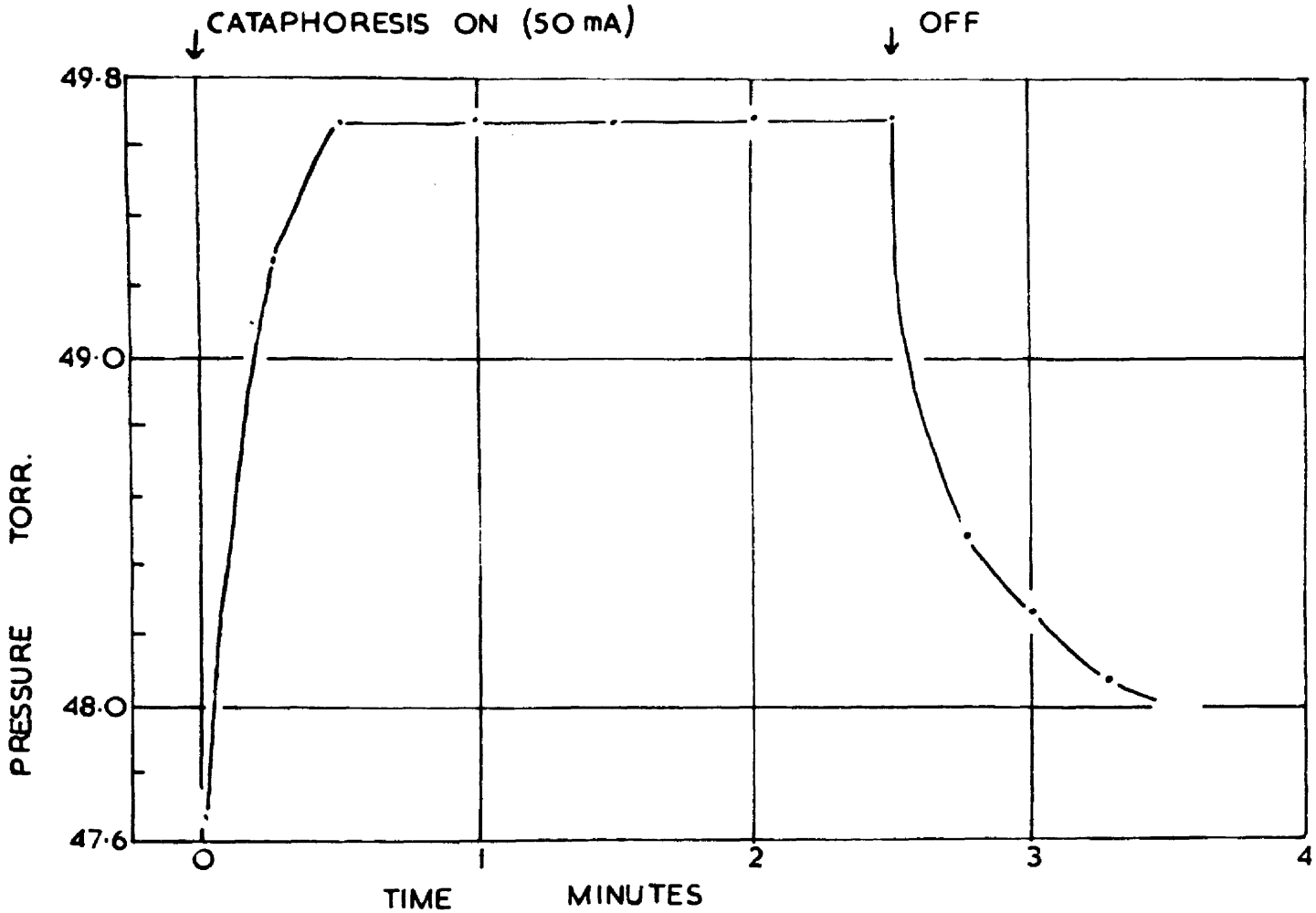

FIG. 28

PASCHEN CURVE SHOWING THE EFFECT OF CATAPHORESIS.

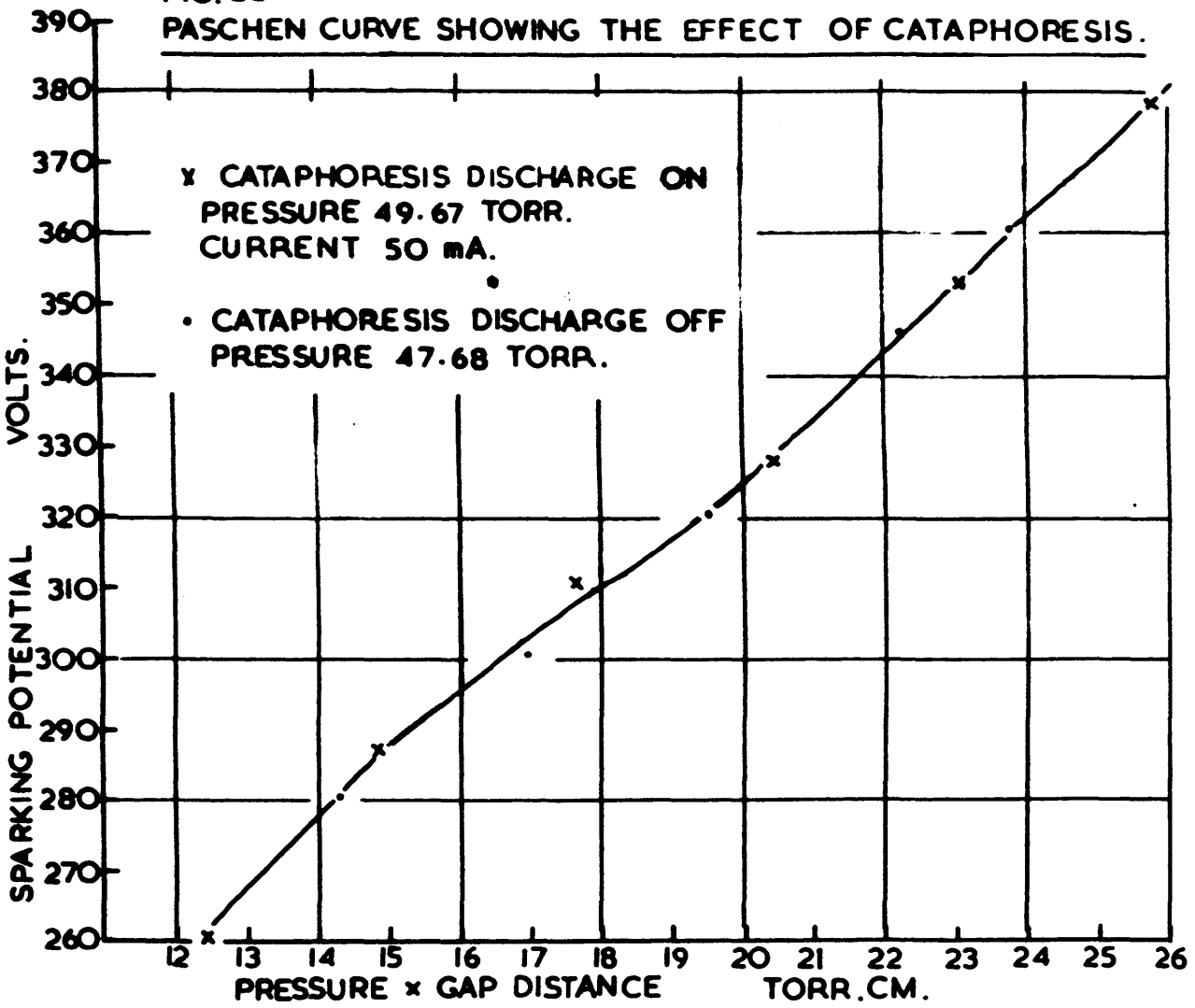

5.5. THE EFFECT OF CATAPHORESIS WITH TUBE 2

As observed with tube 1, the cataphoresis discharge caused an increase in the sparking potential of tube 2 (measured in the way described for tube 1). Fig.26 shows the increase in the sparking potential after starting the cataphoresis discharge. The change was reversible, falling back to the original value after switching off the cataphoresis. The results shown were obtained with a gap of .456 cm. between the electrodes. The neon pressure corrected to $0^{o}C$ was initially 47.68 torr rising to an equilibrium value of 49.67 with a cataphoresis current of 50 mA. The cataphoresis tube was kept cool by a small fan. The corresponding pressure changes could be followed with the improved spiral gauge system. Fig. 27 shows the increase in pressure after switching on the cataphoresis discharge. The pressure reached equilibrium after 30 to 45 seconds. The sparking potential values as a function of $p_o d$ are shown in Fig. 28 with and without the action of a cataphoresis discharge. All the V_s values fall on the same curve within the limits of experimental error. Thus the apparent change in V_s when the cataphoresis discharge is switched on is completely accounted for by the change in pressure of the system.

The effect of the cataphoresis discharge on the temporal growth of current was investigated by measuring the formative time lag as a function of ΔV the overvoltage, with and without cataphoresis.

FIG. 29 FORMATIVE TIME LAGS IN NEON SHOWING THE EFFECT OF CATAPHORESIS WITH TUBE 2

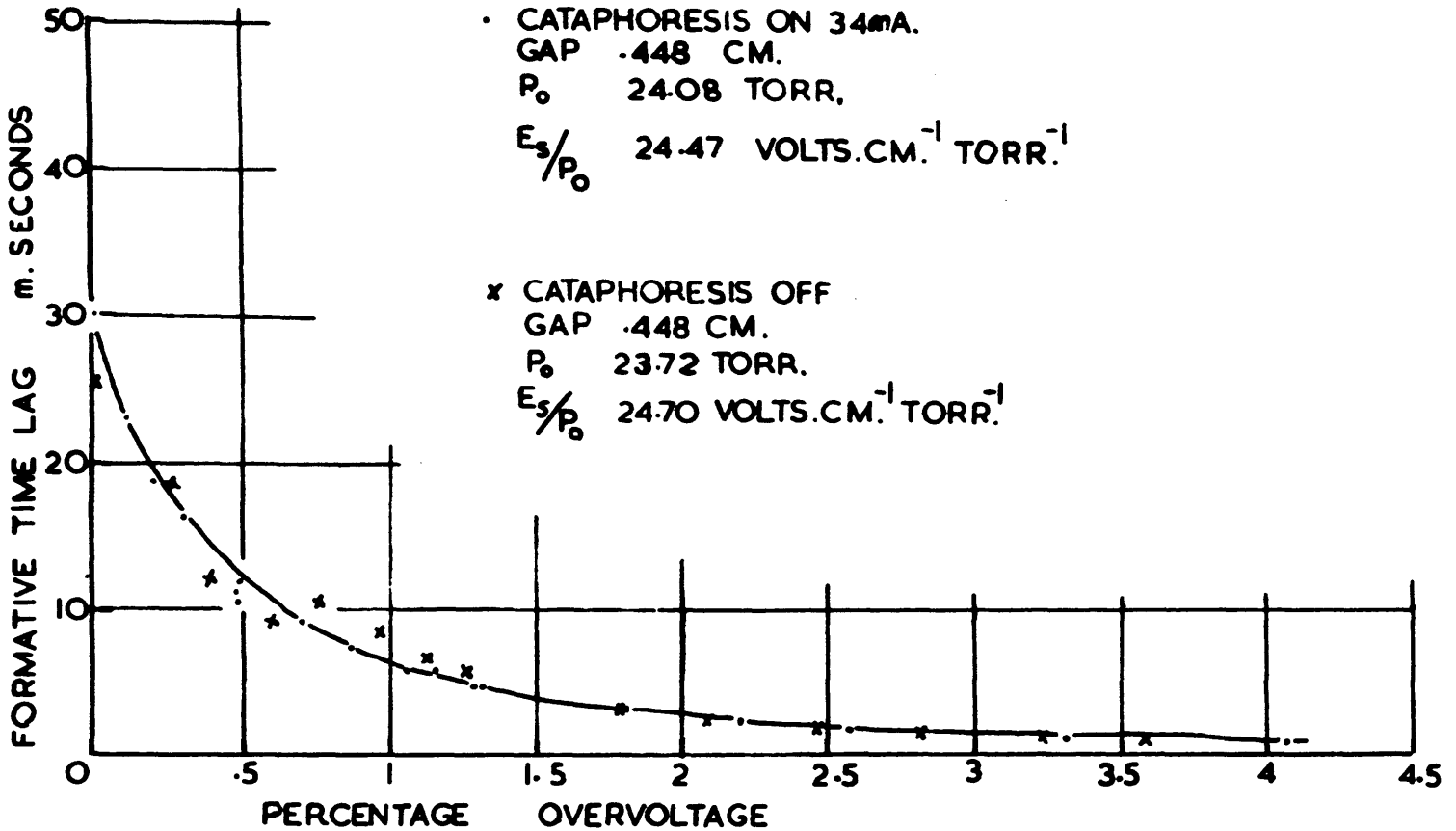

A period of at least half an hour was allowed for the gas composition in the system to reach equilibrium in each case. Fig. 29 shows the measured formative time lags with and without cataphoresis with reduced pressures of 24.08 and 23.72 torr respectively and a gap distance of .448 cm. The cataphoresis current was 34 mA. There is no detectable difference between the two curves. The difference in E_s/p_o for the two curves is small enough to be neglected, so that for these experimental conditions the breakdown of the gap is unaffected by the operation of the cataphoresis discharge. Thus the gas was sufficiently pure without cataphoresis or the cataphoresis discharge was ineffective in removing impurities.

5.6. FORMATIVE TIME LAG RESULTS OBTAINED WITH TUBE 2.

Formative time lags were measured as a function of the overvoltage $\Delta V\%$ for a given value of pressure and gap distance. The formative time lag was taken as the time required for the current in the gap to rise to a value of 5×10^{-7} Amp. An initial current of electrons from the cathode was induced by continuous illumination of the cathode surface with ultra-violet radiation which entered the tube through a quartz window. Five formative time lags were measured for each value of overvoltage, with a standard interval of 10 seconds between each application of the voltage. The breakdown voltage V_s was measured between each set of time lag measurements.

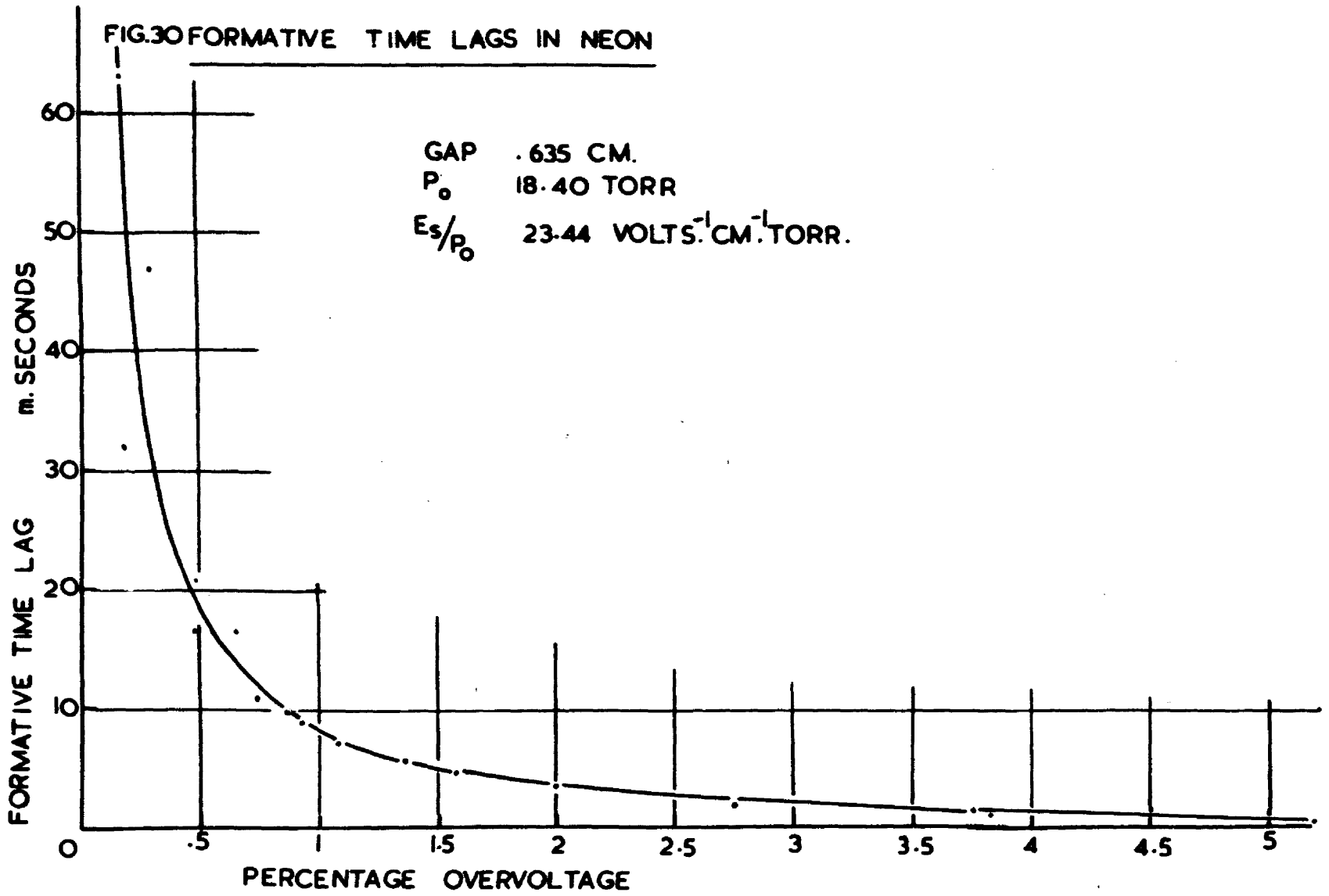
FIG.30 FORMATIVE TIME LAGS IN NEON
GAP .635 CM.
P_o 18.40 TORR
E_s/P_o 23.44 VOLTS^{-1}CM^{-1}TORR.
FORMATIVE TIME LAG m. SECONDS
60
50
40
30
20
10
0
.5
1
1.5
2
2.5
3
3.5
4
4.5
5
PERCENTAGE OVERVOLTAGE

FIG. 31 FORMATIVE TIME LAGS IN NEON

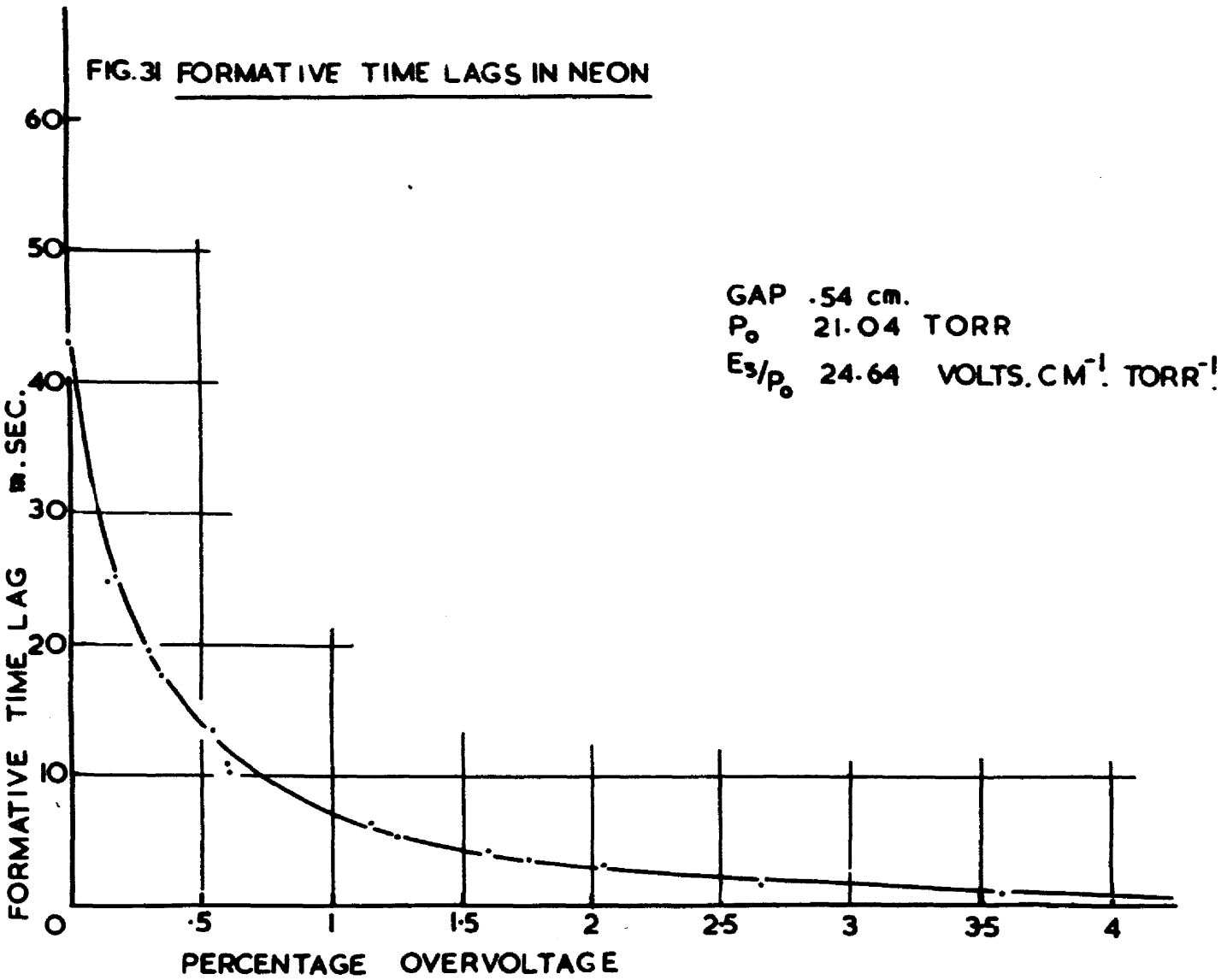

FIG. 32
FORMATIVE TIME LAGS IN NEON

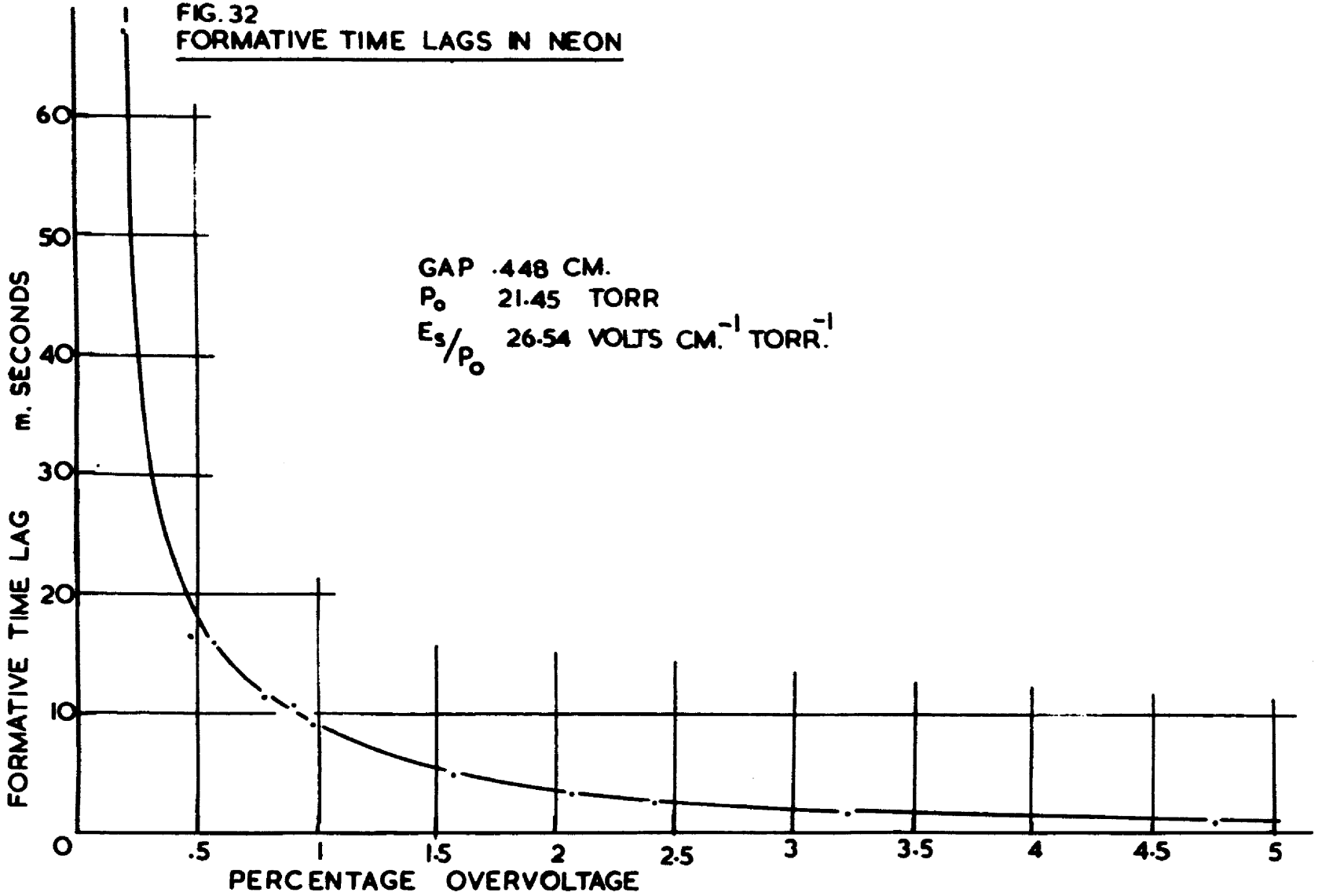

FIG. 33
FORMATIVE TIME LAGS IN NEON

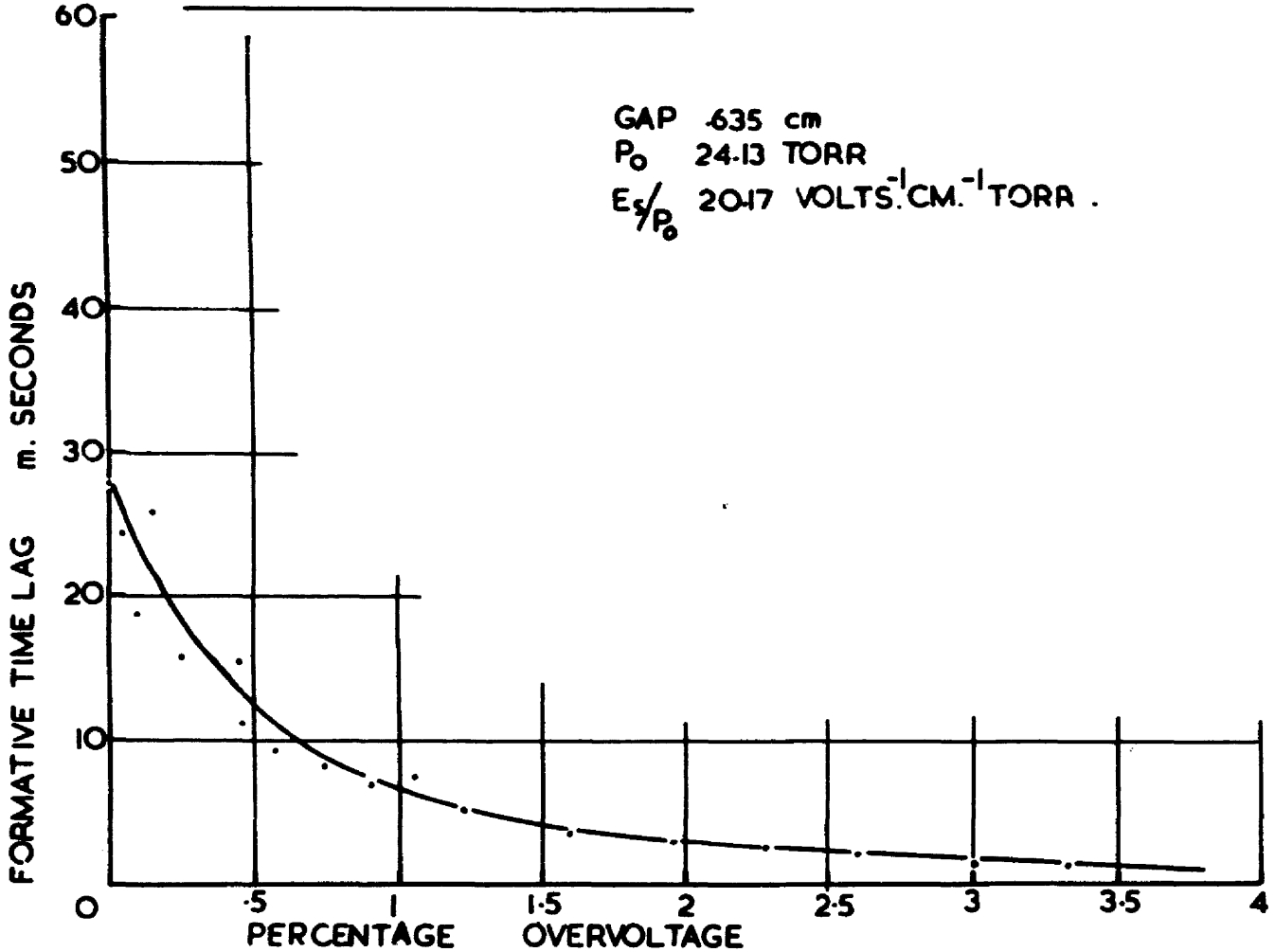

FIG. 34
FORMATIVE TIME LAGS IN NEON

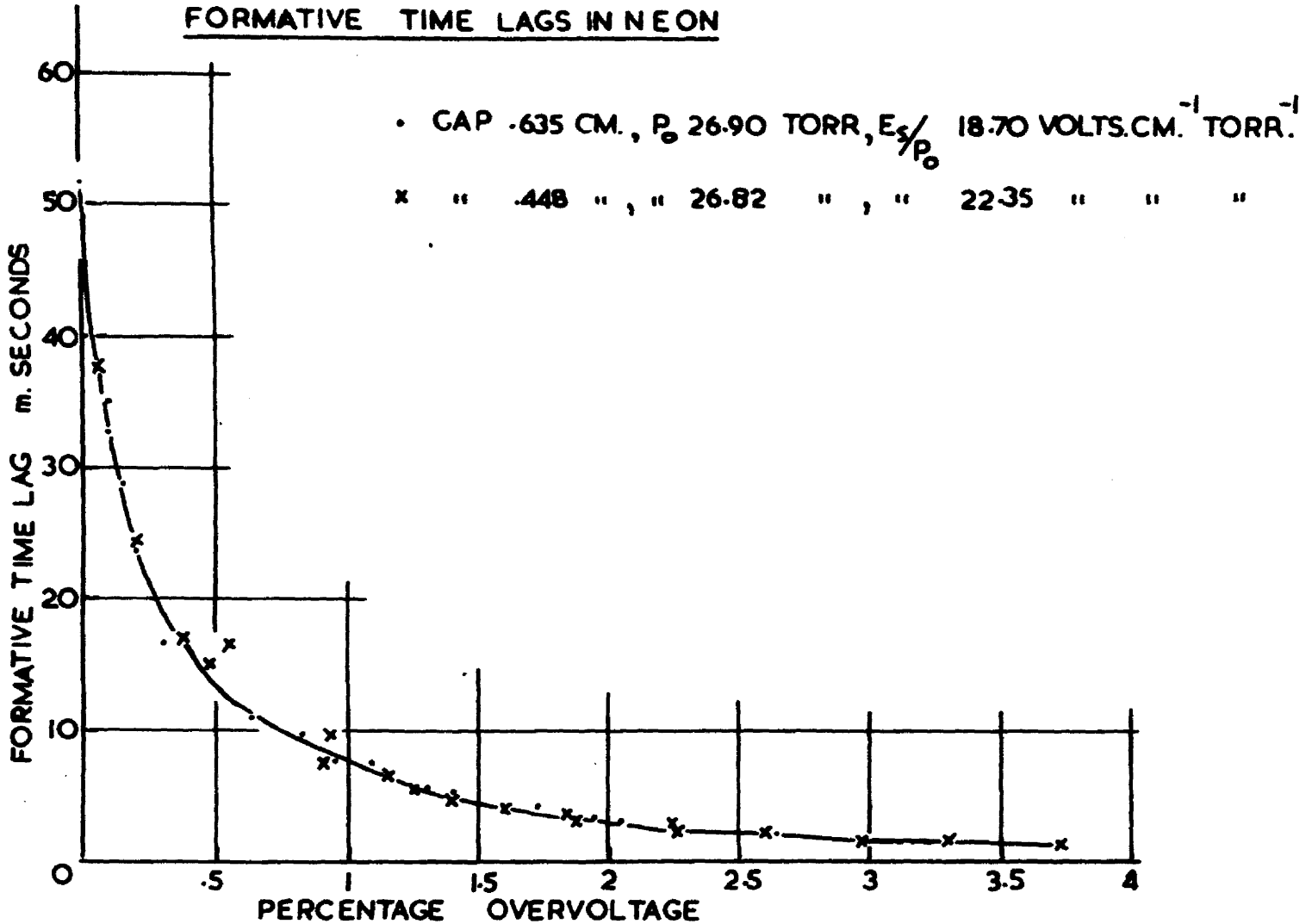

FIG. 35
FORMATIVE TIME LAGS IN NEON.

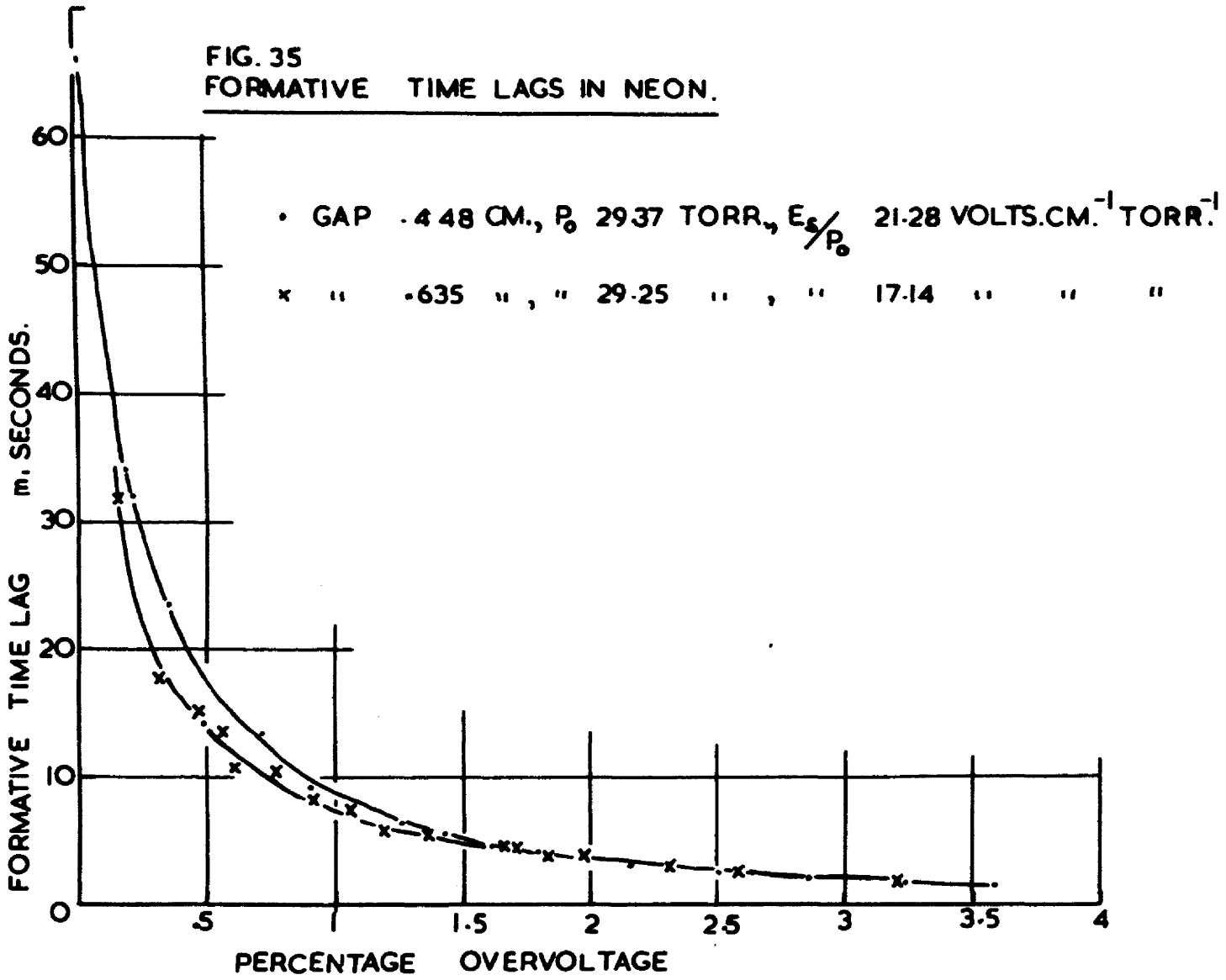

FIG. 36
FORMATIVE TIME LAGS IN NEON

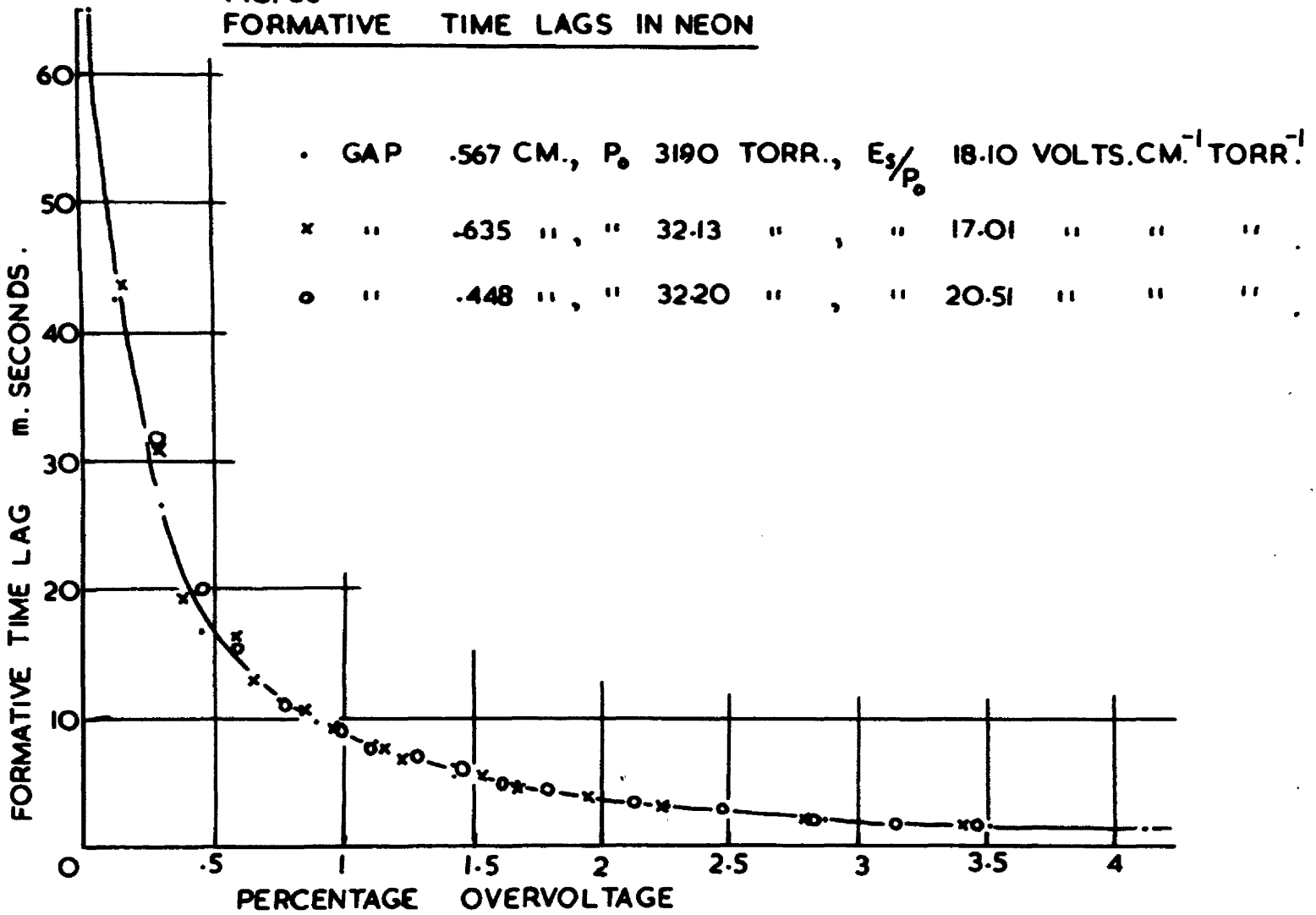

FIG. 37
FORMATIVE TIME LAGS IN NEON

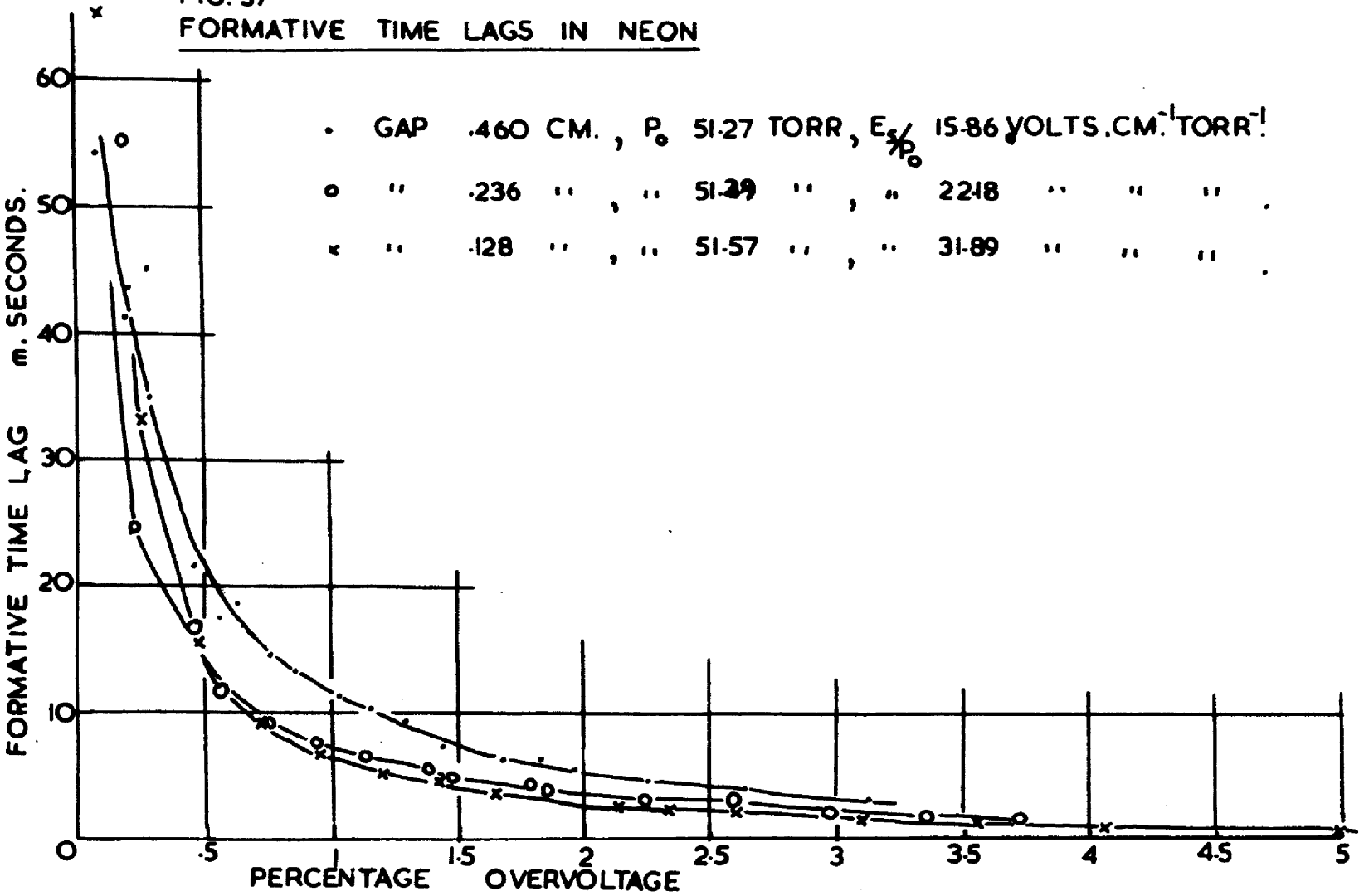

FIG. 38
FORMATIVE TIME LAGS IN NEON.

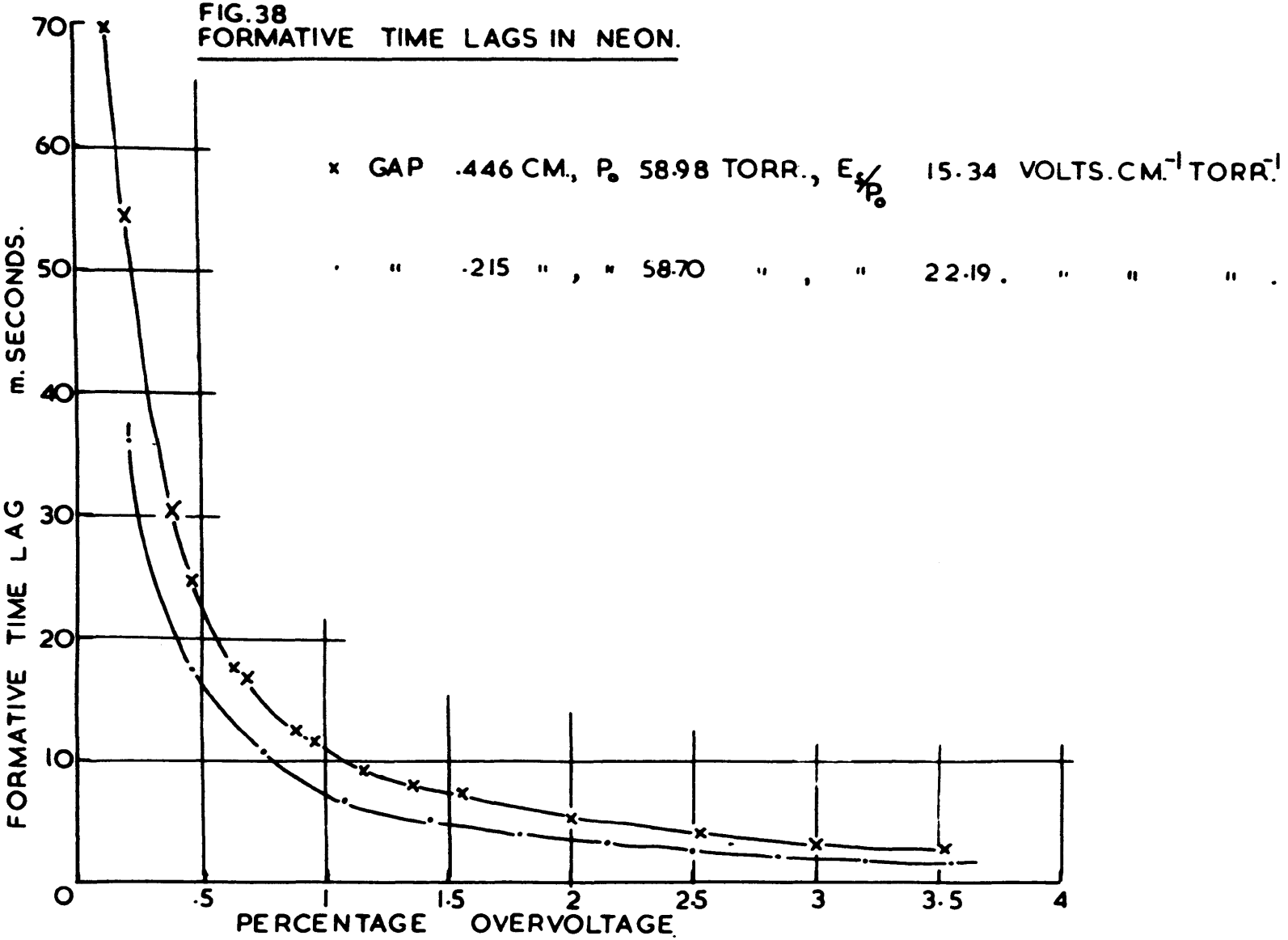

The consistency of the time lags for a given overvoltage was checked over a period of about 30 minutes. A check over a longer period of time was not possible, because of the continuous slow rise in neon pressure resulting from the imperfect closure of taps 2 and 3. All measurements of formative time lag were made with the cataphoresis discharge in operation. Curves of formative time lag as a function of the percentage overvoltage were obtained for pressures from 18.4 to 59 torr and E_s/p_o values from 15.34 to 31.89 volt cm^{-1} $torr^{-1}$. (Expressed in terms of E/N, the field per unit gas density in molecules per cm^3, this is the range 4.35×10^{-16} to 9.00×10^{-16} volt cm^{-1} cm^3.) The electrode separation used varied between .128 and. .635 cm. These curves are shown in Figs. 29-38. For a typical curve the coefficient of variation was approximately 2% at an overvoltage of .2%. For overvoltage above 1% the coefficient of variation fell to below .5%. The data for Figs. 29-38 is included in Table 4 in Chapter VI. The experimental results shown in Figs. 37 and 38 are considered less reliable because of the possibility of gas contamination. Any interpretation of secondary ionization coefficients based on these curves must therefore be considered less certain. Despite this, the experimental results cover a sufficient range of p_o, E_s/p_o and d for broad interpretation to be possible. The analysis and interpretation of the results is given in the final chapter.

CHAPTER VI

DETERMINATION OF SECONDARY IONIZATION COEFFICIENTS USING DAVIDSON'S THEORY

6.1. INTRODUCTION

The theories developed by Davidson, which have been described in Chapter III, enable the formative time lag to be calculated as a function of the overvoltage assuming various secondary ionization processes. The simple theory assumes that electrons may be emitted from the cathode by ions or undelayed photons. Theory I is an extension of this, allowing also for the emission of electrons from the cathode by metastable atoms. This assumes that destruction of metastable atoms in the gas is negligible. Theory II allows for destruction of metastable atoms in the gas with the consequent arrival of delayed photons at the cathode. These theories are used in turn to calculate theoretical formative time lag curves. Comparison with the experimental curves enables possible processes to be eliminated and the important secondary ionization coefficients to be estimated.

6.2. THE SIMPLE THEORY FOR POSITIVE IONS AND PHOTONS

An attempt was made to calculate theoretical formative time lag curves, which agreed with the experimental ones, assuming that the only significant secondary ionization processes were

the emission of secondary electrons from the cathode by photons and positive ions formed in the discharge. The theoretical curves were calculated using Davidson's approximate solution given in Chapter III (page 40). Using the data for the results shown in Fig. 32 the longest possible formative time lags were calculated by assuming that only the slower positive ion process was operative, using the method of solution given on page 41 . The time required for the current to reach a value of 5×10^{-7} Amp with an overvoltage of 1% was calculated. This time was found to be 7.5×10^{-6} seconds which was still about 100 times faster than the experimental time lag. It was therefore concluded that some other, slower, ionization process was required to explain the experimental results.

6.3. DAVIDSON'S THEORY I ALLOWING FOR EMISSION OF ELECTRONS FROM THE CATHODE BY METASTABLE ATOMS

Using Davidson's simple theory, for the positive ion and photon processes, it was possible to solve the equations for λ fairly easily by trial and error. In the more complicated case where the emission of electrons by metastable atoms is considered, this would become an unduly tedious process. The programme outlined below were therefore written to obtain the solution using an IBM 1620 computer.

The solution of equation 29 (Chapter III page 49) for λ could in theory be obtained by an automatic programme which would adjust the value of λ until a sufficiently accurate solution had been obtained. In practice there were some difficulties in using such a programme because it was found that for certain values of the imput data a non-trivial solution for λ did not exist (as will be seen later). It was found more convenient to find λ graphically from values of $F(\lambda)$ as a function of λ calculated by the computer. In the following programmes some of the symbols have been changed from those used in chapter III to make the programme acceptable in Fortran Computer Language. The corresponding symbols are listed below.

$A(I) \equiv \alpha$ primary ionization coefficient.

$G(J) \equiv \gamma' + \delta/\alpha$ positive ion and photon secondary ionization coefficients taken together.

$E(J) \equiv \varepsilon/\alpha$ secondary ionization coefficient for metastable atoms.

$T \equiv \Gamma = \dfrac{\varepsilon/\alpha(\alpha^2 d)(e^{\alpha d}-1)}{(e^{\alpha d} - \alpha d - 1)}$

$F \equiv F = 1 - (\gamma' + \delta/\alpha)(e^{\alpha d} - 1)$

$B \equiv \lambda$

$X \equiv \theta(\lambda)$

$D \equiv d$

The secondary ionization coefficients for the positive ion and undelayed photon processes are taken together in G(J) since both these processes are so much faster than the $\mathcal{E}/\alpha$ process for metastable atoms that they cannot be distinguished by the analysis.

The primary ionization coefficient A(I) is subscripted with the variable I so that the calculations can be performed for several values of A corresponding to different values of overvoltage by means of a "DO" loop. The I values 1, 2, 3, 4 correspond to overvoltages of .5, 1, 1.5, 2%. The subscript J applied to the ionization coefficients G and E enables the calculations to be performed for four choices of the coefficients satisfying the relation:

$$\omega/\alpha = G(J) + E(J).$$

The relationship between X (= $\Theta(\lambda)$) and B (= λ) is obtained by first putting B = A(I) and then decreasing B in small steps since it is known that the required non-trivial solution for which X = 0 lies in the range 0 < B < A(I).

The input data required for programme (1a) is as follows:

4 values of A corresponding to 4 overvoltages.

4 choices of G and E.

D the gap distance.

X AS A FUNCTION OF B FOR DIFFERENT VALUES OF (I,J)

FIG. 39

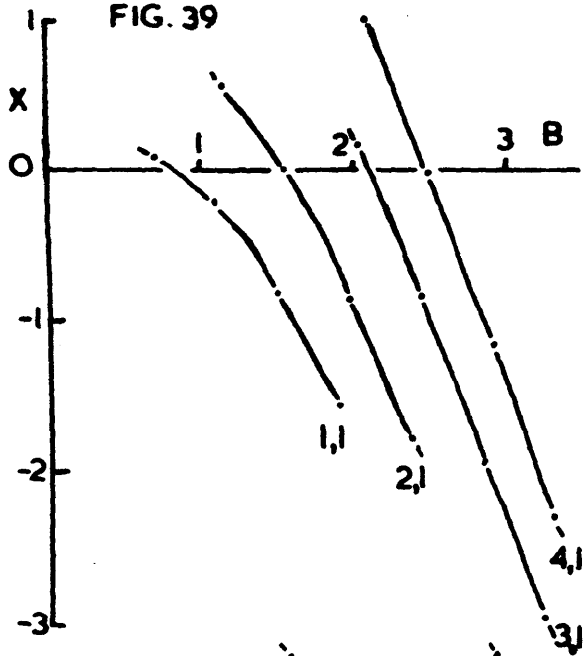

FIG. 41

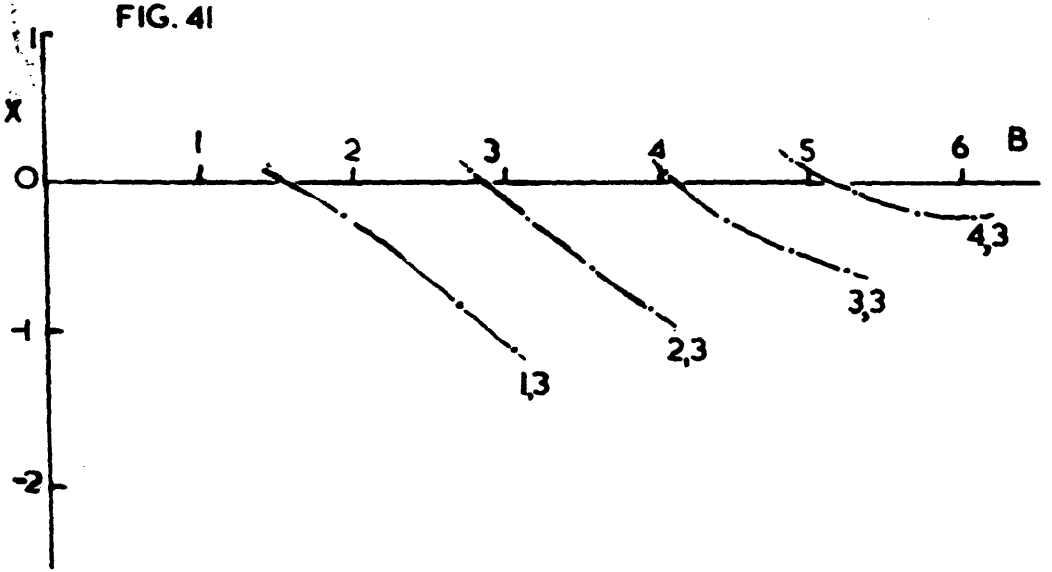

FIG. 40

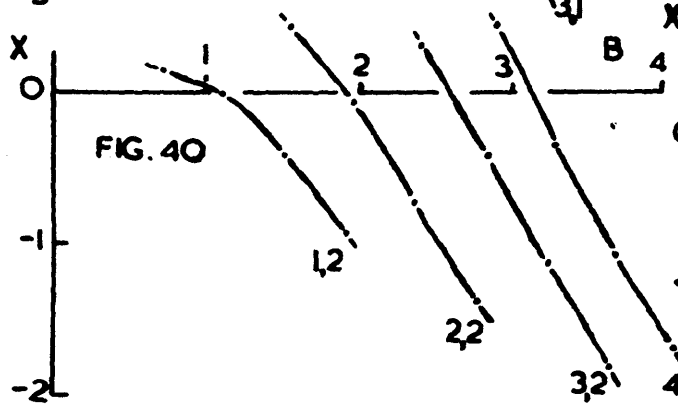

FIG 42

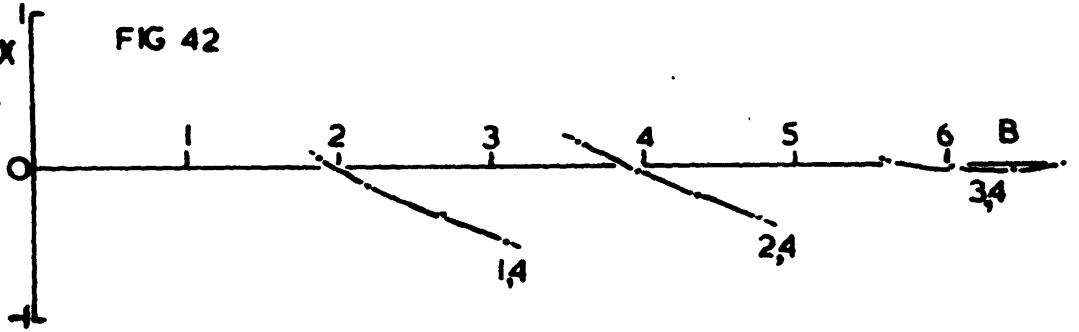

Fortran Programme 1(a)

```
DIMENSION A(4),G(4),E(4)
ACCEPT TAPE 1,A,D,G,E
1 FORMAT (4F10.4)
DO 20J = 1,4
DO 13I = 1,4
T = E(J)*A(I)**2.*D*(EXPF(A(I)*D)-1.)/(EXPF(A(I)*D)-A(I)*D-1.)
F = 1.-G(J)*(EXPF(A(I)*D)-1)
PRINT 8,T,A,F
8 FORMAT (3F10.4)
B = A(I)
9 X = (A(I)-B)*((A(I)+B)*F+T)/EXPF(2.*B*D)+2.*T*B*EXPF((A(I)-B)*D)
      - (A(I)+B)*((A(I)-B)*F+T)
PRINT 11,X,B,I,J
11 FORMAT (2F10.4; 2I2)
1F(X)12,12,13
12 B = B-0.4
GO TO 9
13 PRINT 11, X, B, I, J
20 PRINT 21, I, J
21 FORMAT (2I2)
END
```

This programme calculates X as a function of B for 16 different conditions. The value of B for which X = 0 can then be found graphically giving the value of λ which is required for calculation of the formative time lag. Some typical curves of X as a function of B are shown in Figs. 39 - 42. The values of the subscript I and J are indicated on the curves. Figs. 39-42

are the results of calculations for the experimental conditions of the formative time lag curve shown in Fig. 36 for a pressure of 32.2 torr. It can be seen that as J is increased, increasing the ratio G/E, the curves cut the X = 0 axis at increasingly shallow angles and for the case J = 4, there was only a solution for the first three I values (the three lowest overvoltages).

It is difficult to see any physical reason which would account for this lack of solution at the high overvoltage (2%).

Having determined graphically the value of B to give X = 0, the corresponding formative time lag was calculated using a second programme. This corresponds to equation 26 (Chapter II, page 49), writing

Q for $\frac{i_-(0,t)}{I_o}$, TF for t the formative time lag

DM for D the diffusion coefficient of the metastable atoms.

Fortran Programme 1(b)

```
DIMENSION A(4), B(4,4), F(4,4), T(4,4)
ACCEPT TAPE 1,A,B,F,T,D,Q,DM
1 FORMAT (7F10.4)
DO 20 I = 1,4
DO 18 J = 1,4
P = 2.*B(I,J)*F(I,J)-T(I,J)-2.*T(I,J)*(B(I,J)*D-1.)*EXPF((A(I)
   - B(I,J))*D)-EXPF(-2.*B(1,J)*D)*(2.*F(I,J)*D*(A(I)**2.-B
   (I,J)**2.)+2.*D*T(I,J)*(A(I)-B(I,J))+2.*B(I,J)*F(I,J)+T(I,J))
R = (Q*B(I,J)*P)/((2.*(B(I,J)**2.-A(I)**2.))*(1.-EXPF(-2.*B(I,J)*D)))
TF = LOGF(R)/B(I,J)**2.*DM)
18 PRINT 19,I,J,P,Q,R,TF
19 FORMAT (2I2,4F10.5)
20 PRINT 21,I,J
21 FORMAT (2I2)
END
```

The evaluation of the expression P is the determination of $(\frac{\partial \theta}{\partial z})_\lambda$ (equation 27). R is an intermediary used to simplify the calculations.

The value of the neon metastable diffusion coefficient DM used initially was calculated from Molnar's data. (Molnar 1953). He gave DM as 120 ± 10 cm^2 sec^{-1} for the $^3P_2$ metastable atoms at a pressure of 1 torr. It was assumed that DM varied inversely with pressure. Dixon and Grant (1957) showed that the $^3P_2$ and the

FIG. 43
EXPERIMENTAL AND THEORETICAL FORMATIVE TIME LAGS FOR ε/α, γ, AND δ/α PROCESSES.

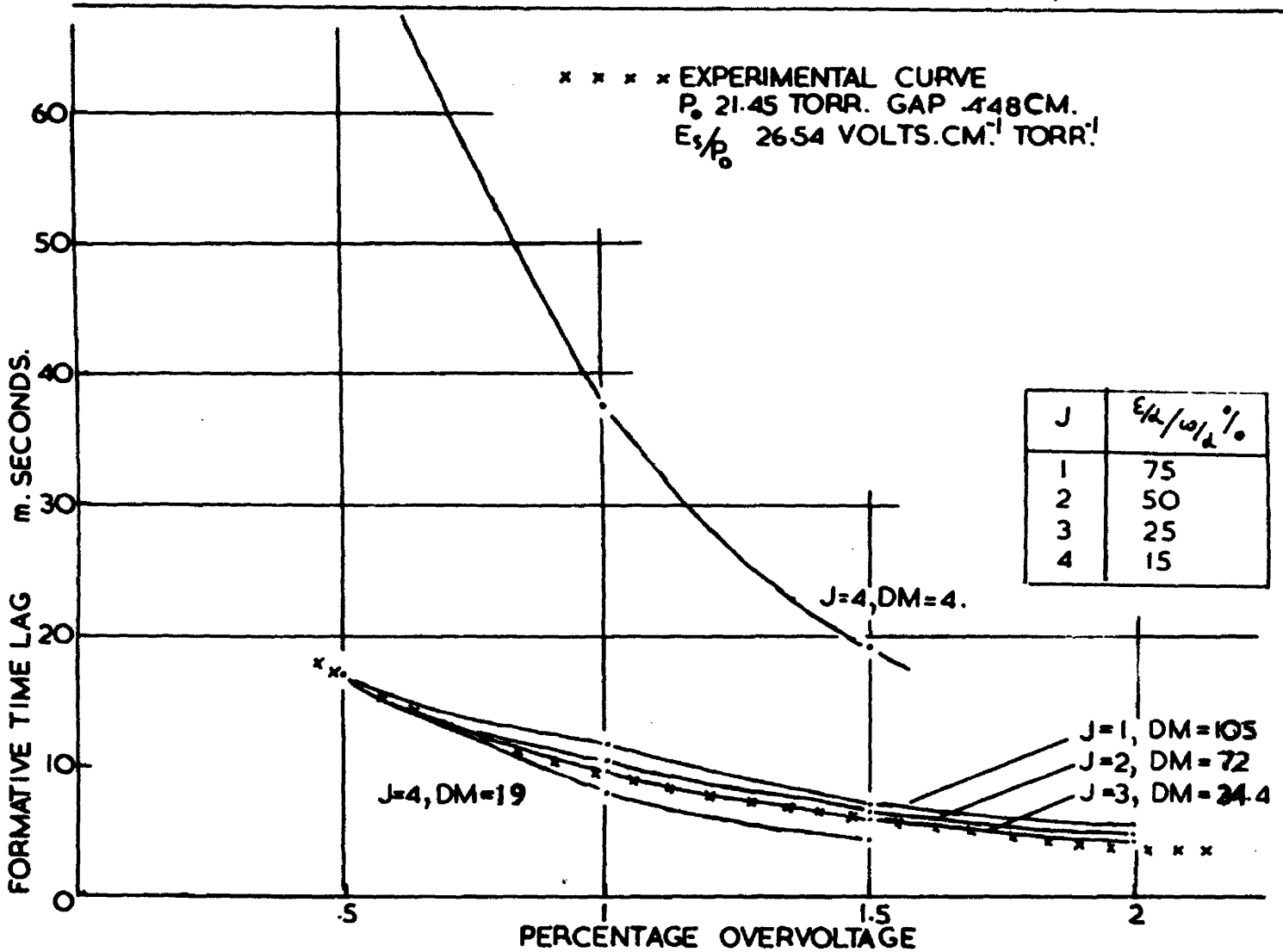

FIG. 44
EXPERIMENTAL AND THEORETICAL FORMATIVE TIME LAGS FOR δ/α, γ, AND δ/α PROCESSES.

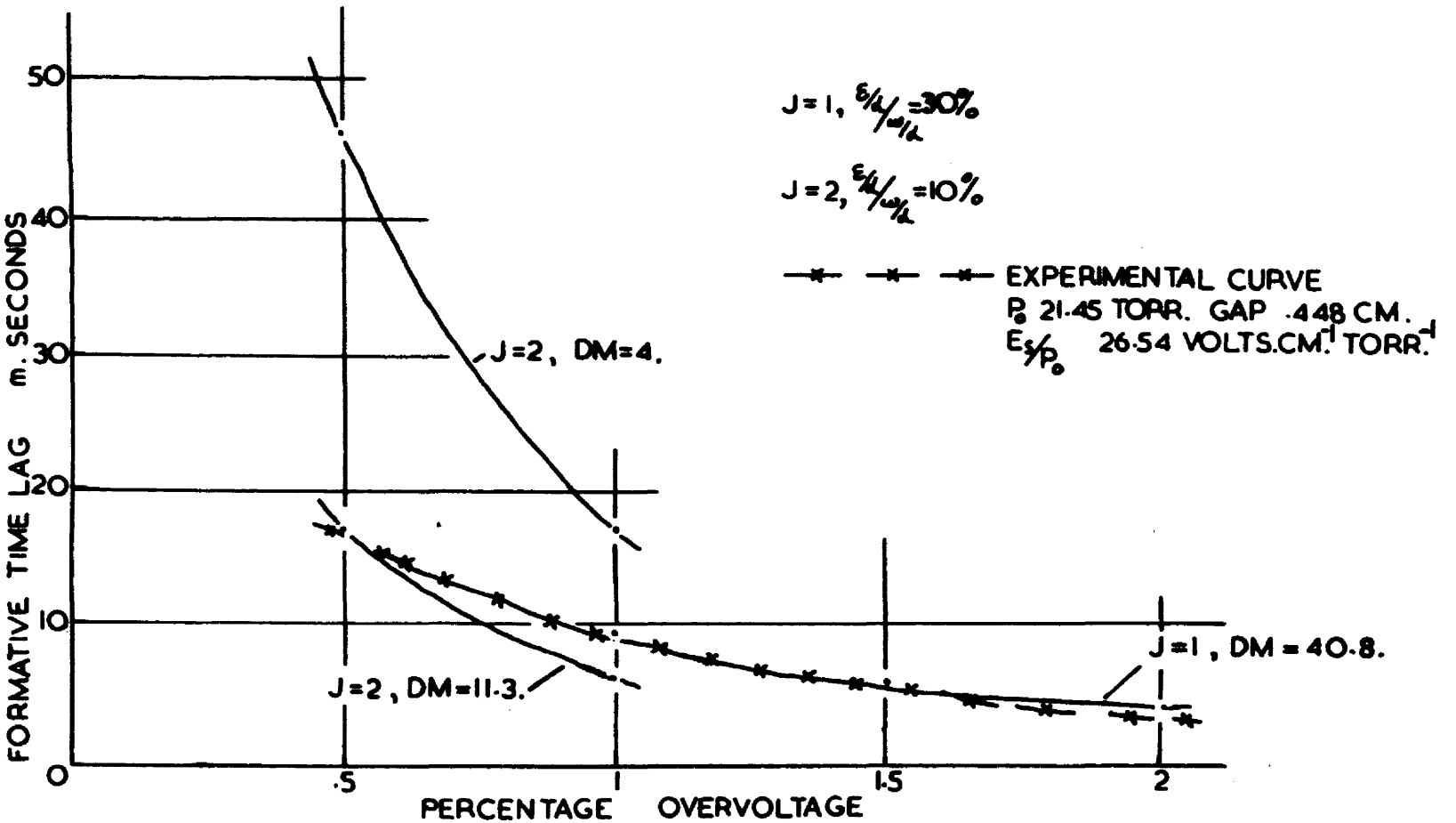

FIG.45 $\frac{\varepsilon/d}{\omega/d}$ AS A FUNCTION OF METASTABLE DIFFUSION COEFFICIENT

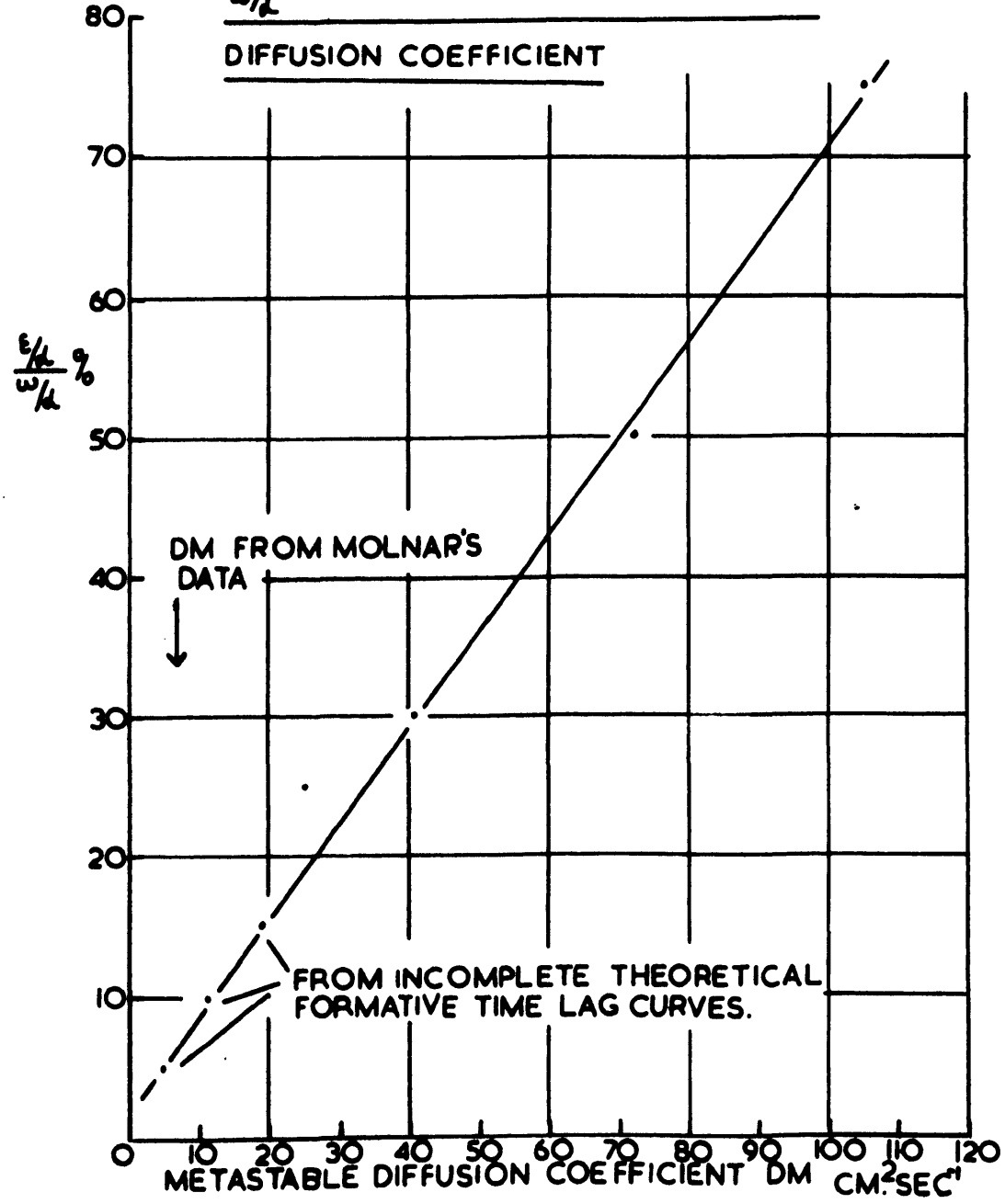

$^3P_0$ metastable atoms had the same diffusion coefficient at low pressures, namely 170 cm^2 sec^{-1} at 1 torr. The value of DM used for the conditions of the experimental results shown in Fig. 36 for a pressure of 32.2 torr was 4 cm^2 sec^{-1}.

The ratio of the breakdown current to the externally induced current Q was taken as 300. In fact the calculated formative time lag was not a sensitive function of Q. Figs. 43 and 44 show theoretical formative time lag curves calculated for the conditions of experimental curve shown in Fig. 32. The curves shown are the ones where closest agreement between experimental and calculated formative time lags was obtained. The analysis showed that a reasonable fit between experimental and theoretical curves could only be obtained using larger values for the diffusion coefficient. The results are summarised in Table 3. Fig. 45 shows these results expressed as a graph of $\frac{\varepsilon/a}{a/a}$ % against DM. From Molnar's data the diffusion coefficient should be $\simeq$ 6 cm^2 sec^{-1} at this pressure. For the lowest values of DM the solutions of the equation X(B) = 0 were incomplete. For DM = 5.5 the analysis only gave a solution at .5% overvoltage so that only one point was obtained on the theoretical formative time lag curve. This cannot be regarded as a fit with the experimental results. Similar calculations for the results shown in Fig. 36 for a pressure of 32.2 torr led to a similar conclusion.

TABLE 3

	J	$\frac{G}{\omega/\alpha}\% = \frac{\gamma_+ \delta/\alpha}{\omega/\alpha}\%$	$\frac{E}{\omega/\alpha}\% = \frac{\varepsilon/\alpha}{\omega/\alpha}\%$	DM
Fig.43	1	75	25	105
	2	50	50	72
	3	25	75	24.4
	4	15	85	19
Fig. 44	1	30	70	40.8
	2	10	90	11.3
	3	5	95	5.5

It was concluded that Davidson's theory for the case where secondary electrons are emitted from the cathode by ions, undelayed photons or metastable atoms cannot account for the breakdown of the gap over a range of overvoltage except for a value of diffusion coefficient which is much too high. In other words the diffusion of neon metastable atoms is too slow to account for the growth of the current. The more approximate theory used by McClore, for the same secondary ionization process in neon, also failed to describe the results satisfactorily (McClure 1962).

6.4. DAVIDSON'S THEORY II ALLOWING FOR DESTRUCTION OF METASTABLE ATOMS AT COLLISIONS WITH GAS ATOMS

Davidson's theory II for the temporal growth of current includes emission of secondary electrons from the cathode by delayed photons released from the destruction of metastable states at collisions with neutral gas atoms. This theory has already been described in chapter III. The detailed application to the practical case of the Townsend breakdown in neon will be given here.

Some of the variables used in equations 47-53 of chapter III have to be changed to suit the Fortran computer programme. The corresponding variables are given below:

A(I)	≡	α	primary ionization coefficient.
D	≡	d	electrode separation.
DT(I,J)	≡	δ_1	where δ_1/α is the ionization coefficient for the delayed radiation process.
P(J)	≡	γ	ionization coefficient for the positive ion process.
T(K)	≡	τ_1	the mean lifetime in seconds of the metastable states.
U	≡	w_-	the electron drift velocity
V	≡	w_+	the positive ion drift velocity
R	≡	$\frac{i_-(o,t)}{I_o}$	
TF	≡	t	the formative time lag.

$B \equiv (e^{\alpha d} - 1)$

$Q \equiv$ p the solution of $F(p) = 0$

$F1 \equiv F'(p)$ the first differential with respect to p of $F(p)$ evaluated at the solution p of $F(p) = 0$

C, G, and H are intermediate expressions used to simplify the programme. The expressions

$$\psi = \alpha - \frac{p}{w_-} \tag{50}$$

and

$$\phi = \alpha - \frac{p}{w} \tag{51}$$

can be simplified if p is small compared with w_- and w ($\frac{1}{w} = \frac{1}{w_-} + \frac{1}{w_+}$). Fortunately, in all practical cases examined the solution of $F(p) = 0$ was such that these approximations were justified. This made the solution of $F(p) = 0$ very much simpler since an explicit expression for p could be written as follows.

If $p \ll w_-$ and $p \ll w$

then $\psi = \alpha$

$\phi = \alpha$

and $$F(p) = 1 - (e^{\alpha d} - 1)\left[\frac{\delta_1}{\alpha}\frac{1}{(1+p\tau_1)} + \gamma\right] \tag{55}$$

If $F(p) = 0$

then $$p = \frac{\frac{\delta_1}{\alpha}\left[\frac{e^{\alpha d} - 1}{1-\gamma(e^{\alpha d}-1)}\right] - 1}{\tau_1} \tag{56}$$

The calculation of the formative time lag, for a given choice of the secondary ionization coefficients σ_1/α and δ and for a given α value corresponding to the value of the overvoltage, is then merely a matter of evaluating a number of complicated expressions.

Fortran Programme 2

```
      DIMENSION A(4),DT(4,4), P(4), T(3)
      ACCEPT TAPE 1,(A(I),I = 1,4)
      ACCEPT TAPE 1,((DT(I,J),J = 1,4), I = 1,4)
      ACCEPT TAPE 1,(P(J),J = 1,4)
      ACCEPT TAPE 2,(T(K),K = 1,3)
      ACCEPT TAPE 3,D
      ACCEPT TAPE 4,U,V,R
1     FORMAT (4F10.5)
2     FORMAT (3F9.0)
3     FORMAT (F10.5)
4     FORMAT (3F9.0)
      DO 20 I = 1,4
      DO 18 J = 1,4
      DO 16 K = 1,3
      B = EXPF(A(I)*D) - 1.
      Q = ((DT(I,J)*B)/(A(I)*(1.-P(J)*B))-1.)/T(K)
      C = DT(I,J)/(U*A(I)**2.*(1.+Q*T(K)))
```

```
      G = U*A(I)*T(K)*B+(1.+Q*T(K))*((A(I)*D-1.)*EXPF(A(I)*D)+1.)
      H = A(I)*P(J)*((A(I)*D-1.)*EXPF(A(I)*D)+1.)/(V*(A(I)**2.))
      F1 = C*G+H
      TF = (LOGF(R*Q*F1))/Q
   16 PRINT 17,Q,C,G,H,F1,TF,I,J,K
   17 FORMAT (3E14.8/3E14.8 3I2)
   18 CONTINUE
   20 CONTINUE
      END
```

This programme used 3 subscripts and 3 DO loops. The subscript I determines the value of α corresponding to one of four values of overvoltage. The subscript J corresponds to the choice of δ_1/α and γ such that $\delta_1/\alpha + \gamma = \omega/\alpha$. γ(=P) is then determined by J and DT ($=\xi_1$) by I and J together. The third subscript K enables the calculations to be repeated for three values of the mean metastable lifetime τ_1.

The Variation of TF with T

The effect of small variations of the metastable lifetime on the formative time lag could be observed by using the approximate relationship between TF and T given below

$$Q \propto \frac{1}{T}$$

$$C \propto \frac{1}{1+QT}$$

FIG.46 THEORETICAL AND EXPERIMENTAL FORMATIVE TIME LAGS

FOR $\delta_{1/2}$, γ, $\delta_{1/2}$ PROCESSES

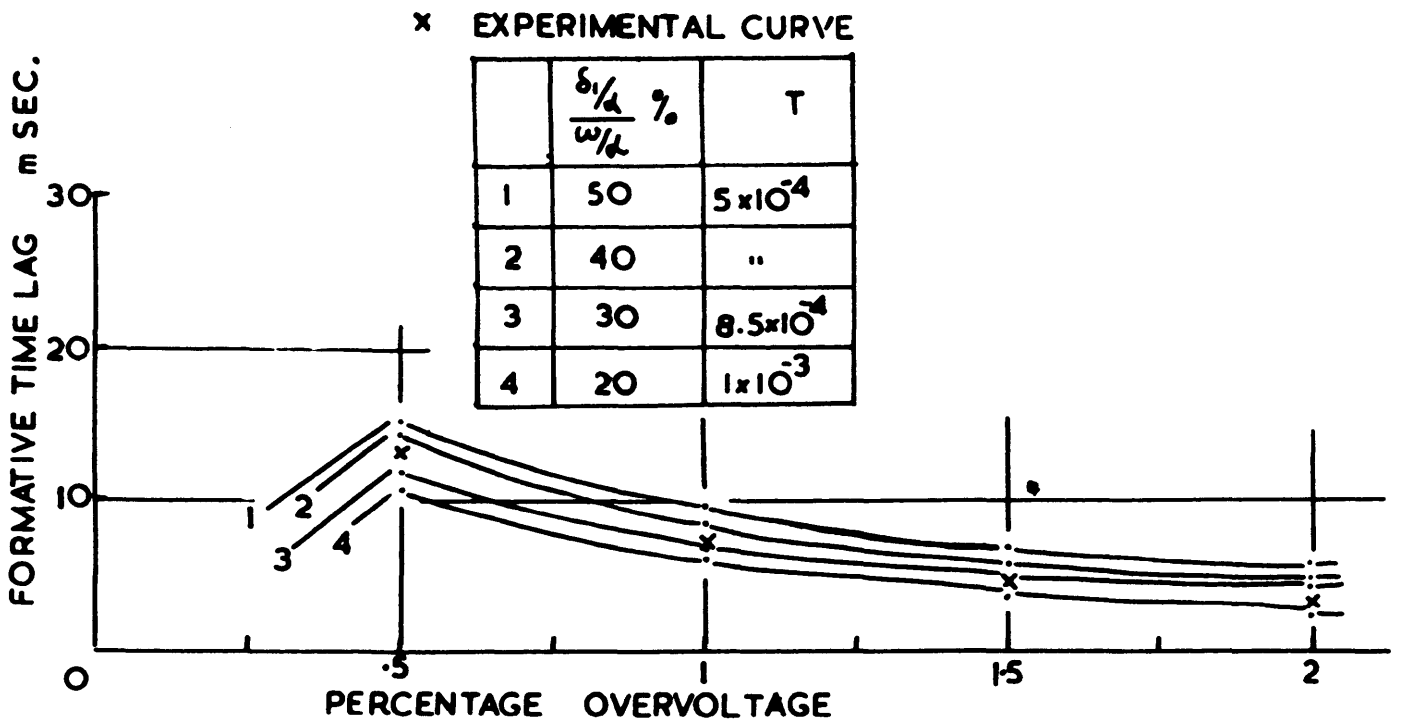

	$\frac{\delta_{1/2}}{\omega_{1/2}}$ %	T
1	50	5×10^{-4}
2	40	"
3	30	8.5×10^{-4}
4	20	1×10^{-3}

But QT is independent of T and therefore C is independent of T. The variation of G with T is mainly determined by the first term so that G $\propto$ T. This is confirmed by the fact that G values calculated for different values of T follow the relationship

$$\frac{G_1}{G_2} = \frac{T_1}{T_2} \text{ to a good approximation.}$$

H is independent of T so that Fl $\propto$ T. The product R*Q*Fl is independent of T. $TF = \frac{LOGF(R*Q*Fl)}{Q}$ is therefore $\propto$ T to a good approximation. This relationship could be used to adjust the value of T to give a better fit between theoretical and experimental curves of formative time lag TF against overvoltage.

The analysis was applied to 17 experimental curves of formative time lag against overvoltage (Figs. 29-38). In most cases a rough fit was found first by using choices of the ratio $\frac{\delta_1/\alpha}{\omega/\alpha}$ covering a wide range (for example 100%, 75%, 50% and 25%). The programme was then re-run covering a narrower range to give a more precise fit. Each programme used 4 choices of $\frac{\delta_1/\alpha}{\omega/\alpha}$, and 3 choices of T giving 12 formative time lag curves covering 4 values of overvoltage (.5%, 1%, 1.5% and 2%). Fig. 46 shows a typical plot of experimental and theoretical time lag results. These are for the experimental results of Fig. 31 with a gap distance of .54 cm, reduced pressure p_o of 21.04 torr, and E_s/p_o at sparking of 24.64 volt cm^{-1} $torr^{-1}$. Only the 4 closest theoretical curves are included.

FIG. 47 $\frac{\delta_{1/2}}{\omega_{1/2}}$ % AS A FUNCTION OF METASTABLE LIFETIME T

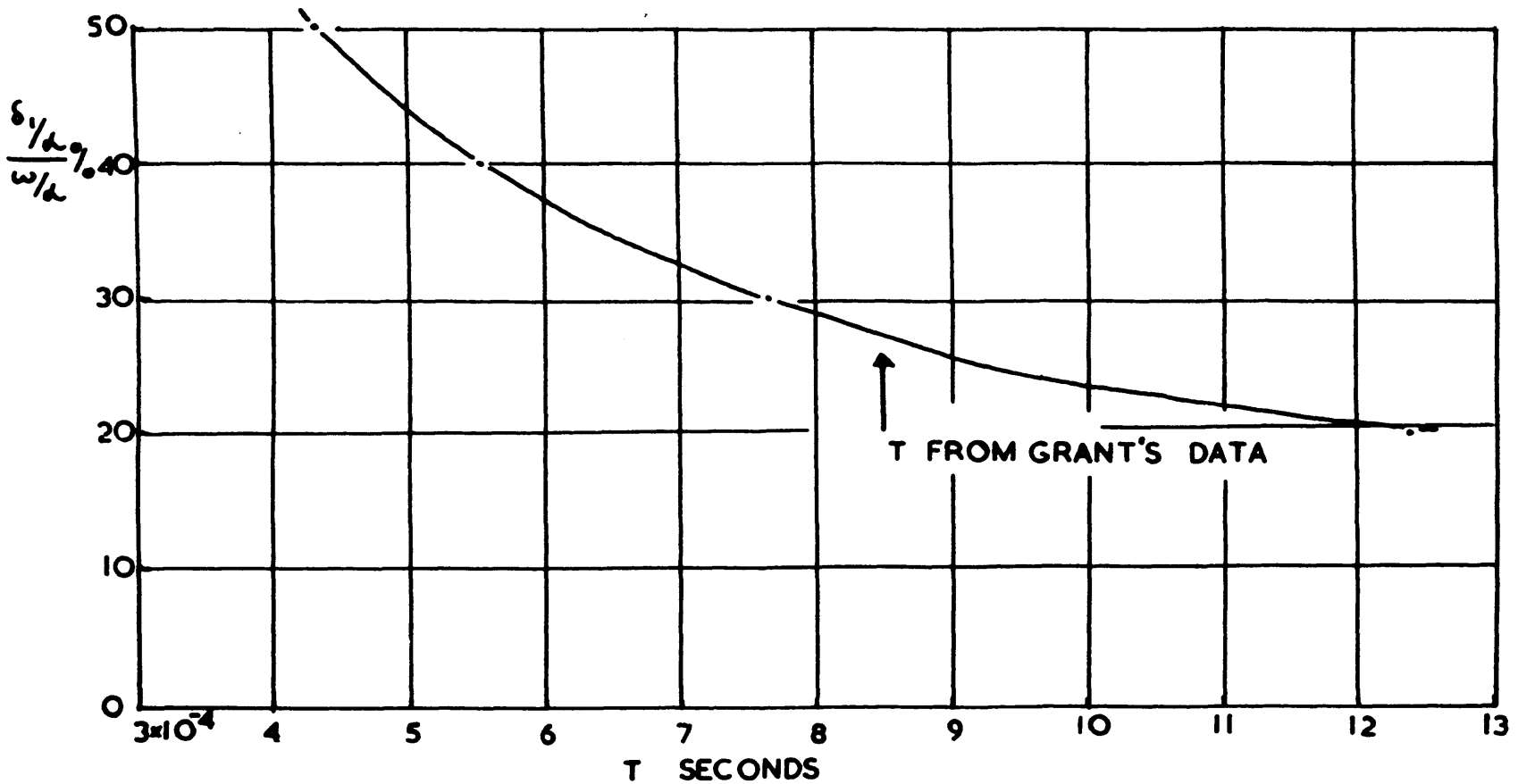

The metastable lifetime, calculated from Grant's empirical relationship (Grant 1951), was 8.5×10^{-4} seconds at this pressure. The theoretical formative time lag curve for $\frac{\delta_{1/a}}{\omega/a} = 30\%$ agrees with the experimental curve within the limits of experimental error. The four theoretical curves shown were adjusted using the approximate proportionality between TF and T to give an exact fit between the theoretical and experimental curves at .5% overvoltage. The relation between $\frac{\delta_{1/a}}{\omega/a}$ % and T is shown in Fig. 47. For a metastable lifetime of 8.5×10^{-4} seconds this curve shows a value for $\frac{\delta_{1/a}}{\omega/a}$ of 27%. For a shorter lifetime a higher $\frac{\delta_{1/a}}{\omega/a}$ value would be obtained.

For all the 17 cases examined it was found that the agreement between the experimental and theoretical curves was adequate in view of the experimental accuracy, the accuracy of data used in the calculations, and approximations involved in the theory. The results of the analysis are summarised in Table 4.

TABLE 4

GRAPH	d	p_o	V_s	E_s/p_o	$p_o d$	$\frac{\omega^2}{c^2}\frac{d^2}{2}$	ξ_1/a	$\frac{\omega^2}{c^2}\frac{d^2}{3}$	γ	ω/a	E_s/N
30	.635	18.40	274	23.44	11.68	20	.011	80	.042	.053	6.60×10^{-16}
31	.54	21.04	280	24.64	11.36	27	.013	73	.035	.048	6.69 "
33	.635	24.13	309	20.17	15.32	15	.007	85	.041	.048	5.88 "
34	.635	26.90	319	18.70	17.08	33	.017	67	.035	.052	5.30 "
* 34	.448	26.82	269	22.35	12.02	21-25	.013 -.017	79 -75	.049 -.047	.062	6.30 "
35	.635	29.25	329.5	17.14	18.57	27	.014	73	.039	.053	4.85 "
* 35	.448	29.37	280	21.28	13.16	29-35	.017 -.021	71 -65	.042 -.038	.059	5.95 "
29	.448	24.08	264	24.47	10.79	23	.013	77	.044	.057	7.05 "
36	.635	32.13	347	17.01	20.40	42	.021	58	.030	.051	4.82 "
36	.567	31.90	327.5	18.10	18.09	39	.021	61	.032	.053	5.40 "
36	.448	32.2	295.7	20.51	14.43	23	.012	77	.041	.053	5.80 "
32	.448	21.45	255	26.54	9.61	26	.015	74	.042	.057	7.50 "
* 37	.46	51.27	374	15.86	23.58	55-62	.026 -.029	45 -38	.021 -.018	.046	4.48 "
* 38	.446	58.98	403.5	15.34	26.30	60-75	.025 -.031	40 -25	.017 -.011	.042	4.35 "
37	.128	51.57	205	31.89	6.60	40	.035	60	.052	.037	9.00 "
37	.236	51.39	269	22.18	12.13	40	.025	60	.038	.064	6.25 "
38	.215	58.70	280	22.19	12.62	35	.020	65	.036	.056	6.26 "

The last column of Table 4 shows the values of E_s/N volt cm^2 where E_s is the electric field at the sparking potential (volt cm^{-1}) and N is the gas density in molecules cm^{-3}. This parameter is now commonly used in place of E_s/p_o (Huxley et al. 1966).

The last five results of Table 4 were considered slightly less reliable because of the possibility of contamination of the neon as discussed in the previous chapter.

For the four results marked with an asterisk a reasonable fit between experimental and calculated time lag curves could be obtained over the range of values of δ_1/α and γ shown. This is because the calculated formative time lag is not always a sensitive function of the ratio $\frac{\delta_1/\alpha}{\gamma}$ and is an intrinsic weakness of the method.

6.5. THE VALUE OF THE PRIMARY IONIZATION COEFFICIENT USED IN THE CALCULATIONS

The value of the primary ionization coefficient α is often a sensitive function of the purity of the gas. The effect is particularly important for neon where the introduction of a small impurity of argon leads to an increase in the value of α because the Penning effect can then operate. In the study of the breakdown of helium by D. K. Davies and Griffiths α measurements were made

FIG.48 α/p_0 VALUES USED IN CALCULATIONS.

(FROM CHANIN AND RORK 1963)

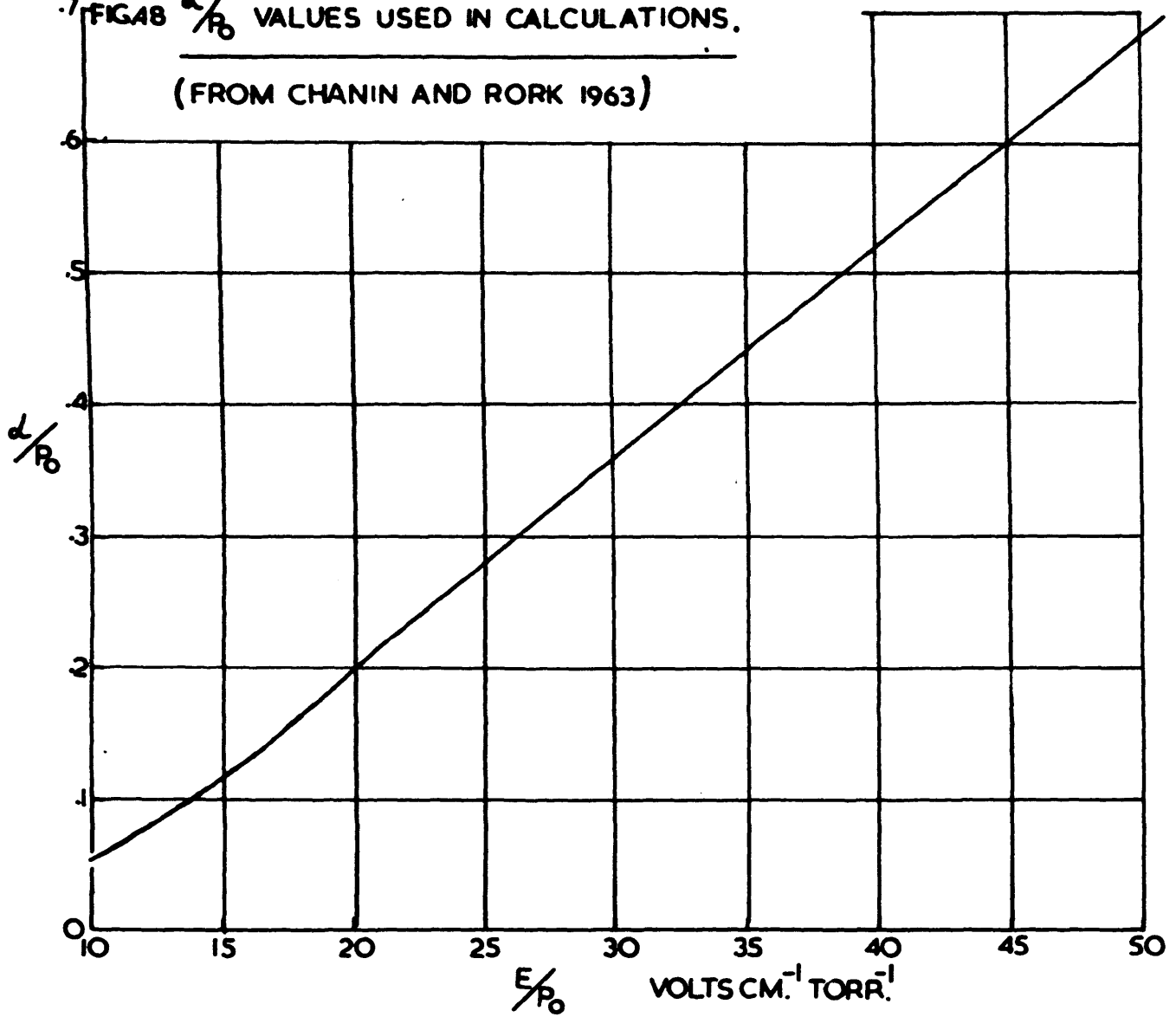

in the same sample of gas. This obviously desirable procedure did not prove possible in the present investigation because of the continuous rise in neon pressure which occurred. The α measurements used were taken from data by Chanin and Rork (1963). These results were obtained using gold electrodes with guard rings, the cathode being illuminated with ultra-violet light through small perforations in the anode. The neon purity was good, the system being equipped with a liquid nitrogen cooled trap, bakable valves and a cataphoresis discharge running at 50 mA. Fig. 48 shows α/p_o as a function of E/p_o. These results agreed surprisingly well with results obtained much earlier under more primitive conditions by Townsend and McCallum (1928) and Knuitoff and Penning (1937). Measurements by Fletcher (1963) made with a system using grease taps for E/p_o values greater than 30 gave lower values of α/p_o than those of Chanin and Rork.

Recent work by Lucas (1965 1 and 2) has shown that α values calculated from the prebreakdown current may be in error as a result of the loss of electrons by diffusion where large electrode gaps are used. Calculation for the case of helium have shown that the error in the α value obtained is significant for low values of E/p_o (up to about 40 V cm^{-1} $torr^{-1}$). In some cases the α value obtained was larger than the true value by a factor of 4. Unfortunately complete analysis to give the correct α value requires a knowledge of the secondary ionization processes under the conditions

FIG.49 ELECTRON DRIFT VELOCITY IN NEON.

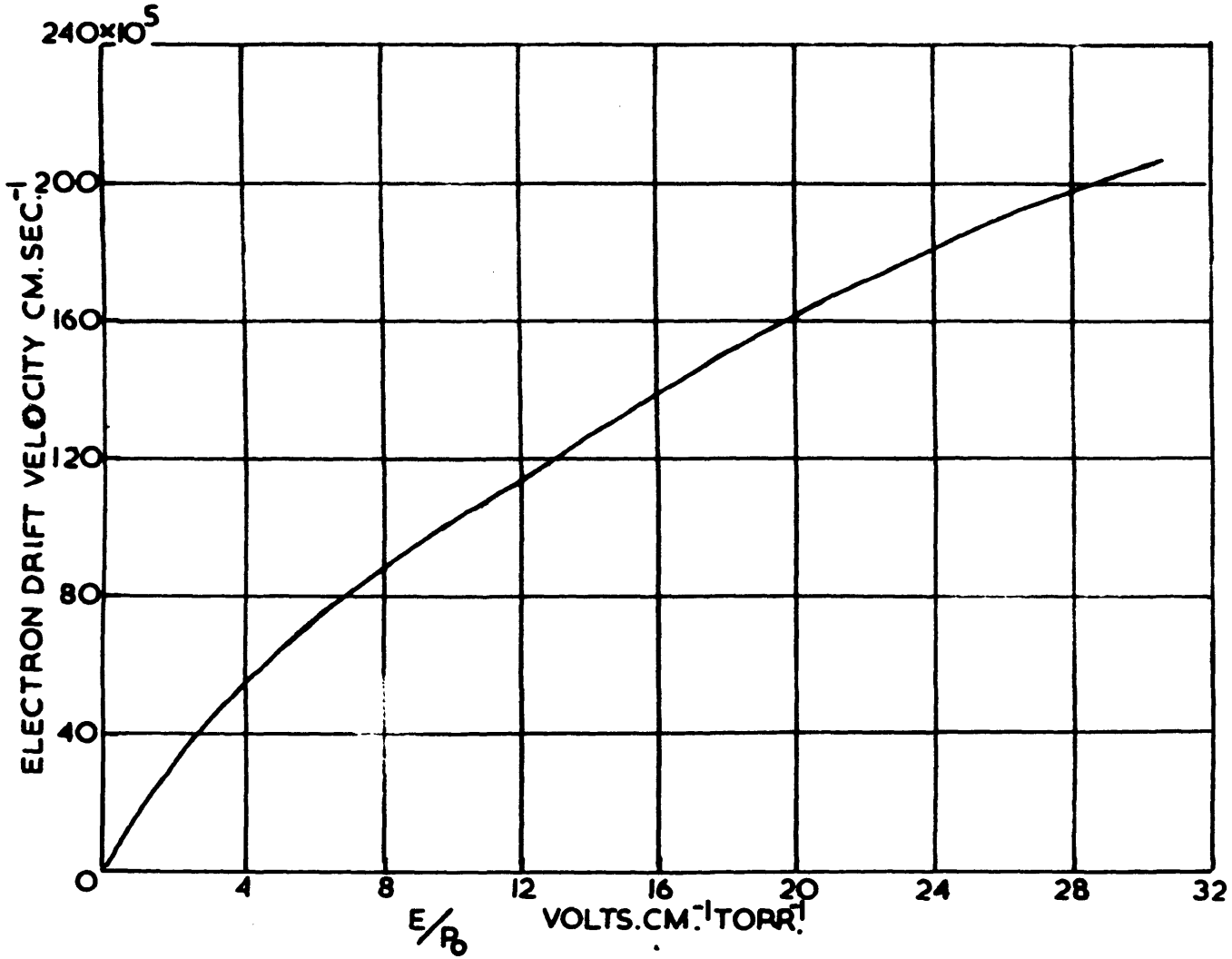

of the α measurements. The effect of the error for the case of neon α values cannot therefore be simply determined, but the work of Lucas stresses the danger of using incorrect α values in formative time lag calculations. The error involved in the calculated time lag TF is all the more serious since the calculation involves the function $B = e^{\alpha d} - 1$.

6.6. THE DRIFT VELOCITY OF ELECTRONS IN NEON

The values of electron drift velocity in neon used in the calculations are shown in Fig. 49 as a function of E/p_o. This graph has been extrapolated to higher E/p_o from data by Bradbury and Nielson (1936 1,2) and Nielson (1936) assuming that the drift velocity becomes proportional to E/p_o for the E/p_o region where inelastic collisions become significant. (Von Engel 1955 page 106). It was seen from Programme 2 that provided $p \ll w_-$ (or Q << U in Fortran notation) and the approximation $\psi = \alpha$ can be made the electron drift velocity appears only in the expression F1 the derivative of F(p). F1 = C*G + H where $C \propto \frac{1}{U}$, and $G \propto U$ since the first term of G is much larger than the second term. Thus C*G is approximately independent of U so that F1 is not sensitive to small change in U. In practice it was found that a change of an order of magnitude in the U value used resulted in a changes in the theoretical formative time lag which was well within the limits

FIG.50 DRIFT VELOCITY OF Ne^+ IN NEON.

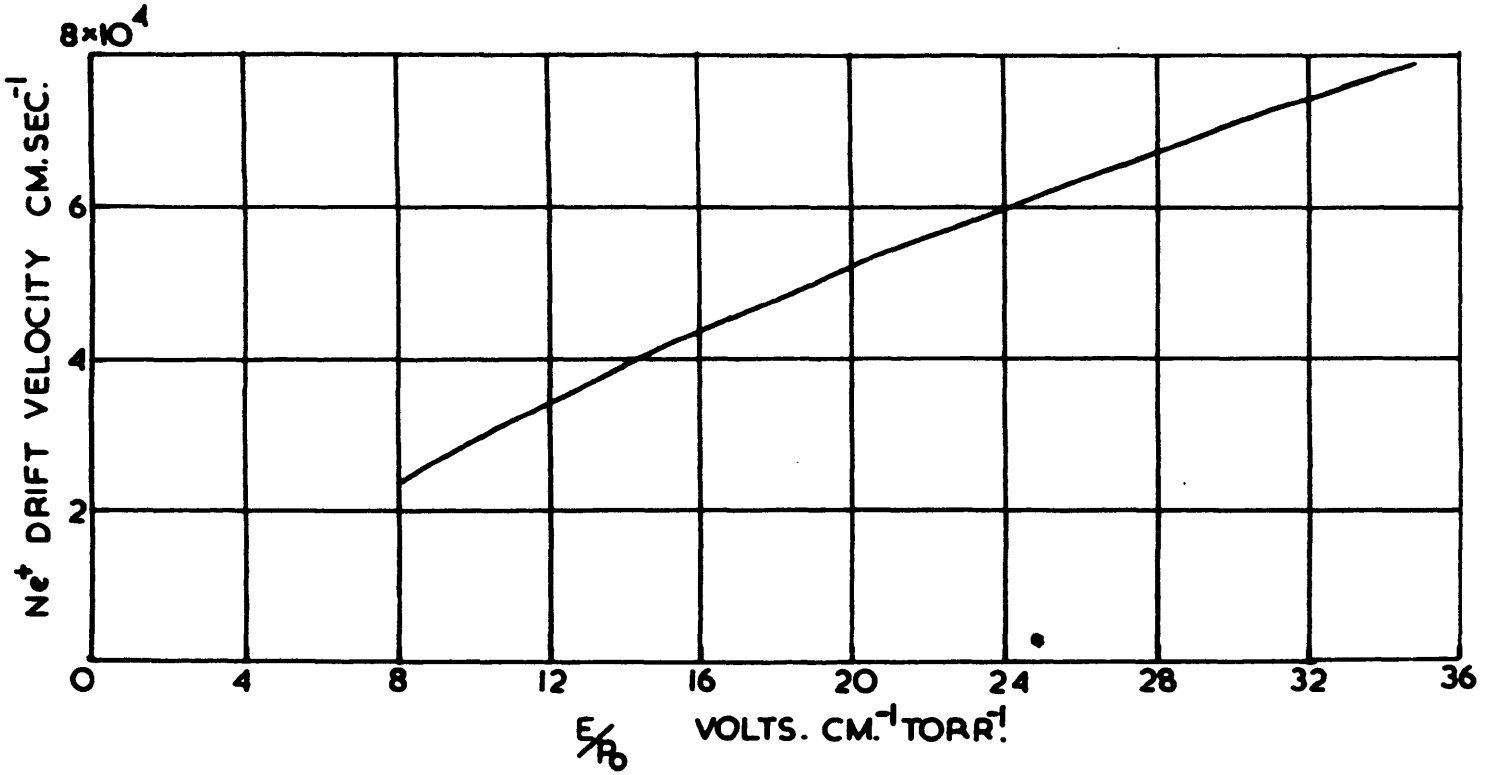

of accuracy of the analysis. The extrapolated values of U used in the calculations were therefore of adequate accuracy.

6.7. THE DRIFT VELOCITY OF POSITIVE IONS IN NEON

The values of the drift velocity of neon positive ions used in the calculations were taken from data by Hornbeck (1951). Fig. 50 shows the drift velocity of a singly charged neon ion as a function of E/p_o. The value of w (or V) used in Programme 2 is related to the ion and electron drift velocities by the formula:

$$\frac{1}{w} + \frac{1}{w_-} + \frac{1}{w_+}.$$

Since $w_+ << w_-$, w is mainly determined by the positive ion drift velocity w_+. In practice it was found that the calculated formative time lags, and the ratio $\frac{\zeta_1/a}{\omega/a}$ determined by curve fitting, were not significantly affected by order of magnitude changed in U, V or R.

6.8. THE LIFETIME OF NEON METASTABLE ATOMS

The values of mean metastable neon lifetime τ_1 or T, used in the calculations were obtained by using Grant's empirical formula [Grant 1951]

$$\frac{1}{\tau_1} = \frac{B}{p_o} + Cp_o^n \qquad (57)$$

where B = 66

C = 135

n = .7 p_o is the reduced pressure in torr.

The first term depends on the geometry of the system, and becomes significant at low pressures. Tabel 5 shows the relative importance of the two terms of the two ends of the pressure range used. The effect of the geometrical term is very small.

TABLE 5

PRESSURE	$\frac{1}{Cp_o^n}$	$\frac{1}{B/p_o + Cp_o^n}$
20 torr	9.3×10^{-4} sec	8.9×10^{-4} sec
50 torr	4.82×10^{-4} sec	4.83×10^{-4} sec

Most of the present experimental results were obtained with an electrode gap of about .5 cm in a tube of diameter 6 cm. The lifetimes measured by Grant were for a longer tube (150 cm) so that the geometrical term used in equation (57) may be an underestimate for the present work.

A similar formula for τ_1 has been described by Phelps and Molnar (1953):

$$\frac{1}{\tau_1} = \frac{D_o}{p_o \Lambda^2} + Ap_o + Bp_o^2 \qquad (4)$$

The first term is again a geometrical term. D_o is the diffusion coefficient for the metastable atoms at a pressure of 1 torr. Λ is the diffusion length given by

$$\frac{1}{\Lambda^2} = \left(\frac{\pi}{L}\right)^2 + \left(\frac{2.4}{R}\right)^2 \qquad (5)$$

where L is the length and R the radius of a cylindrical chamber. The second term Ap_o of the expression for $\frac{1}{\tau_1}$ accounts for destruction of the metastable atoms in the gas by two body processes. A is the frequency of destruction at two body collisions determined by Phelps and Molnar as 50 sec^{-1} $torr^{-1}$ at 300°K. The third term accounts for destruction at three body collisions. The destruction frequency B was shown by Phelps to be zero at 300°K and only important at lower temperatures.

The diffusion length of the apparatus used for the present work was 1/6 cm for a gap of .5 cm between the electrodes. For D_o of 150 $cm^2 sec^{-1}$ the geometrical term could then be evaluated as a function of pressure. Table 6 below shows the relative importance of the two terms over the range of pressure used.

FIG.5I LIFETIME OF NEON METASTABLE ATOMS AS A FUNCTION OF PRESSURE

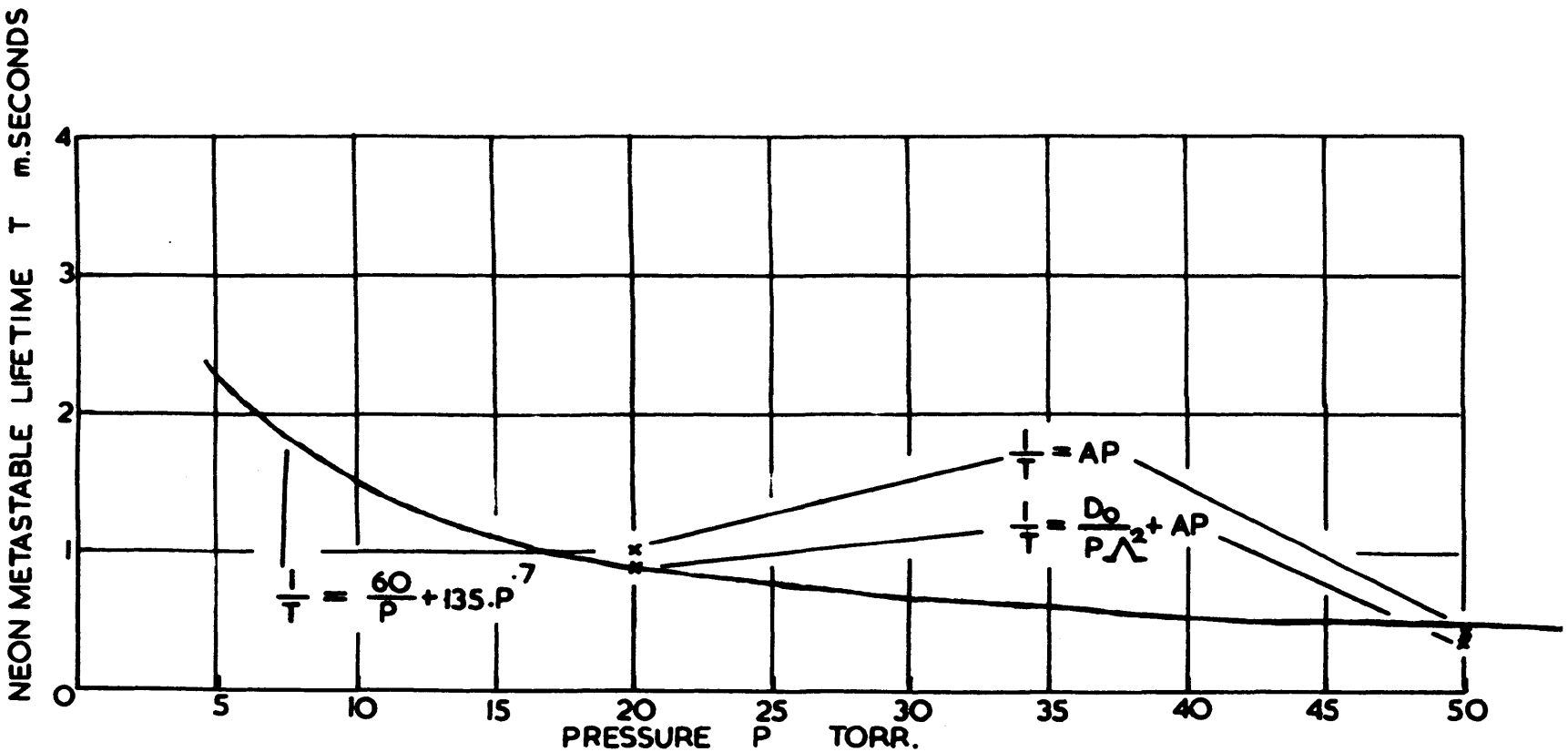

TABLE 6

PRESSURE	$\frac{1}{Ap_o}$	$\frac{1}{\frac{D_o}{p_o^2} + Ap_o}$
20 torr	1×10^{-3} sec	7.9×10^{-4} sec
50 torr	4×10^{-4} sec	3.8×10^{-4} sec

These results show that the geometrical effect on τ_1 is probably larger than it appears from Grant's formula because of the longer diffusion length used by Grant. Fig. (51) shows the metastable lifetime τ_1 or T as a function of pressure calculated by using Grant's formula, and also the values obtained by Phelps' and Molnar's formula. The latter values are slightly lower but the difference is not serious. The experimental variation of $\frac{\delta_1/a}{a}$ % against T shown in Fig. 47 for a typical set of results, shows that the value of δ_1/a would not be seriously affected by a small discrepancy in T in view of the other inaccuracies of the method. Measurements of τ_1 by Dixon and Grant (1957) over a rather restricted pressure range indicated that the lifetimes of the $^1P_2$ and $^3P_0$ metastable states coincide and the two types of atom both have the same diffusion coefficient. Thus the analysis used in the present work does not enable the two metastable states to be distinguished.

FIG.52 SECONDARY IONIZATION COEFFICIENTS ω/α, γ AND δ_1/α AS FUNCTIONS OF E_s/P_o.

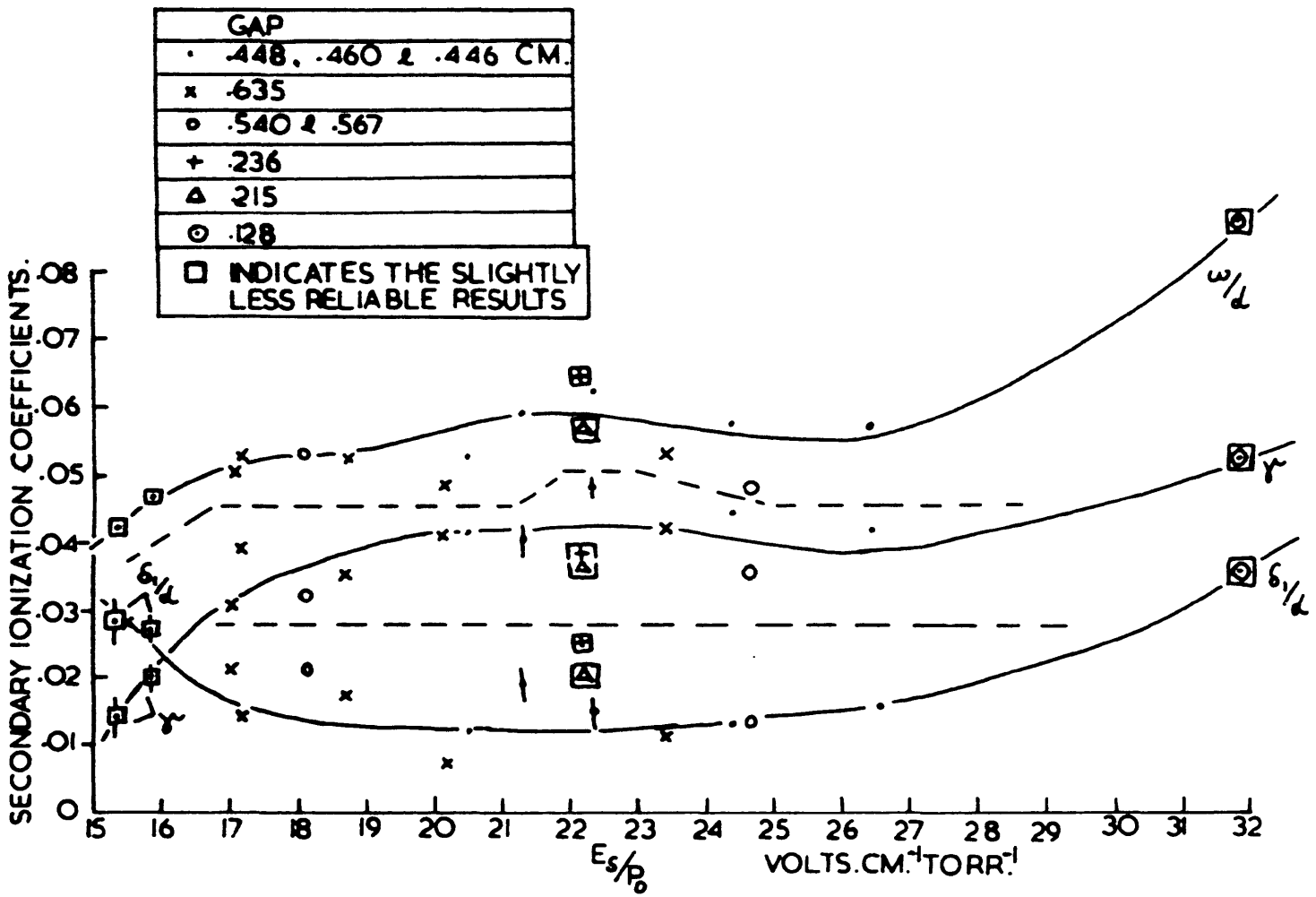

In section 6.3 the secondary emission from the cathode due to positive ions, undelayed photons and metastable atoms, failed to explain the experimental current growth. The metastable lifetime values shown in Table (6) give some indication of the reason for this failure since even at the lowest pressure a considerable number of the metastable atoms are destroyed by two body collisions in the gas and will never reach the cathode.

6.9. VARIATION OF THE SECONDARY IONIZATION COEFFICIENTS WITH E_s/p_o

Fig. 52 shows the secondary ionization coefficients ω/α, δ_1/α and γ as functions of E_s/p_o. The last 5 results for which the gas purity was slightly doubtful are indicated on the graphs. Because of the intrinsic inaccuracy of the method previously mentioned and the possibility of an inappropriate α value having been used the δ_1/α and γ curves are not of high accuracy, but they do provide an estimate of the value of the secondary coefficients and show general trends.

For the E_s/p_o range from 17 to 27 there is no clear evidence for any variation of ω/α with gap distance ranging from .215 cm to .635. The slightly less reliable results indicate a fall in ω/α for E_s/p_o below 17 and a rise for E_s/p_o above 27, but further data would be required to confirm this. The secondary coefficients δ_1/α and γ obtained from the analysis show a wider

FIG.53 PASCHEN CURVE. V_s AS A FUNCTION OF $P_0 d$

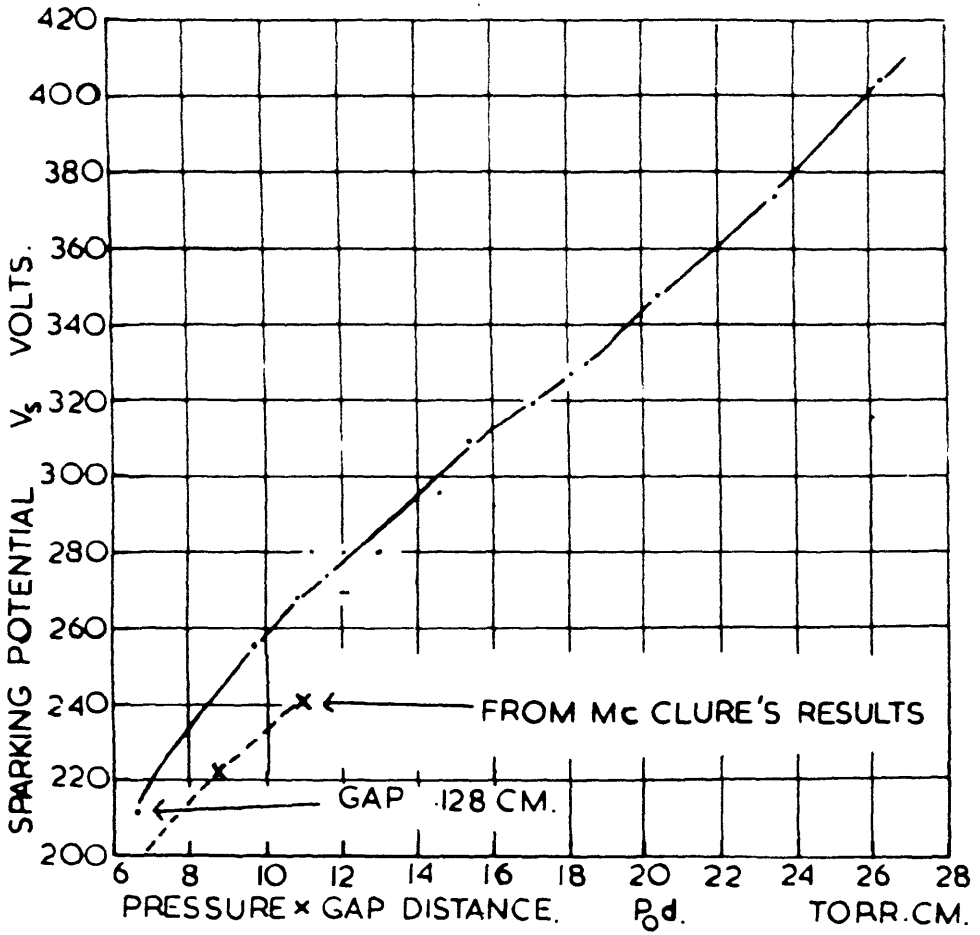

scatter because of inaccuracies introduced in the calculations. For low E_s/p_o there is a fall in γ and a rise in $\delta 1/\alpha$ for decreasing E_s/p_o. (The γ values include secondary emission resulting from undelayed photons (δ/α) since the two processes are not distinguishable.) The results for $\delta 1/\alpha$ obtained by D.K. Davies for helium showed a similar rise in $\delta 1/\alpha$ at low E_s/p_o as shown in Fig. 14. At high E_s/p_o (above 27) $\delta 1/\alpha$ rises faster than γ with increasing E_s/p_o. However further evidence would be required to confirm this since the apparent rise depends on only one experimental point where the gas could have been contaminated and where a very small gap distance (.125 cm) was used. The increase in $\delta 1/\alpha$ could be due to a geometrical effect, since with the smaller gap distance a larger fraction of the radiation from the decayed metastable atoms would arrive at the cathode.

Graph 53 shows the sparking potential measurements obtained during the formative time lag experiments plotted as a Paschen curve against $p_o d$. There is no serious deviation from Paschen's law for the range of gap distances used with the exception of the smallest gap used, so that geometrical effects were not serious. The result for the smallest gap distance falls below the extrapolated curve for the rest of the results. This lower V_s value could be accounted for by the high $\delta 1/\alpha$ coefficient described above. The sparking potential values from McClure's work with molybdenum disc

FIG.54 VARIATION OF SECONDARY IONIZATION COEFFICIENTS $\delta_{1/\alpha}$ AND γ WITH PRESSURE.

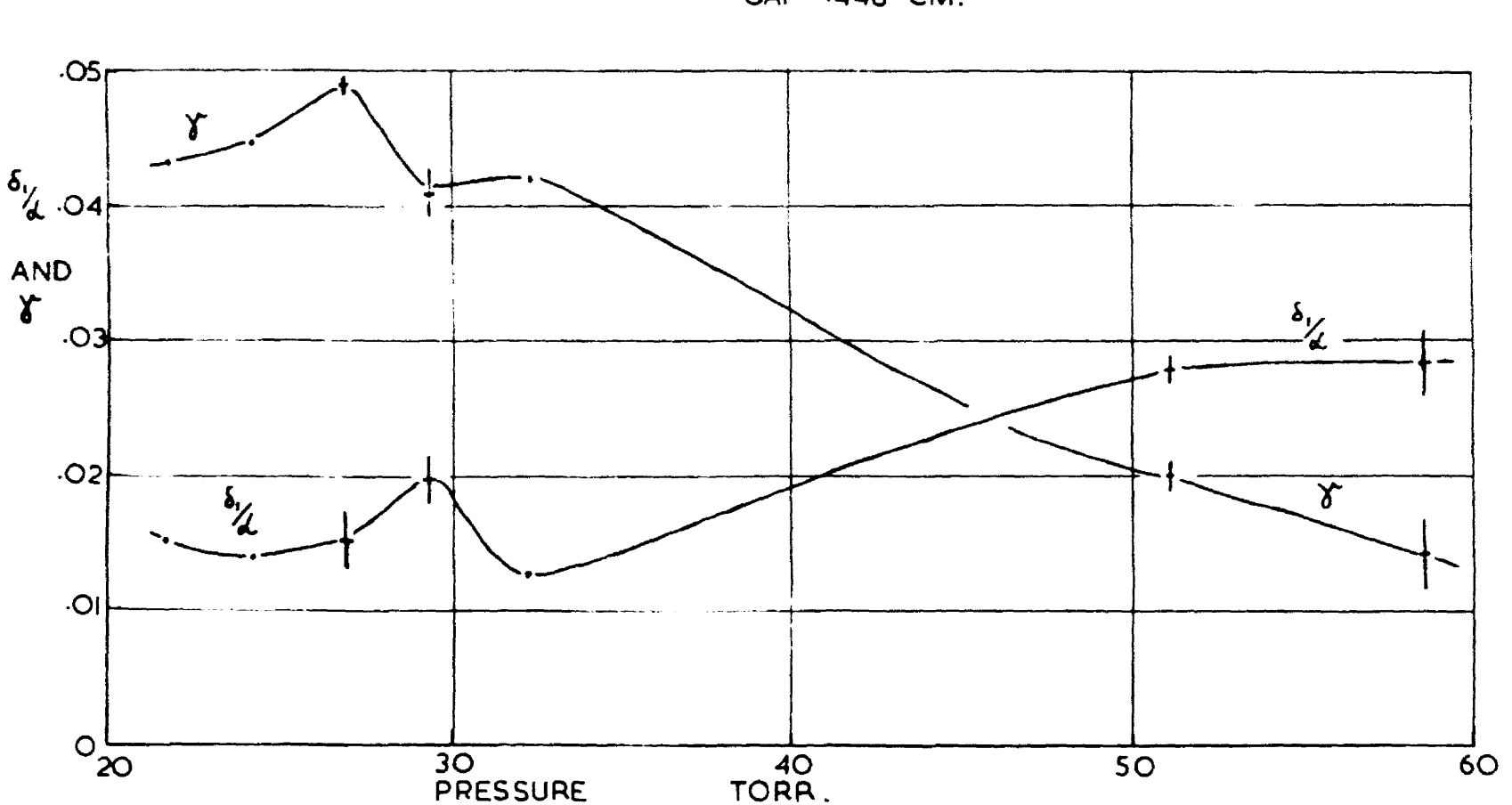

FIG. 55 ELECTRON YIELD AS A FUNCTION OF ION ENERGY FOR NOBLE GAS IONS ON TUNGSTEN

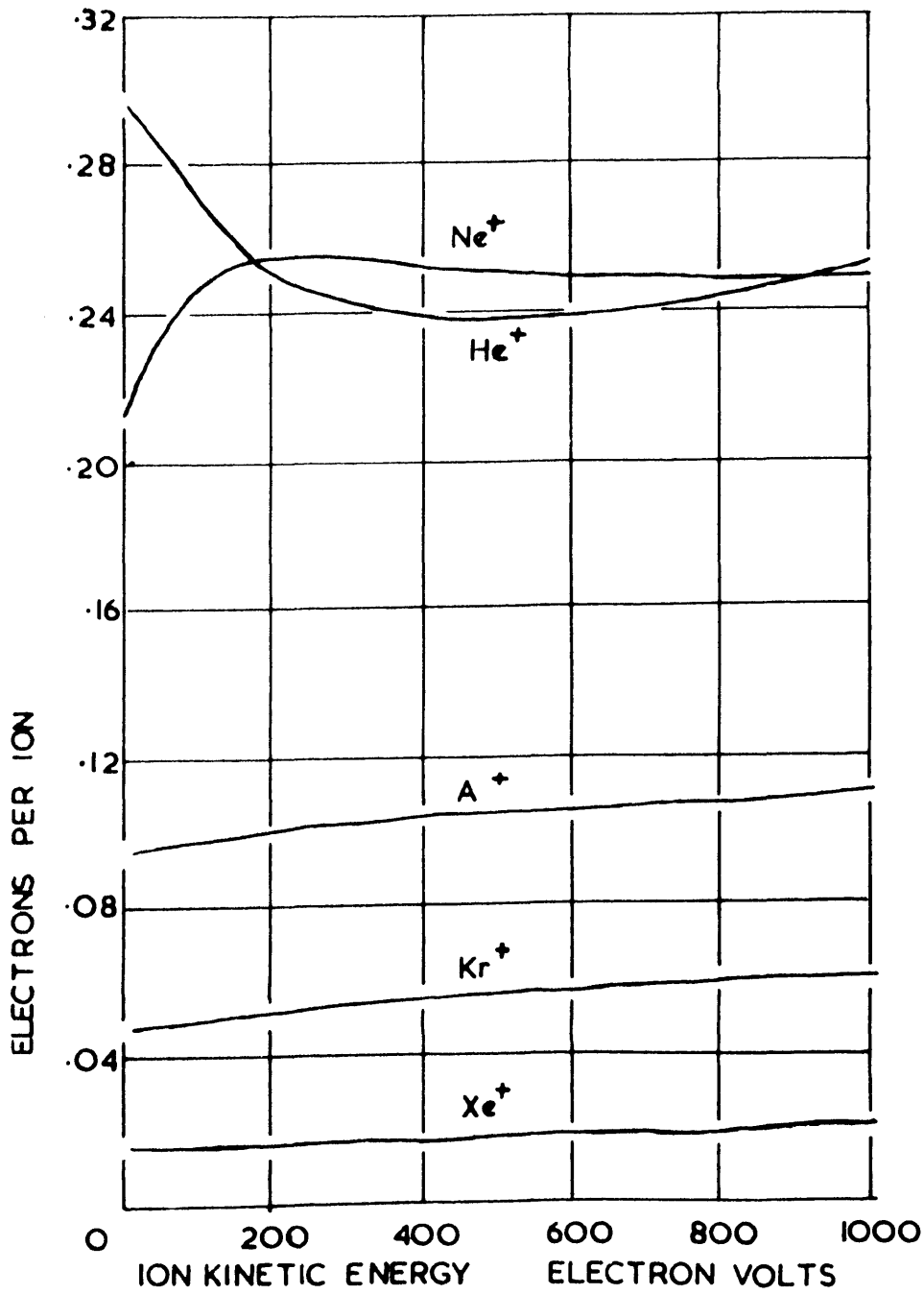

electrodes fall well below the curve. This could be due to a lower cathode work function, contamination of the neon or non-uniform field near the edge of his electrodes.

The predominance of the $\delta 1/\alpha$ process at low E_s/p_o shown on Fig. 52 is not the result of a geometrical effect, since it is still true of results for a single gap distance. Fig. 54 shows the variation of γ and $\delta 1/\alpha$ with p_o for a gap distance of .448 cm. The results for gaps of .46 and .446 cm are also included. For pressures below 46 torr the γ process predominates, but above 46 torr the $\delta 1/\alpha$ process becomes more important. This may be partly due to the fact that the life-time of the metastable states decreases with increasing pressure so that less metastable atoms diffuse out of the gap before collision with a neutral atom releases a photon.

The γ values obtained in the present work are considerably lower than values of γ_i, the secondary electron yield per incident ion, measured by Hagstrum (1954) using mono-energetic ions on atomically clean tungsten (Fig. 55). Hagstrum's measurements, using ion beams in vacuum, are not susceptible to errors due to the operation of the Penning effect and may be considered as reliable since they are in agreement with more recent work by Rakhimov and Dzhurakulov (1964). In the present work, the operation of the Penning effect was considered as a possible reason for the discrepancy. Contaminated neon would have a lower sparking potential than pure neon (Penning 1929). Unfortunately no sparking potential measurements for high purity neon are

In addition to this effect, Penning showed that contaminated neon would have higher α values than pure neon. The α effect is larger and would therefore cause a reduction in ω/α calculated from $\omega/\alpha = \frac{1}{e^{\alpha d}-1}$. However, if α values are not measured in the experiment and values for pure neon are used instead (as in the present work), any unsuspected Penning effect would result in an increase in the calculated value of ω/α and would not therefore account for the difference between the γ coefficient of the present work and Hagstrum's γ_i values. This difference could only be accounted for if the α values used were obtained under Penning effect conditions and applied to the case of pure neon. This is thought to be unlikely since the α measurements of Chanin and Rork were obtained under good experimental conditions.

A similar difference arises between the helium γ values of Griffiths and Hagstrum's measurements of γ_i for helium, although the γ values of D.K. Davies are consistent with Hagstrum's data. The data of Griffiths' experiment shows slightly higher sparking potentials than those of D.K. Davies for E_s/p_o values of about 25 volt cm^{-1} $torr^{-1}$ for similar experimental conditions. Griffiths also measured higher α values than D.K. Davies. These two factors would give a lower value ω/α and lead to a lower value of γ for Griffiths' work. If the helium purity for Griffiths' experiment was inferior to that of D. K. Davies, as suggested by Griffiths, this would lead to higher α values, but on the other hand V_s would be lower. Thus the Penning effect is not sufficient to explain these results. The low ω/α and γ values obtained by Griffiths may be the result of a high cathode work function or possibly

FIG.56 FORMATIVE TIME LAG AS A FUNCTION OF E/P_0 FOR A GIVEN OVERVOLTAGE.

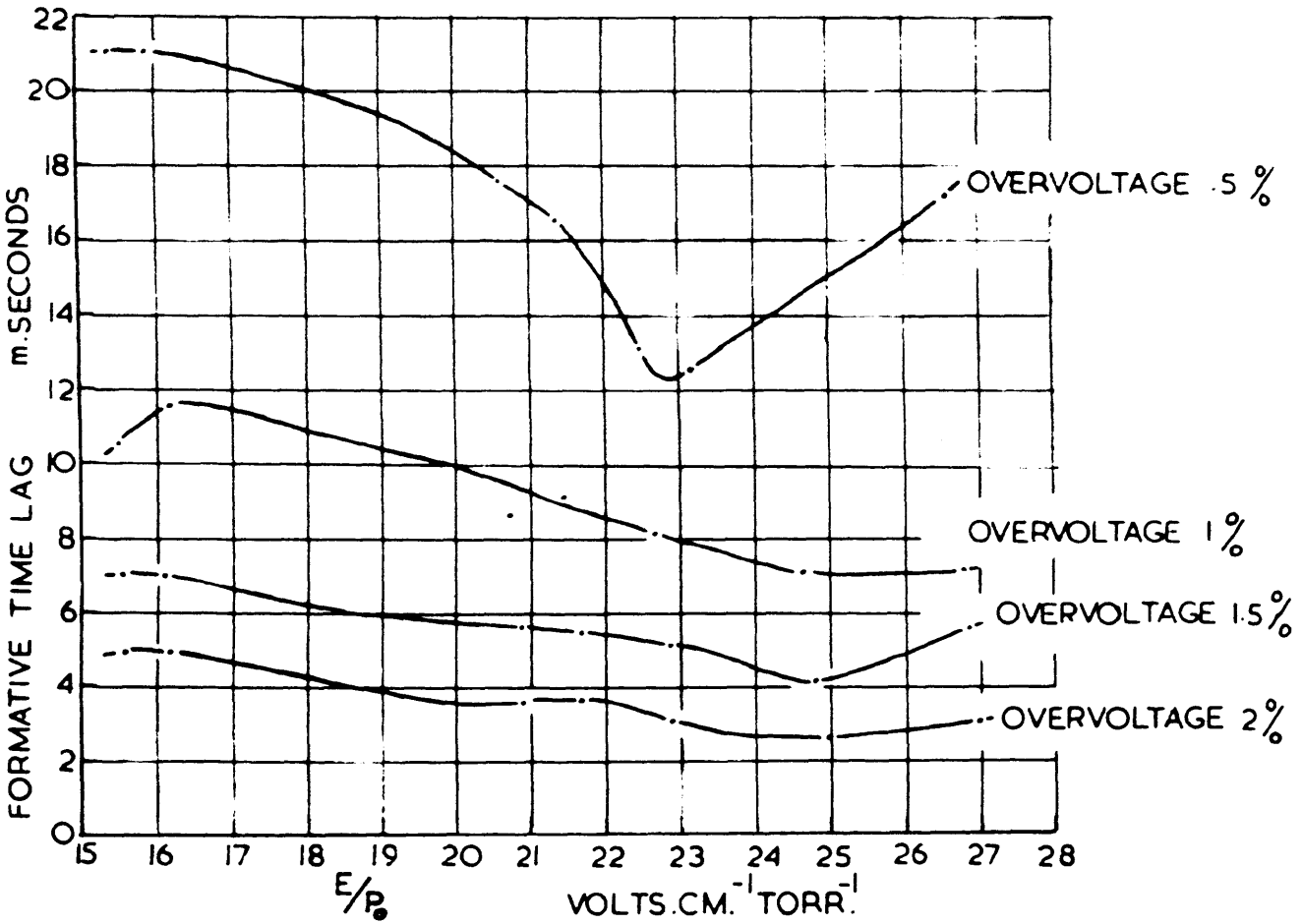

gas sample (a low ω/α value resulting from the use of an α value which is too high).

The γ_i values of Hagstrum and Rakhimov and Dzhurakulov were measured for atomically clean tungsten and molybdenum respectively. Both workers observed that γ_i decreased as the surface became contaminated. Under conditions of a Townsend discharge the cathode surface may be contaminated and the possibility of an oxide layer cannot be ruled out. In the present work in neon using a nickel cathode, an oxide layer, once formed, would not be removed by the electrode outgassing techniques used. Such a layer could increase the work function by more than 2 eV (Farnsworth 1958) and would have a γ coefficient considerably lower than that for a clean nickel surface. This is the most likely explanation of the low γ values obtained in the present work.

Graph 56 shows the experimental formative time lags plotted as a function of E/p_o for 4 different overvoltages for a gap of .448 cm. These curves show a rise in the formative time lag at low E/p_o and at high E/p_o. The helium results of D.K. Davies showed a peak at low E_s/p_o. The rise of formative time lag for decreasing E/p_o and increasing pressure for low E/p and high pressure is difficult to explain qualitatively since the life-time of the metastable state decreases with increasing

pressure leading to a decrease in the delay of the trapped energy in reaching the cathode.

6.10. THE EFFECT OF METASTABLE NEON MOLECULES

The work of Griffiths in helium, which has been described in Chapter III, showed that the temporal growth of current at the Townsend breakdown for pressures above 30 torr and E_s/p_o below 10 volt cm^{-1} $torr^{-1}$ could be explained by a combination of three secondary processes. These were emission of electrons from the cathode by (a) ions, (b) delayed photons from helium metastable atoms destroyed by two-body collisons, and (c) delayed photons from the destruction of diatomic metastable molecules. These metastable molecules were believed to be formed by three-body collisons involving two ground state atoms. Phelps (1960) also showed that the action of these metastable molecules could account for the current growth in helium for low values of the growth constant and pressures of more than 100 torr.

For neon, for the range of pressure and E_s/p_o used in the present investigation, it was not found necessary to include a metastable molecule process in order to explain the results. The other two processes were sufficient. It would, however, be of interest to extend the work to higher pressures where such a three body process would become more important. At the time of writing the diatomic neon metastable molecule has not been observed in a gas discharge. The situation is, in any case, likely to be more complicated than for helium, since neon has four energy levels close enough for transitions between them to be caused by the thermal energy of neutral gas atoms.

6.11. THE EFFECT OF NEON MOLECULAR IONS

Neon molecular ions have been observed by Hornbeck and Molnar (1951) and are thought to be formed by the two stage process

$$Ne + e + K.E. \longrightarrow Ne^* + e$$

$$Ne^* + Ne \longrightarrow Ne_2^+ + e$$

where Ne^* is a high lying excited state.

The appearance potential of Ne_2^+ was slightly less than the ionization potential for Ne^+. The excited state involved in the

formation process cannot therefore be either the $^3P_2$ on the $^3P_0$ metastable state. If the formation of Ne_2^+ involves a radiating state the effect on the temporal growth of current would not be distinguishable from the Ne^+ ions since the theoretical formative time lags are not a sensitive function of ion drift velocity.

Niles and Robertson (1965) consider the formation of Ne_2^+ to be a single stage three body process $Ne^+ + 2Ne \rightarrow Ne_2^+ + Ne$. Theoretical calculations showed that the reaction rate for neon was much less than for He, A, Kr or Xe. Thus the neon molecular ion is unlikely to have a distinguishable effect on the temporal growth of current.

6.12. EMISSION OF SECONDARY ELECTRONS FROM THE CATHODE BY METASTABLE NEON ATOMS

Recent measurement by MacLennan (1966) of the secondary electron emission coefficient for metastable atoms of He and Ne on atomically clean tungsten have shown that the metastable atoms are almost as efficient as low energy ions for causing emission of secondary electrons, as would be expected from the Auger theory of secondary emission. For neon metastable atoms (an unresolved mixture of the $^3P_0$ and $^3P_2$ states) incident on clean tungsten, it

was found that .215 electrons were emitted per incident metastable atom. It was also shown that gas contamination of the surface caused a considerable reduction in the yield. For helium metastable atoms the yield was reduced by 80% by air contamination. However it is clear that, in the present work, metastable neon atoms which reach the cathode will be able to cause electron emission. At the higher pressures used (~ 50 torr) few metastable atoms are likely to reach the cathode before being destroyed in the gas. At the lower pressures used however the process described above may have a significant contribution to secondary ionization. The formative time lag method used would not be sufficiently sensitive to distinguish this effect unless it were comparable with the other secondary processes considered. An extension of the work to lower pressure using very small gap distances may enable this point to be resolved.

6.13. CONCLUSIONS

The analysis of experimental formative time lag curves using Davidson's analysis enables the secondary ionization processes, which predominate in the Townsend breakdown of neon, to be distinguished. This procedure does, however, have its limitations. The analysis only provides a possible explanation of the results. There may exist some other theory which would explain the

results equally well. The calculated formative time lags are not always sensitive functions of the assumed values of the secondary ionization coefficients. In such cases the coefficients cannot be determined with high accuracy. The accuracy of results is also particularly dependent on the use of the correct value for the primary ionization coefficient. Some of the possible ionization processes are not distinguishable, for example the secondary ionization coefficients for electron emission from the cathode by ions (γ') and undelayed photons (δ/α) cannot be distinguished from each other. The values of γ' which have been calculated in this work in fact include δ/α. It has been assumed that δ/α is small compared with γ', but this is difficult to justify because of a lack of information on the probability of excitation to the various excited states of the neon atom. Work by Phelps and Dixon and Grant suggests that the lowest non-metastable state ($^3P_1$) may be involved in a relatively slow resonance radiation process. The effect of diatomic molecular ions cannot be distinguished from atomic ions. Any ionization process which has only a small contribution to the total secondary ionization will not be distinguishable. The contributions of the $^3P_0$ and $^3P_2$ metastable states to the secondary ionization cannot be distinguished from each other because the mean lifetimes of the two states are not sufficiently different.

Despite these considerations the use of Davidson's analysis has shown that for an E_s/p_o range from 15 to 32 volt cm^{-1} $torr^{-1}$ (or E/N range from 4.3 to 9.0 x 10^{-16} volt cm^2) and a pressure range from 18 to 59 torr, the initial stage of the neon Townsend discharge can be successfully explained by assuming that the secondary ionization processes predominating are the γ and $\delta 1/\alpha$ processes. The $\delta 1/\alpha$ process involves the destruction of atomic neon metastable states by two body collisions with gas atoms, the resulting photon causing secondary electron emission from the cathode. The coefficient $\delta 1/\alpha$ has the value .015 $\pm$ .005 electrons per primary ionizing collision in the gas, and is approximately independent of E_s/p_o over the range 18 to 27 volt cm^{-1} $torr^{-1}$. $\delta 1/\alpha$ rises for E_s/p_o below 18, and for E_s/p_o below 16 the $\delta 1/\alpha$ process provides most of the secondary ionization.

The secondary ionization coefficient γ, for emission of electrons from the cathode by positive ions, has the value .040 $\pm$ .005 approximately independent of E_s/p_o over the range 18 to 27 volt $cm^{-1}torr^{-1}$. For E_s/p_o below 18 the value of γ falls. For E_s/p_o above 16 the γ process provides most of the secondary ionization. The value of γ includes any ionization resulting from the action of undelayed photons at the cathode (δ/α process).

The γ_i values measured by Hagstrum (1954) and Rakhimov and Dzhurakulov (1964) for mono-energetic neon ions on clean tungsten and molybdenum are considerably higher than the γ values for a nickel cathode obtained in the present work. This is thought to be due to a high cathode work function caused by the formation of an oxide layer.

6.14. SUGGESTIONS FOR FURTHER WORK

In any further measurements of formative time lags it would be an advantage to improve the conductance of the pumping system. This would give a shorter pump down time, a better ultimate pressure and less contamination of the test gas. Effective closure of the valves in the system is of course most important since this makes it possible to check the reproducibility of the results at a given pressure. This was not possible in the present work. Good pressure stability would also make it possible to measure the primary ionization coefficient in the same sample of gas as used for formative time lag measurements. This could be done with the type of experimental tube used in the present work. Such α measurements would greatly improve the accuracy of the calculated secondary ionization coefficients.

It would be useful to extend the range of the measurements particularly to higher pressures (above 60 torr) to ascertain whether a diatomic metastable molecular process needs to be considered. Further work at lower pressure (< 20 torr) using small gaps (<.1 cm), where the destruction of metastable states in the gas will be reduced, may enable the emission of electron from the cathode by incident metastable atoms to be observed. There is now sufficient data available for the formative time lag analysis to be used for argon. Some of the sources of argon data have been mentioned in Chapter II.

In formative time lag experiments where impurities are likely to have an important effect considerable weight is added to the conclusions if proof of gas purity can be obtained. The effectiveness of cataphoresis purification could also be directly determined. Unfortunately the addition of a mass spectrometer to the system would require the complication of a differentially pumped system to reduce the pressure of the test gas to a level at which a mass spectrometer, such as an omegatron, could be used.

It is clear from the results of the present work, and the work in helium by D. K. Davies and Griffiths, that the state of the cathode surface has an important effect on the secondary ionization coefficients operating at the cathode. It is therefore important to be able to measure the work function of the cathode surface under the conditions of the experiment. This could be done by the Kelvin vibrating electrode method provided that the practical difficulties of incorporating this in an already complicated tube can be overcome. (See for example Llewellyn Jones and Davies 1951.) To obtain stable work functions electrodes should preferably be of a noble metal and be outgassed at a high temperature. Alternatively, noble metal films put down in high vacuum could be used provided that the difficulties, experienced with such electrodes in the present work, can be avoided.

REFERENCES

Anderson, J.M. 1930. Can. J. Res., 2, 13

Arnot, F.L., & M'Ewan, M.B. 1938. Proc.Roy.Soc.Lond.A, 166, 543

Arnot, F.L., & M'Ewan, M.B. 1939. Proc.Roy.Soc.Lond.A, 171, 106

Baker, M.A., & Laurenson, L. 1966. Vacuum, 16/11, 633-637

Baly, E.C. 1893. Phil.Mag., 55, 35/214, 200-205

Bartholomeyczyck, W. 1940. Z. Phys., 116. 235

Betts, B.P. 1963. M.Sc. Thesis, Birmingham

Biberman, L.M. 1947. J.Expt.Thr.Phys. U.S.S.R., 17, 416

Biberman, L.M. 1949. J.Expt.Thr.Phys. U.S.S.R., 19, 584

Biberman, L.M., & Gurevich, I.M. 1950. J.Expt.Thr.Phys. U.S.S.R., 20, 108

Biordi, M.A. 1952. Phys. Rev., 88/3, 660-665

Bradbury, N.E., & Neilson, R.A. 1936(1) Phys. Rev., 49, 388

Bradbury, N.E., & Neilson, R.A. 1936(2) Phys. Rev., 51, 69

Buttner, H. 1939 Z. Physik., 111, 750

Chanin, L.M., & Rork, G.D. 1963 Phys. Rev., 132/6, 2547-53

Colli, L. 1954. Phys. Rev., 95/4, 892-894

Compton, K.J., & Van Voorhis, C.C. 1926. Phys. Rev., 27, 724

Davidson, P.M. 1955. Phys. Rev., 99, 1072

Davidson, P.M. 1958. Proc.Roy.Soc.A, 249, 237-247

Davidson, P.M. 1962. Proc.Roy.Soc.A, 80, 143-150

Davies, D.K. 1961. Ph.D. Thesis, Swansea

Davies, D.K., Llewellyn Jones, F., & Morgan, C.G. 1963. Proc.Phys.Soc., 81, 677-681

Davies, D.K., Llewellyn Jones, F., & Morgan, C.G. 1964. Proc.Phys.Soc., 83, 137-143

Davies, R.D., & Llewellyn Jones, F. 1965. International Conference on Ionization Phenomena in Gases, Belgrade. to be published

Dornestein, R. 1942. Physica, 9, 422

Dixon, J.R., & Grant, F.A. 1957. Phys.Rev., 107/1, 118-124

Druyvesteyn, M.J. 1935. Physica, 2, 255-266

Dutton, J., Haydon, S.C., Llewellyn Jones, F., & Davidson, P.M. 1953. B.J.App.Phys., 4, 170

von Engel, A.H. 1955. Ionized Gases, Oxford

von Engel, A.H. & Corrigan, S.J.B. 1958. Proc.Phys.Soc., 72, 782

von Gugelburg, H.L. 1947. Helv.Phys.Acta, 20, 250, 307

Engstrom, R.W., Huxford, W.S. 1940. Phys.Rev., 58, 670

Farnsworth, H.E., 1958, Proc. Phys. Soc. A218, 566.

Fletcher, J. 1963. Ph.D. Thesis, Keele

Fulker, M.J. 1963. M.Sc. Thesis, Birmingham

Gogna, C.F. 1960. Ph.D. Thesis, Birmingham

Grant, F.A. 1950. Can.J.Res. A, 28, 339-358

Grant, F.A. 1951. Phys. Rev., 84, 844

Griffiths, D. 1964. Ph.D. Thesis, Swansea

Hagstrum, H.D. 1953. Phys. Rev., 91, 543-551

Hagstrum, H.D. 1954. Phys. Rev., 96, 325, 336-365

Holstein, T. 1947. Phys. Rev. 72, 1212

Holstein, T. 1951. Phys. Rev., 83, 1159

Hornbeck, J.A., & Molnar, J.P. 1951. Phys.Rev., 84, 621-625

Huxley, L.G.M., Crompton, R.W., & Elford, M.T. 1966. Bulletin of the Institute of Physics, 17/7, 251

Kenty, C. 1958. Bull.Am.Phys.Soc., II/3, 82

Kruitoff, A.A., & Penning, F.M. 1937. Physica, 4, 430

Langmuir, I. 1923. Journ.Frankl.Inst., 196, 751

Little, P.F. 1956. Handbuch.der Physik, 21, 618

Llewellyn Jones, F. and Davies, D.E. 1951, Proc.Phys.Soc., B64, 397.

Llewellyn Jones, F. 1957. Ionization and Breakdown in Gases, Methuen, London

Llewellyn Jones, F., Morgan, C.G., & Davies, D.K. 1965 Proc.Phys.Soc., 85, 351-354

Loeb, L.B. 1958. J.Appl.Phys., 29/9, 1369-1379

MacLennon, D.A. 1966. Phys.Rev., 148/1, 218-223

Magnuson, G.D., & Carlston, C.E. 1963. Phys.Rev., 129/6, 2403-2408

McClure, T. 1962. Phys.Rev., 125/1, 11-16

McLure, C.W. 1961. Phys.Rev., 124, 980

Lucas, J. 1965(1) Int.J.Electronics, 18, 419-430

Lucas, J. 1965(2) Inst.J.Electronics, 19, 439-452

Meisner, K.W., & Graffunder, W. 1927. Ann.Physik, 84, 1009

Mitchell, A.C.G., & Zemansky, M.W. 1934. Resonance Radiation and Excited Atoms, Macmillan, London

Molnar, J.P. 1951(1) Phys.Rev., 83/5, 933-940

Molnar, J.P. 1951(2) Phys.Rev., 83/5, 940-952

Morgan, C.G., Llewellyn Jones, F., & Davies, D.K. 1965. Proc.Phys.Soc., 85, 351-354

Nielson, R.A. 1936. Phys. Rev., 50, 950

Niles, F.E., & Robertson, W.W. 1965. J.Chem.Phys., 43/3, 1076-8

Penning, F.M. 1929(1) Proc.Acad.Sci.Amst., 32, 341

Penning, F.M. 1929(2) Z.Physik, 57, 723

Penning, F.M. 1930. Physica, 10, 47

Penning, F.M. 1934. Physica, 1, 763

Phelps, A.V., & Molnar, J.P. 1953. Phys.Rev., 89/6, 1202-1207

Phelps, A.V. 1955. Phys.Rev., 99, 1657, A.

Phelps, A.V. 1959. Phys.Rev., 114/4, 1011

Phelps, A.V. 1960. Phys.Rev., 117/3, 619-632

Pike, E.W. 1936. Phys.Rev., 49, 513

Rakhimov, R.R., & Dzhurakulov, Kh. 1964. Instrum.Exper. Tech. (U.S.A.), 2, 263-279

Reize, R., & Dieke, G.H. 1954. J.Appl.Phys., 25/2, 196-201

Schade, R. 1937. Z.Physik, 105, 595

Schade, R. 1938. Z.Physik, 108, 353

Schmeltekopf, A.L. 1964. J.App.Phys., 35/6, 1712-1717

Townsend, J.S. 1910. The Theory of Ionization of Gases by Collision, Constable, London, 56-58

Townsend, J.S., & McCallum, S.P. 1928. Phil.Mag., 8, 857

Utterbach, N.G., & Miller. G.M. 1961. Phys.Rev., 124, 1477

Weissler, G.L. 1965. Handbuch der Physik, 21, 347

Zemansky, M.W. 1929. Phys.Rev., 34, 213